POLITECNICO DI TORINO

Master's Degree in AEROSPACE ENGINEERING

Master's Degree Thesis

Analysis of the effects of orbital parameters and phase angle on missions to near-Earth asteroids

Supervisor

Prof. Lorenzo CASALINO

Candidate

Alessandro DI NICOLA

July 2024

Abstract

In this thesis will be analyzed a strategy of optimization of trajectories for missions to near-Earth asteroids. Near-Earth Asteroids, also known as NEA, are a class of asteroids of sizes ranging from meters to tens of kilometres that orbit the Sun and whose orbits come close to that of Earth's, and this aspect makes them interesting, firstly in order to monitor their positions and predict eventual potential impacts with Earth. In addition, NEAs are interesting both from the perspective of studying the genesis of the Solar System and the life on our planet, and with the aim of a space economy also based on the extraction of the minerals they contain. With the continuous discovery of new NEAs through sky observations, employing eletrical propulsion becomes advantageous. Unlike chemical propulsion, it significantly reduces propellant consumption, leading to substantial savings in missions.

A technique known as optimal control theory, with indirect methods of resolution of the fundamental equations, which are characterized by a significant numeric precision, with a low number of parameters and limited time of calculation, is used to optimise trajectories: through the definition of additional equations to be aggregated to the system of differential equations governing the problem, it is possible to minimise a cost function representing the parameter to be optimised, in this case the mass at the end of the journey. Using a list of asteroids with a close passage to Earth in the next few years, an optimisation has been carried out to find the optimal phase angle to maximise the final mass. Furthermore, it was analysed how the variation of orbital parameters and phase angle impact trajectory optimization, highlighting which asteroids may be easier to reach in terms of cost. The objective was to optimize the trajectory in a way that required the least amount of propellant, showcasing the practical application of the research findings. This approach not only emphasizes the efficiency of electric propulsion but also underscores its potential in enabling cost-effective and environmentally sustainable space missions, including missions to explore celestial bodies within our solar system.

Acknowledgements

Ringrazio il mio relatore, il Professor Casalino, per la sua guida preziosa, la disponibilità e il sostegno continuo. La sua esperienza è stata fondamentale per lo sviluppo di questo lavoro.

Grazie di cuore alla mia famiglia, per il loro amore e supporto costante durante tutto il mio percorso accademico.

Infine, un ringraziamento ai miei amici, sia nuovi che di vecchia data, con cui ho condiviso questi anni universitari. Grazie per il vostro incoraggiamento e per i momenti che abbiamo vissuto insieme. La vostra presenza è stata essenziale per mantenere l'equilibrio e la motivazione.

Table of Contents

List of Tables

List of Figures

Chapter 1

Introduction

1.1 Thesis overview and objectives

The introductory chapter presents a general introduction to space trajectory optimisation, low-thrust propulsion and the workflow followed. When speaking of optimal trajectories, the link with low-thrust propulsion is very close, as it is the small forces that make the trajectory continuous and optimisable.
The aim of the thesis work presented in this paper is to research the trajectories that a probe will have to make in order to visit some asteroids that are near the Earth. To achieve this, a low-thrust propulsion system will be used, which is inherently more complex to analyse due to the weak forces and the long actuation times. On the other hand, these characteristics allow great freedom in the choice of trajectory, allowing the implementation of optimisation techniques to find the best one. After a brief reminder of the principles of orbital mechanics, the preliminary selection of asteroids in the solar system will be discussed, which excludes the most difficult bodies for a probe to reach, in order to focus on missions to objects in near-earth space. The chapters that follow outline the theory of space trajectory optimisation, reporting on high-level logic flows. The last chapters focus on the calculations performed, in particular describing the algorithm that was used, the analysis of asteroids trajectories and the results obtained from the implemented optimisation processes.

1.2 Spacecraft trajectory Optimisation

Optimisation of space trajectories can be defined as the search for the control law for which a particular parameter, known as the *performance index*, is optimised and the imposed constraints are met. The control law describes the time evolution of the thrust in modulus and direction. It is possible to apply this control law to a model of equations describing the motion of the spacecraft, and the result is, after numerical integration, an optimal trajectory that satisfies the boundary conditions, the initial conditions and those along the trajectory itself, which may be integral functions over the mission time (or on the entire trajectory) or values at a precise instant, very often the final one of the path.

Optimisation of trajectories for space missions, especially long-distance ones, is of key importance because it is closely linked to propellant consumption: following a non-optimal trajectory means allocating more mass for the propellant, which leads to a greater vehicle mass at departure with an increase in the overall cost of putting into orbit and mission time. A non-optimal trajectory also means carrying less payload for the same cost, a situation that is equally undesirable.
Optimisation of trajectories does not have an unambiguous path. There are different mathematical models that can be used, each of which may correspond to a different objective, hence a different performance index. Different approaches can also be used, in which different methods, techniques and algorithms can be followed. It is clear that each of these approaches has its own disadvantages and advantages, so it is necessary to make an accurate choice that is justified by the desired result.

1.3 Fundamentals of space propulsion

There are two main energy sources for space propulsion: chemical and electrical. Chemical propulsion is not very well suited to optimisation calculations because very often the thrust involved is so great that manoeuvres can be regarded as impulses, that is, as abrupt changes in the vehicle's speed at a certain fixed position at a given time. An impulsive manoeuvre can be optimised in terms of the direction and modulus of the thrust and by choosing the right moment at which to execute it. Very often this does not require numerically complex calculations, but it is also possible to arrive at the optimum analytically, take the Hohmann's transfer for example.
For optimal low-consumption trajectories, electric propulsion is used in its three forms: electro-thermal propulsion, electrostatic propulsion and electromagnetic propulsion. The most suitable propulsion for the mission analyzed in this thesis is electrostatic propulsion due to the orders of magnitude of specific impulse, thrust and power used. The specific impulse can be defined as:

$$I_{sp} = \frac{T}{\dot{m}_p \cdot g_0} \tag{1.1}$$

with T, thrust of the system, $\dot{m}_p$ propellant flow rate and g_0 acceleration of gravity at sea level. If the flow rate is fixed, a propellant with a higher specific impulse is capable of producing more thrust than one with a lower value, that means it has an higher performance. A clear comparison of the different propulsion techniques can be seen in Fig. 1.1: it is evident that electric propulsion is the one with by far the greatest specific impulse, but the accelerations produced are 3 to 8 orders of magnitude lower than those generated by chemical propulsion. This is because chemical propulsion exploits the energy released by a reaction, typically combustion, and accelerates the gases produced in a nozzle. This implies a flow rate of expelled propellant on the order of hundreds of kg/s, which then produces a considerable force, despite lower efficiencies. This allows achieve short but very intense ignitions. Electric propulsion uses an external source of energy. This results in a substantial independence between flow and power, so you can either increase one and have lower specific energy, hence higher thrusts at low efficiencies, or increase the other and have a very energetic propellant, which leads to high efficiencies and low thrusts. The first

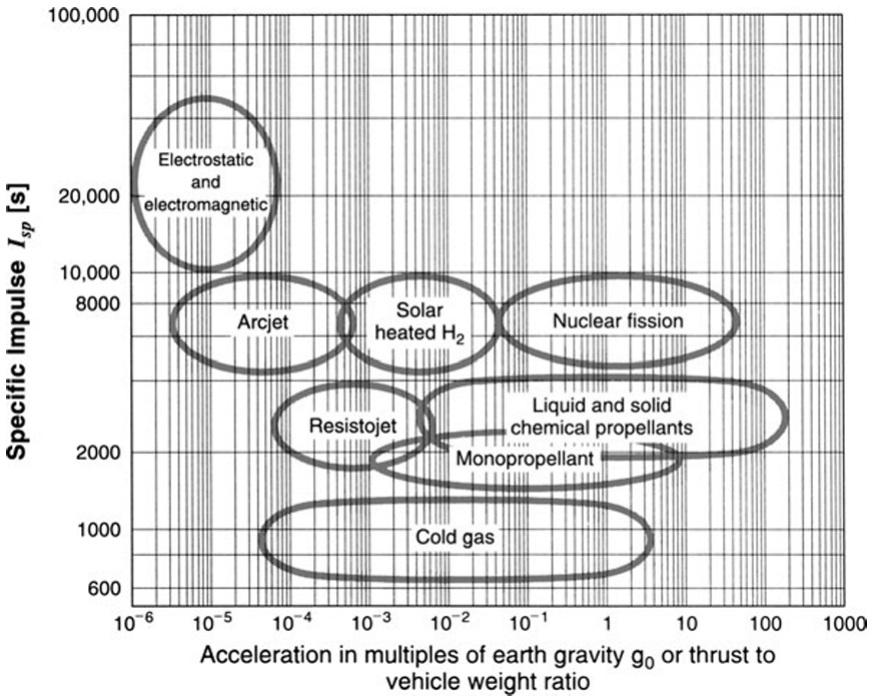

Figure 1.1: Specific impulse and specific thrust of different propulsion systems. [1]

case is unimportant for the purposes of this thesis, because it could be achieved more easily and effectively with chemical propulsion, the second is the peculiarity of electric propulsion that is exploited. This does not allow electric propulsion to be used for the manoeuvre of ascension and exit from the atmosphere, but it proves to be of excellent use for missions that require a large propulsive effort after insertion into orbit, i.e. interplanetary transfers or to geostationary orbits, *sample & return* missions or multiple flybys.
The reduced propulsive force also becomes an advantage when trying to achieve an optimal trajectory as it allows a very precise manoeuvre and allows the thrust to be shaped in the most appropriate manner to achieve the desired objective.
However, there are many disadvantages associated with this technology: they arise from the small control authority of the thruster, which could become critical at certain stages of the mission as perturbations could be orders of magnitude equal to to the thrust, if not larger. Furthermore, small thrusts give small accelerations, which in turn lead to very long manoeuvre times compared to impulsive manoeuvres with chemical propulsion. Considering that the mission time is directly proportional to the vehicle's handling time by a Mission Control Centre, this could increase mission costs considerably.
Mathematically, a manoeuvre with electric propulsion must be treated as a trajectory in which not only the force of gravity but also the propulsive force acts a large part of the time. The thrust varies from instant to instant generally in modulus (very often discontinuously) and direction, so that the known term of the differential equations is non-zero and generally time-dependent. Another mathematical complication arises from

the small modulus of the thrust, which only slightly modifies the trajectory. Very small time integration steps are therefore required, which increases the computational cost of the problem. The continuity of the thrust, although it generates all the problems mentioned, is precisely the characteristic that makes trajectory optimisation possible and drastically decreases propellant consumption.

1.4 Workflow

The work process is basically divided into three steps:

1. Selection of asteroids;
2. Optimisation of a trajectory;
3. Analysis of results.

1.4.1 Pre-selection of asteroids

It is necessary, before carrying out any optimisation, to make a pre-selection of the asteroids in order to find the most easily reachable ones and the points on their trajectory where it is possible to arrive with the least possible expense. This makes it possible to choose candidate asteroid classes for the mission under consideration.
In order not to have excessive propellant consumption, it is intuitive that the vehicle must stay within the ecliptic, as changes in inclination are very costly due to the very high orbital velocity of the Earth around the Sun. In addition, efforts must be made to reduce displacements, both in terms of radius and right ascension relative to the Earth. The chosen asteroids will therefore pass very close to the Earth and the vehicle will intercept them at the ascending or descending node of its orbit. In the case of low inclination, any point in the orbit is a good meeting point if close enough to the Earth, but it is preferred to meet the asteroid at one of the apses to reduce the velocities relative to the passage.
The asteroid selection process will be explored in more detail in 3.3.

1.4.2 Optimisation of a trajectory

The optimisation process can be divided into four main sections, as described in fig. 1.2:

1. Definition of the mathematical **model** describing the system dynamics;
2. Definition of the appropriate **objectives**;
3. Development of an **approach**;
4. Achievement of the **solution**.

The first step is necessary not only for optimisation, but for every orbital mechanics problem. It consists in understanding the dynamics of the system in which one is moving and choosing the mathematical model that describes it. In other words, it consists in

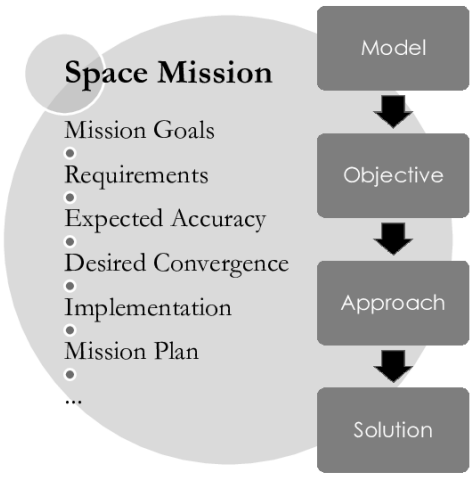

Figure 1.2: Steps for a space trajectory optimisation process [2]

defining the state vector, which unambiguously indicates the state of the system and the respective differential equations of motion of the spacecraft, as well as the control vector with which the thrust influences the dynamics.
The second step concerns the choice of mission objectives, in particular the objectives according to which the vehicle's trajectory is to be optimised. This is operationally done by defining a cost function, which consists of a parameter or combination of parameters that one wants to keep as low or as high as possible. We basically have two categories for this step, one according to the type of objectives and a second one according to the number of objectives.
The third step is represented by the methods and techniques employed to solve the trajectory design problem. In this phase, two main ways are possible, which are the analytical and numerical approaches. The analytical approach is mainly based on the theory of optimal control, which will be central in this work. Optimal control theory, which is the theory that determines the time-dependent control vector such that the constraints are met and the cost is minimised, derives the equations underlying optimisation, although the treatment in itself is fully analytical, this does not imply that the approach is analytical, in fact indirect methods are based on numerical integration of these analytical equations. The numerical approach does not involve analytical functions and is divided into methods: *direct methods*, which find the minimum of the cost function directly by means of non-linear programming, starting from the state and control vectors appropriately discretized in time, and *indirect methods*, which involve analytically deriving the necessary conditions for the optimum, from which other variables and equations emerge, known as 'additions', and transform the optimisation problem into an boundary condition problem solvable by numerical integration that can be solved by numerical integration in time and Newton's method. The latter is based on Pontryagin's principle.
The fourth and final step is to solve the problem formulated in the previous steps. If

the developed approach is an analytical one, the solution will likely be a closed-form analytical solution, otherwise, if the numerical approach is adopted, the problem will be an optimisation problem, thus needing a numerical algorithm to get the solution. However, most of the optimisation problems are solved by a numerical technique. The numerical approach is the most used for space trajectories, because they are too complex and inherently non-linear to present a solution in closed form. The analytical approach can only be used if stringent assumptions are made or under specific conditions that severely limit the conformity of the solution found with the real one. Which will be discussed in more detail in Chapter 6.

Chapter 2

Fundamentals of Astrodynamics

This chapter presents a brief overview of the essential theoretical concepts on which the physics of the problem analysed in the thesis is based. The fundamentals law governing the motions of spacecrafts and planets and the main elements used in the definition of orbits will be described. Finally, concepts related to propulsion will be introduced in order to present the main characteristics of orbital manoeuvres. For the drafting of the chapter, the following were used [3], [4].

In the following sections, the notation in bold will indicate a vector, while the same non-bold symbol indicates its modulus, e.g. $|\mathbf{r}| = r$.

2.1 Introduction to astrodynamics

2.1.1 Kepler's Law of planetary motion

First Law: *The orbit of each planet is an ellipse, with the sun at a focus.* **Second Law**: *The line joining the planet to the sun sweeps out equal areas in equal times.* **Third Law**: *The square of the period of a planet is proportional to the cube of its mean distance from the sun.*

2.1.2 Universal law of gravitation

The starting point of mechanics of celestial bodies was given by Isaac Newton who formulated the law of universal gravitation, which states that:

> *Given two material points M and m located at two distinct points in space and separated by a distance r, they attract each other along their conjuction with a force proportional to the product of their masses and inversely proportional to the square of their distance:*

$$F = G\frac{M \cdot m}{r^2} \tag{2.1}$$

where $G = 6.673 \cdot 10^{-11} m^2 kg^{-1} s^{-2}$ *is the universal gravitational constant.*

The law can be written in vector terms defining the vector $\mathbf{r}$ as the distance between M and m. The force exerted by M on m is:

$$\mathbf{F} = -G\frac{M \cdot m}{|\mathbf{r}|^3}\mathbf{r} \tag{2.2}$$

The negative sign indicates that the gravitational force is attractive and it moves m towards M, in an opposite direction to $\mathbf{r}$.
In real cases the two masses are not point-like, nevertheless the law can be applied also to bodies with spherical symmetry and bodies of any shape as long as their distance is greater than their characteristic size.

2.1.3 The N-Body Problem

Given a spacecraft travelling in space, it is subject at each instant to N different gravitational forces from N different bodies with different gravitational masses (fig. 2.1). Other forces may be present on the spacecraft such as thrust, drag or pressure produced by solar radiation, but they are neglected in the discussion.

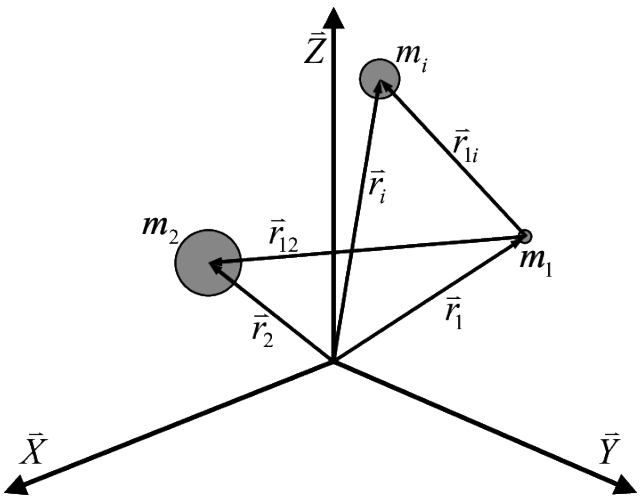

Figure 2.1: The N-Body problem [2]

Considering a system, in an Euclidean space, of N-bodies (m_1, m_2, m_3, ..., m_n) one of which is the body whose motion we wish to study, the following assumptions are made:

- The bodies are spherically symmetric. This allows to treat the bodies as though their masses were concentrated at their centers.
- Masses are constant over time.
- There are no external nor internal forces acting on the system other than the gravitational forces which act along the line joining the centers of the two bodies.

Assuming an inertial reference frame centered at any point O, the force that body n exerts on body i can be written as:

$$\mathbf{F}_{in} = -G\frac{m_n \cdot m_i}{r_{ni}^3}\mathbf{r}_{ni} \tag{2.3}$$

with $n \neq i$ and $\mathbf{r}_{ni} = \mathbf{r}_i - \mathbf{r}_n$. The resultant will be:

$$\mathbf{F}_i = -\sum G\frac{m_n \cdot m_i}{r_{ni}^3}\mathbf{r}_{ni} \tag{2.4}$$

Merging the equation above with Newton's second law and making the relative distances explicit, the following formulation is found:

$$\ddot{\mathbf{r}}_{ij} = -G\frac{(m_i + m_j)}{r_{ij}^3}\mathbf{r}_{ij} - \sum_{n\neq i, m\neq j} Gm_n\left(\frac{\mathbf{r}_{nj}}{\mathbf{r}_{nj}^3} - \frac{\mathbf{r}_{ni}}{\mathbf{r}_{ni}^3}\right) \tag{2.5}$$

The first member of the equation indicates the force between two bodies and the other one indicates the gravitational disturbances of the other bodies. It is possible to write $n-1$ differential vector equations of this type. They are second order differential equations, all coupled together. They can not be solved analytically but only numerically.

2.1.4 The two-body problem

The N-body problem can be simplified to a system consisting of only two bodies, in the case in which two bodies are much closer to each other than to the rest of the bodies present in the universe.
The result is the same equation of the N-body problem where the summation term disappears.

$$\ddot{\mathbf{r}}_{ij} = -G\frac{(m_i + m_j)}{r_{ij}^3}\mathbf{r}_{ij} \tag{2.6}$$

If one of the two bodies is much smaller than the other, the two-body problem becomes a *restricted two-body problem*. The force exerted by the small body on the large body is very small and can be neglected. A reference frame centered in the larger body is inertial and relative distance becomes absolute distance. The differential equation changes to:

$$\ddot{\mathbf{r}} = -G\frac{M + m}{r^3}\mathbf{r} \tag{2.7}$$

Considering $M \gg m$, the equation becomes:

$$\ddot{\mathbf{r}} = -G\frac{M}{r^3}\mathbf{r} \tag{2.8}$$

It is possible to define the gravitational constant of the bigger body as $\mu = GM$.

2.1.5 Constants of the motion

The gravitational field is conservative and radial, so an object moving under the influence of gravity alone does not lose or gain mechanical energy but only exchanges one form of energy, *kinetic*, for another form called *potential energy*. Since the gravitational field is radial, the angular momentum of the satellite about the center of the reference frame (the large mass) does not change.

Conservation of Mechanical Energy

The energy constant of motion can be derived with a scalar multiplication between the motion equation and the velocity $\dot{\mathbf{r}}$:

$$\dot{\mathbf{r}} \cdot \ddot{\mathbf{r}} + \frac{u}{r^3}\dot{\mathbf{r}}\mathbf{r} = 0 \tag{2.9}$$

From which it is possible to obtain:

$$\frac{d}{dt}(\frac{V^2}{2} - \frac{\mu}{r}) = 0 \tag{2.10}$$

If the derivative is equal to zero, that means the function to be derived is constant in time. This function is the specific mechanical energy. The integration constant of the potential energy is taken to be zero at infinite radius, so it is zero.

Conservation of angular momentum

The angular momentum constant of the motion can be obtained by cross multiplying the motion equation with $\mathbf{r}$:

$$\mathbf{r} \times \ddot{\mathbf{r}} + \mathbf{r} \times \frac{\mu}{r^3}\mathbf{r} = 0 \tag{2.11}$$

In general $\mathbf{r} \times \mathbf{r} = 0$, the second term vanishes and using the product rule of differential calculus it is possible to obtain the following equaion:

$$\frac{d}{dt}(\mathbf{r} \times \dot{\mathbf{r}}) = 0 \tag{2.12}$$

The expression $\mathbf{r} \times \dot{\mathbf{r}}$ is the vector $\mathbf{h}$, called *specific angular momentum*. Since $\mathbf{h}$ is the vector cross product of $\mathbf{r}$ and $\mathbf{v}$ it must always be perpendicular to the plane containing $\mathbf{r}$ and $\mathbf{v}$, but $\mathbf{h}$ is a constant vector so $\mathbf{r}$ and $\mathbf{v}$ must always remain in the same plane. Therefore, it is possible to conclude that the satellite's motion must be confined to a plane which is fixed in space, called *orbital plane*.

2.1.6 The Trajectory Equation

It is possible to easily obtain a partial solution which will tell us the size and shape of the orbit. The complete solution with an explicit time dependence is difficult to derive because it requires a double integration.
By cross multiplying the equation of motion by the angular momentum $\mathbf{h}$, we arrive at the equation:

$$\ddot{\mathbf{r}} \times \mathbf{h} = \frac{\mu}{r^3} \tag{2.13}$$

In a few step, the equation becomes:

$$\frac{d}{dt}(\dot{\mathbf{r}} \times \mathbf{h}) = \frac{d}{dt}(\mu\frac{\mathbf{r}}{r}) \tag{2.14}$$

Integrating the above equation, appears a vector integrative constant **B** and deriving the radius in modulus:

$$r = \frac{\frac{h^2}{\mu}}{1 + \frac{B}{\mu}\cos\nu} \tag{2.15}$$

where ν is the angle between the vector **B** and the radius. $\frac{B}{\mu}$ shall be smaller than 1, in order to guarantee the existance of the solution. It is important to notice that when the angle ν is zero, the radius is minimal, when ν is equal to π, the radius is maximum. Equation 2.15 is the trajectory equation expressed in polar coordinates. To determine the type of curve it represents, is necessary to compare it to the general equation of a conic section written in polar coordinates:

$$r = \frac{p}{1 + e\cos\nu} \tag{2.16}$$

In the above equation, p is a geometrical constant of the conic called *semilatus rectum*, e is the eccentricity and it determines the type of conic section represented by the equation. It can be concluded that:

1. The family of curves called conic sections, i.e. circle, ellipse, parabola, hyperbola, represents the only possible paths for an orbiting object in the two-body problem.
2. The focus of the conic orbit must be located at the center of the central body.
3. The mechanical energy of a satellite does not change as the satellite moves along its conic orbit.
4. The orbital motion takes place in a plane which is fixed in inertial space.
5. The specific angular momentum of a satellite about the central attracting body remains constant.

2.1.7 Types of orbits

The name *conic* derives from the fact that a conic section may be defined as the curve of intersection of a plane and a right circular cone. All orbits have a symmetry and two foci, for the circle the two foci are coincident in the centre, for ellipse and hyperbola, the two foci are separated and for the parabola one of the foci is at infinite distance. The parabolic orbit represents a boundary between closed and open orbits and it is the minimum energy orbit to escape the gravitazional influence of a body. In an orbit is possible to define fundamental geometric quantities:

- Semilatus rectum p: half width of the curve at the focus.
- Semi-major axis a: half of the length of the chord passing through the foci.
- Focal distance c: distance between the two foci.
- Semi-minor axis b: half of the length of the chord passing through the center of the curve.

With the quantities above is possible to obtain other quantities:

$$e = \frac{c}{a} = \sqrt{1 + \frac{2Eh^2}{\mu^2}}$$

$$p = a(1 - e^2)$$

$$r_{min} = \frac{p}{1 + e} = a(1 - e)$$

$$r_{max} = \frac{p}{1 - e} = a(1 + e)$$

Elliptical orbit

The orbit of all planets in the solar system is elliptical, is a closed curve with a constant period. An elliptical orbit has the following properties:

$$r + r' = 2a$$

The sum of the radii of each point from the two foci is constant. In addition, the radii of the apsides are so connected:

$$r_a - r_p = 2c$$

$$e = \frac{2c}{2a} = \frac{r_a - r_p}{r_a + r_p}$$

The period of an elliptical orbit is equal to:

$$T = 2\pi\sqrt{\frac{a^3}{\mu}}$$

Circular orbit

In a circular orbit, the two foci are coincident and the eccentricity is zero. The above equations for the elliptical orbit are valid also for the circular one, with the difference that the radius is constant and equal to the semi-major axis of the orbit. The circular velocity of the orbit is equal to:

$$V_c = \sqrt{\frac{\mu}{r_c}}$$

Parabolic orbit

The parabolic orbit is characterised by one of the two foci at infinite distance and eccentricity equal to 1. It is a very rare orbit to find in nature. It is an open orbit with:

$$p = 2r_p$$

with r_p periapsis radius. The parabolic orbit has a characteristc velocity that is the escape velocity, which is the minimum velocity that a body must have at a given radius in order

to escape the sphere of influence[1] of the central body. When the radius tends to infinity, the velocity tends to zero, so the overall energy of the parabolic orbit is zero.

$$V_{esc} = \sqrt{\frac{2\mu}{r}} = \sqrt{2}V_c$$

Hyperbolic orbit

The hyperbolic orbits are characterised by positive energy, which means that at infinite radius the velocity is not equal to zero, and the velocity is hyperbolic excess velocity. An hyperbolic orbit has two arms, that are asymptotic to two intersecting straight lines (the asymptotes). Only one of the two arms has physical significance. The semi-major axis, the distance between the foci and the semi-minor axis have negative values: the semi-major axis is the distance between the two periapses.

$$c^2 = a^2 + b^2$$

In this case, the eccentricity is bigger than 1 and it determines the slope of the asymptotes using the formula:

$$\frac{1}{e^2} = \cos^2 \phi$$

2.1.8 Position and velocity as a function of time

Knowledge of the shape of an orbit is not sufficient to study the motion of a body, because as it may often be appropriate to know the position of the body at different time instants. To do this, is necessary to solve the equation 2.8. For the conservation of angular momentum it is possible to write:

$$\dot{\nu} = \frac{h}{r^2} \tag{2.17}$$

From Kepler's second law, we know that the areolar velocity is constant, and for a circle:

$$\frac{dA}{dt} = \frac{R}{2}\dot{\nu} = \frac{h}{2} \tag{2.18}$$

For an ellipse we obtain the same result, so:

$$T_p = 2\frac{A_{ellipse}}{h} \tag{2.19}$$

From which, knowing the expression for the area of the ellipse, it is possible to derive the period formula.
The time to travel a certain distance in an orbit from any initial point to any final point is calculated by subtraction between the time to reach the final point from the periapsis and

[1]The sphere of influence of a planet is the oblate-spheroid-shaped region around a celestial body where the primary gravitational influence on an orbiting object is that body.

the time to reach the initial point from the periapsis, $t_{12} = t_2 - t_1 = (t_2 - t_p) - (t_1 - t_p)$. From Kepler's second law, we can write that:

$$t_i = \frac{A_i}{A_{tot}} T_p \tag{2.20}$$

The resolution problem consists of determing A_i as a function of the true anomaly ν. An auxiliary circle is employed to solve the problem, as reported in fig. 2.2. The angle E between the radius from the center to the point Q on the circle and the major axis is the *eccentric anomaly*. From analytical geometry, the equations of the curves in cartesian coordinates are:

$$\text{Ellipse: } \frac{x^2}{a^2} + \frac{y^2}{b^2} = 1 \quad \text{Circle: } \frac{x^2}{a^2} + \frac{y^2}{a^2} = 1 \tag{2.21}$$

From which it is possible to arrive to $y_{ellipse} = \frac{b}{a} y_{circle}$

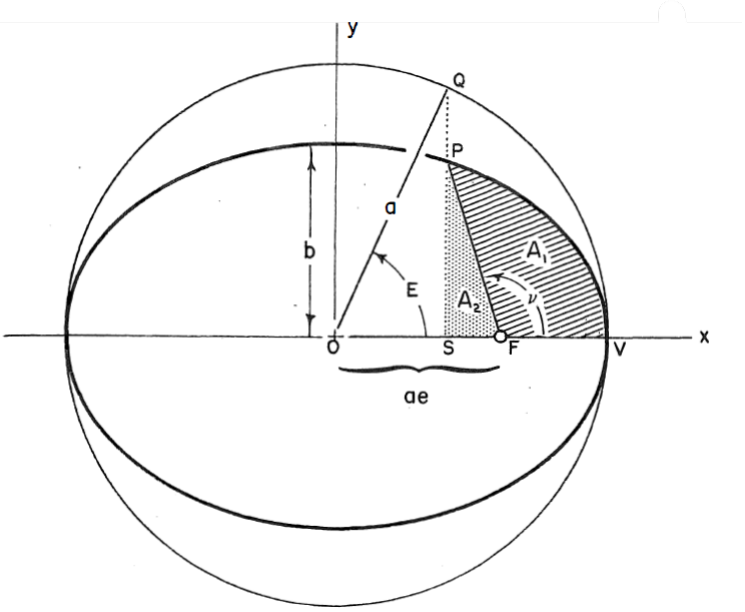

Figure 2.2: Eccentric Anomaly, E [3]

From figure 2.2 we note that the area swept out by the radius vector is Area PSV minus the dotted area, A_2.

$$A_1 = AreaPSV - A_2 \tag{2.22}$$

The area of triangle A_2 can be calculated as:

$$A_2 = \frac{ab}{2}(e \sin E - \cos E \sin E) \tag{2.23}$$

Area-PSV is the area under the ellipse; it is bounded by the dotted line and the major axis. Area-QSV is the corresponding area under the auxiliary circle. From the relationship

between circle and ellipse found above, it is possible to write:

$$AreaPSV = \frac{b}{a}(AreaQSV) \tag{2.24}$$

The area QSV is the area of sector QOV minus the triangle. Hence

$$AreaPSV = \frac{ab}{2}(E - \cos E \sin E) \tag{2.25}$$

Substituting into the expression for area A_1 yields

$$A_1 = \frac{ab}{2}(E - e \sin E) \tag{2.26}$$

The time t_i can be written as:

$$t_i = \sqrt{\frac{a^3}{\mu}}(E_i - e \sin E_i)$$

where $M = (E_i - e \sin E_i)$ is called the *mean anomaly*. The time from the start point to the final point is:

$$t_{21} = \sqrt{\frac{a^3}{\mu}}(E_2 - e \sin E_2 - E_1 + e \sin E_1)$$

In order to use the above equations is necessary to relate the eccentric anomaly, E, to its corresponding true anomaly, ν.

$$\cos E = \frac{ae + r \cos \nu}{a} \tag{2.27}$$

Introducing the radius equation, we obtain:

$$\cos E = \frac{e + \cos \nu}{1 + e \cos \nu} \tag{2.28}$$

The correct quadrant for E is obtained by noting that ν and E are always in the same half-plane; when ν is between 0 and π, so is E. The discussion just concluded can also be generalised to circumferences, where true and eccentric anomaly are the same, and for open orbits.

2.2 Coordinate systems and time measurements

2.2.1 Coordinate systems

The first requirement for describing an orbit is a suitable inertial reference frame. In the case of orbits around the sun such as planets, asteroids, comets and deep-space probes, the heliocentric-ecliptic coordinate system is convenient. For satellites of the earth is used the geocentric-equatorial system. To describe a reference frame we need:

- The origin of the reference frame;
- The orientation of the fundamental plane X-Y;
- The principal direction, which means the direction of the X axis;
- The direction of the Z-axis, perpendicular to the fundamental plane.

The Y-axis is always chosen so as to form a right-handed set of coordinate axes.

The Heliocentric-Ecliptic Coordinate System

The heliocentric-ecliptic system has its origin at the center of the sun. The fundamental plane coincides with the *ecliptic* which is the plane of the earth's revolution around the sun. The line of intersection of the ecliptic plane and the earth's equatorial plane defines the direction of the γ axis as shown in figure 2.3. On the first day of spring a line joining the center of the earth and the center of the sun points in the direction of the positive γ axis. That is called the vernal equinox direction. The earth wobbles slightly and its axis of rotation shifts in direction, about 50 arcseconds per year. This effect is known as precession. As a result the heliocentric ecliptic system is not really an inertial reference frame but in this thesis the duration of the missions will be a maximum of 2 or 3 years, too short to be affected by the phenomenon just described.

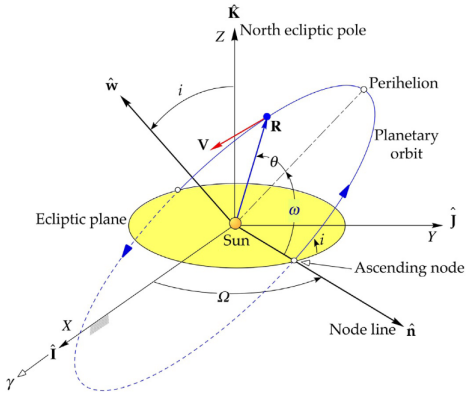

Figure 2.3: Heliocentric-Ecliptic coordinate system [4]

The Geocentric-Equatorial Coordinate System

The geocentric-equatorial system has its origin at the earth's center. The fundamental plane is the equator and the positive X-axis points in the vernal equinox direction. The Z-axis points in the direction of the north pole. The system is not fixed to the earth and turns with it; rather, the geocentric-equatorial frame is nonrotating with respect to the stars and the earth turns relative to it.

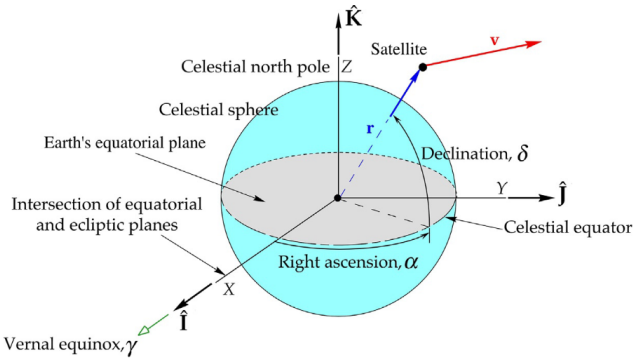

Figure 2.4: Geocentric-equatorial coordinate system [4]

The Perifocal Coordinate System

The perifocal coordinate system is really useful for describing the motion of a satellite. The fundamental plane is the plane of the satellite's orbit. The p-axis points toward the periapsis; the q-axis is rotated 90° in the direction of orbital motion and lies in the orbital plane, the w-axis along **h** completes the right-handed perifocal system.

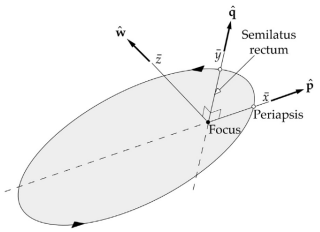

Figure 2.5: Perifocal Frame [4]

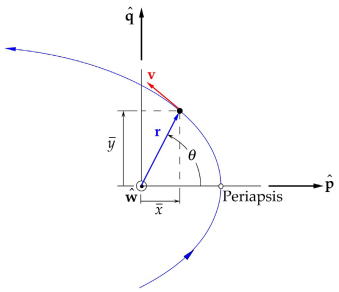

Figure 2.6: Position and velocity relative to the perifocal frame. [4]

2.2.2 Time Measurements

In astrodynamics there are two measures of time: *solar time* and *sidereal time*. The time between two successive upper transits of the sun across our local meridian is called an *apparent solar day*. The earth has to turn through slightly more than one complete rotation on its axis relative to the fixed stars during this interval. The reason is that the earth travels about 1/365th of the way around its orbit in one day. A *sidereal day* consisting of 24 sidereal hours is defined as the time required for the earth to rotate once on its axis relative to the stars. This occurs in about 23 hours, 56 minutes and 4 seconds of ordinary solar time. The two measures are reported in table 2.1. Two types of time can

	Sidereal Time	Solar Time
24 sidereal hours	24h 00m 00s	23h 56m 04s
1 sidereal day	1 day	0.997 days
24 solar hours	24h 03m 56s	24h 00m 00s
1 solar day	1.00274 days	1.00000 day

Table 2.1: Sidereal and solar time.

be distinguished on a revolution: tropical year and sidereal year. The sidereal year is based on a complete rotation, the tropical year is based on the time between two vernal equinoxes. This is because due to the precession of equinoxes, 50 fewer arcseconds are travelled between two spring equinoxes, equivalent to 18 solar minutes, as reported in table 2.2. The difference between the tropical and sidereal year is the reason because there are

Sidereal Year	Tropical Year
365dd 06h 09min 10s	365dd 05h 18min 46s

Table 2.2: Sidereal and tropical year.

two calendars: Julian calendar and Gregorian calendar. The Gregorian calendar is the one used today, as it takes into account the 5 hours and 48 minutes deviation from the usual 365 days of the year. The main differences are reported in table 2.3.

	Julian Calendar	Gregorian Calendar
Cycle (years)	4 years	400 years
Cycle (days)	1461 days	146097 days
Deviation from Sidereal year	1 day / 128 years	1 day / 3323 years
Deviation from Tropical year	0.0278days / year	0.003days / year

Table 2.3: Julian and Gregorian Calendar.

An important moment in the time reference system is the J2000, defined at noon of January 1, 2000. This date is the 2451545th day of the Julian calendar and at this moment are defined the axis directions of the ECI J2000 reference frame. In order to reduce the

order of magnitude of a Julian Date, the Modified Julian Date (MJD) is used. A Modified Julian Date is a Julian Date decreased by 2400000.

2.3 Coordinate Transformations

In astrodynamics is useful to use a coordinate transformation to simplify some calculations, transforming vector quantities from one coordinate system to another. Imagine we want to rotate a triplet of versors (**i**, **j**, **k**) by an α angle along the k-axis. The resulting versors are:

$$\begin{bmatrix} \mathbf{u} \\ \mathbf{v} \\ \mathbf{w} \end{bmatrix} = \begin{bmatrix} \cos\alpha & \sin\alpha & 0 \\ -\sin\alpha & \cos\alpha & 0 \\ 0 & 0 & 1 \end{bmatrix} \begin{bmatrix} \mathbf{i} \\ \mathbf{j} \\ \mathbf{k} \end{bmatrix} \tag{2.29}$$

The 3x3 matrix is the representation of the equations on the directions of the rotated vectors and is called the rotation matrix. It is possible to write the rotations along the other axes:

$$L_1 = \begin{bmatrix} 1 & 0 & 0 \\ 0 & \cos\alpha & \sin\alpha \\ 0 & -\sin\alpha & \cos\alpha \end{bmatrix} \quad L_2 = \begin{bmatrix} \cos\alpha & 0 & -\sin\alpha \\ 0 & 1 & 0 \\ \sin\alpha & 0 & \cos\alpha \end{bmatrix} \tag{2.30}$$

Matrices are orthogonal, so their inverse is equal to their transpose. Note that for successive rotations around different axes, the matrices are simply multiplied by replacing the input vector of one rotation with the output vector of the previous rotation. It is important to remember that the order in which the matrices are multiplied is relevant since matrix multiplication is not commutative. The angle through which one frame must be rotated to bring its axes into coincidence with another frame are commonly referred to as *Euler angles*. A maximum of three Euler angle rotations is sufficient to bring any two frames into coincidence.

2.4 Classical Orbital Parameters

In astrodynamics, five indipendet quantities called *orbital parameters* are sufficient to completely describe the size, shape and orientation of an orbit. A sixth element is required to pinpoint the position of a satellite along the orbit at a particular time. The classical set of six orbital elements, fig. 2.7, are defined as follows:

- a, *semi-major axis*: a constant defining the size of the conic orbit;
- e, *eccentricity*: a constant defining the shape of the conic orbit;
- i, *inclination*: angle between the **K** vector and the angular momentum, **h**;
- Ω, *longitude of the ascending node*: the angle between the **I** vector and the point where the satellite crosses through the fundamental plane in a northerly direction (ascending node);

- ω, *argument of periapsis*: the angle between the ascending node and the periapsis point, measured in the direction of the satellite's motion;
- $\nu(t)$, *true anomaly*: the angle between the radius of the orbiting mass at time t *(r(t))* and the periapsis direction (θ in fig. 2.7).

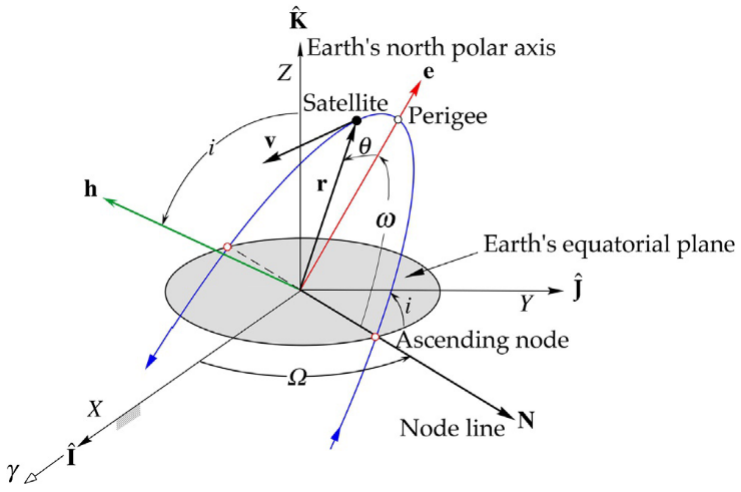

Figure 2.7: Classical orbital parameters

The list of six orbital elements defined above is by no means exhaustive, there are situations in which one or more parameters can be indeterminate:

- If the inclination is zero, Ω and ω can not be determined, an additional parameter Π is used, called *longitude of periapsis*, angle from **I** to periapsis.
- If the eccentricity is zero, ω and ν can not be determined, an additional parameter u is used, called *Argument of latitude*.
- If both eccentricity and inclination are zero, Ω, ω and ν can not be determined, an additional parameter l is used, called *True longitude at epoch*.

2.4.1 Determining the orbital elements from r and v

Assuming that a ground station on the earth is able to provide the vectors **r** and **v** representing the position and the velocity of a satellite relative to the geocentric-equatorial reference frame ata a particular epoch, it is possible to obtain the eccentricity vector through the formula:

$$\frac{\mathbf{B}}{\mu} = \frac{\mathbf{v} \times \mathbf{h}}{\mu} - \frac{\mathbf{r}}{r} = \mathbf{e} \tag{2.31}$$

From **r** and **v**, we can obtain the angular momentum and the specific energy of the orbit, from which a and p can be derived. The other parameters can be obtained with the

following equations:

$$\Omega = \arccos\left(\frac{\mathbf{I}\cdot(\mathbf{K}\times\mathbf{h})}{|\mathbf{K}\times\mathbf{h}|}\right) \quad \omega = \arccos\left(\frac{(\mathbf{K}\times\mathbf{h})\cdot\mathbf{P}}{|\mathbf{K}\times\mathbf{h}|}\right)$$

$$i = \arccos\left(\frac{\mathbf{K}\cdot\mathbf{h}}{|\mathbf{h}|}\right) \quad \nu = \arccos\left(\frac{\mathbf{r}}{|\mathbf{r}|}\cdot\mathbf{P}\right)$$

with **P** direction of periapsis and **I**,**J** and **K** cartesian axes of the reference frame considered.

2.4.2 Determining r and v from the orbital elements

It is assumed that all six orbital parameters are known and we want to calculate the position and velocity of the orbiting body. In the perifocal coordinate system, the position can be written as:

$$\mathbf{r} = r\cos\nu\mathbf{p} + r\sin\nu\mathbf{q} \tag{2.32}$$

with the modulus of r equal to:

$$r = \frac{p}{1 + e\cos\nu} \tag{2.33}$$

To obtain the velocity vector is necessary to differentiate the position vector, assuming the perifocal system as inertial.

$$\dot{\mathbf{r}} = \mathbf{v} = (\dot{r}\cos\nu - r\dot{\nu}\sin\nu)\mathbf{p} + (\dot{r}\sin\nu + r\dot{\nu}\cos\nu)\mathbf{q} \tag{2.34}$$

That can be written as:

$$\mathbf{v} = \sqrt{\frac{\mu}{p}}(-\sin\nu\mathbf{p} + (e + \cos\nu)\mathbf{q}) \tag{2.35}$$

2.5 Orbital manoeuvres

Orbital manoeuvres are performed to change one or more orbital parameters. During manoeuvres, propulsive forces are applied to the spacecraft, implying a change in vehicle mass with the ejection of a mass $\dot{m}_p$. In this section, some impulsive manoeuvres will be reported which, although not those performed by the spacecraft, are very important because they explain in a simplistic way what happens when a thrust is applied in a certain direction.

2.5.1 Manoeuvre cost and propulsion parameters

For an impulsive manoeuvre, using Tsiolkovsky's *rocket equation*, it can be seen that the input of the manoeuvre is a required change in velocity ΔV and the output for this to occur is a certain energy expended by the thruster. For impulsive manoeuvres, it is possible to approximate the position as constant during manoeuvring, which is not possible in the case of continuous manoeuvre.
The cost of the manoeuvre is the energy required to achieve the desired change in velocity, which will be directly proportional to the fuel consumption of the manoeuvre.

Some fundamental quantities are now introduced: ejected propellant flow rate $\dot{m}_p$ and thrust T are related to the *effective exhaust velocity* c, which represents the velocity at which the propellant is expelled from the nozzle under the assumption of zero external pressure.

$$T = \dot{m}_p \cdot c \tag{2.36}$$

Another important parameter is the *total impulse* I_t, which takes into account all thrust contributions during a time interval, typically from the initial instant of thruster ignition t_0 to the final instant t_f:

$$I_t := \int_{t_0}^{t_f} T\, dt \tag{2.37}$$

However, the total impulse is only related to the thrust obtained and does not take into account the propellant consumption required to obtain it. In order to be able to make a more balanced comparison, the specific impulse is defined:

$$I_{sp} := \frac{I_t}{m_p g_0} = \frac{T}{\dot{m}_p g_0} = \frac{c}{g_0} \quad [s] \tag{2.38}$$

with m_p the available fuel mass.
It is possible now to write the Tsiolkovsky's *rocket equation*:

$$\frac{m_f}{m_i} = \exp\left(-\frac{\Delta V}{c}\right) \tag{2.39}$$

This equation is of essential importance for the study of space propulsion: given a type of propulsion and a certain amount of fuel, what is the achievable ΔV? Or, given what is the value of ΔV needed to perform a certain manoeuvre, how much propellant is needed to perform it?
The second question is closely related to the work addressed in this thesis: knowing the positions of the asteroids, a series of manoeuvres must be performed in order to encounter them. Note that the ratio m_f/m_i depends exponentially on the reciprocal of the specific impulse, which means that the greater this parameter, the less propellant will be needed to achieve a certain ΔV, demonstrating how the choice of electric propulsion is ideal for reducing fuel consumption.
Given a spacecraft with velocity $\mathbf{V}_1$, the ΔV is calculated as the velocity variation to be imparted to the spacecraft to obtain a $\mathbf{V}_2$ appropriate to the desired orbit. Since velocities and ΔV are vector quantities, it is necessary to use Carnot's theorem to calculate the modulus:

$$V_2^2 = V_1^2 + \Delta V^2 - 2V_1 \Delta V \cos(\pi - \beta) \tag{2.40}$$

with β the angle between the velocity vectors. Associated with it is a change in energy that the satellite will be subjected to and this represents the cost of the manoeuvre as it is linked to the propellant consumption:

$$\Delta E_g = \frac{V_2^2}{2} - \frac{V_1^2}{2} = \frac{1}{2}\Delta V(\Delta V + 2V_1 \cos\beta) \tag{2.41}$$

To achieve the greatest possible energy variation, the manoeuvre must be carried out when the speed is maximum and when the angle β is zero (or equal to π). The lower the velocity,

the more energy ends up in gravitational losses and the energy effect is low at the same ΔV. The non-zero β on the other hand, results in losses due to thrust misalignment. Finally, it should be noted that the previous two relationships are valid under the assumption that thrust occurs instantaneously, which is not the case with electric propulsion. The considerations made, however, continue to apply in general.

2.5.2 Main impulsive manoeuvres

In this section, the main impulsive manoeuvres will be analyzed; three-pulse manoeuvres or transfers between orbits at different inclinations will be omitted because they are not useful for the trajectories analysed, which will remain at very low inclinations.

Adjustment of Periapsis and Apoapsis height

A very effective way to change the height of an apsis is to increase the speed in the opposite one. This changes the major semi-axis (and eccentricity) without varying its direction. If the increment is Δz, then the change in major semi-axis will be:

$$\Delta a = \frac{\Delta z}{2} \tag{2.42}$$

Knowing the required Δa, it is possible to derive Δz and from there derive the required V_2 and ΔV. Note that the ΔV at periapsis is very effective, while ΔV at apoapsis is inconvenient due to gravitation losses.
It is possible to write:

$$V dV = \frac{\mu}{2a^2} da \tag{2.43}$$

For a near-circular orbit:

$$\frac{dV}{V} = \frac{da}{2a} \tag{2.44}$$

Apses line rotation

The apses line is determined in the orbital plane by the angle ω. To rotate such line by a $\Delta\omega$ angle with a simple impulse, it is necessary that the point at which the impulse occurs is common to the starting orbit and the ending orbit: one of the two intersections of the ellipses.
The manoeuvring conditions will be:

$$r_1 = r_2 \quad \nu_2 = \nu_1 - \Delta\omega \tag{2.45}$$

Energy and angular momentum do not vary since the shape and size of the orbit remain constant. Since the radius is constant, the tangential velocity also remains constant, as does the modulus of the velocity.
To do this, it is necessary to vary the direction of the radial velocity:

$$\Delta V = 2V_r = \frac{2\mu e}{h} \sin\nu \tag{2.46}$$

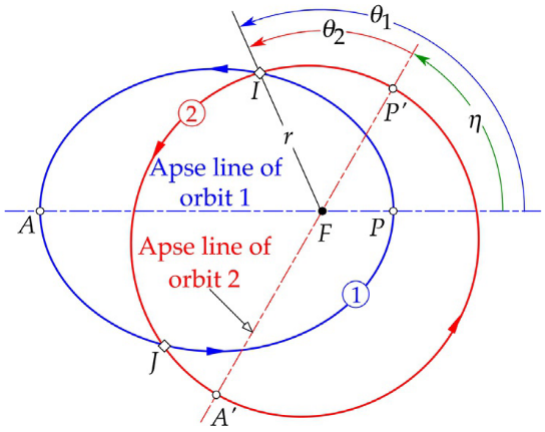

Figure 2.8: Apses line rotation [4]

Orbital plane change

The change of orbital plane requires a ΔV with a component perpendicular to the orbital plane. The manoeuvre takes place with a single impulse at constant radius, energy and angular momentum.
The moduli of V, V_r and V_t remain constant, only the direction of V_t varies in the plane tangent to the two orbits at the manoeuvring point.
The cost of the manoeuvre is equal to:

$$\Delta V = 2V_t \sin \frac{\Delta\psi}{2} \tag{2.47}$$

with $\Delta\psi$ the angle between the tangential velocity in the departure orbit and the tangential velocity in the arrival orbit.
It should be noted that the cost is directly proportional to the orbital velocity, so the change of orbital plane should be done at apoapsis or with a combined manoeuvre. A graphic representation of the manoeuvre is shown in figure 2.9.

Phasing Manoeuvre

A phasing manoeuvre is a two-impulse manoeuvre from and then back to the same orbit, as reported in fig. 2.10. This kind of manoeuvres are used to change the position of a spacecraft in its orbit. If two spacecraft, destined to rendezvous, are at different locations in the same orbit, then one of them may perform a phasing manoeuvre to catch the other one. In fig. 2.10, phasing orbit 1 might be used to return to P in less than one period of the main orbit. This would be appropriate if the target is ahead of the chasing vehicle. If the chaser is ahead of the target, then phasing orbit 2 with its longer period, and bigger major semi-axis, might be appropriate.
The phasing manoeuvre can be done also only with the phasing orbit 2, using a smaller ΔV but waiting more than one orbital period. The whole thing is a compromise between cost

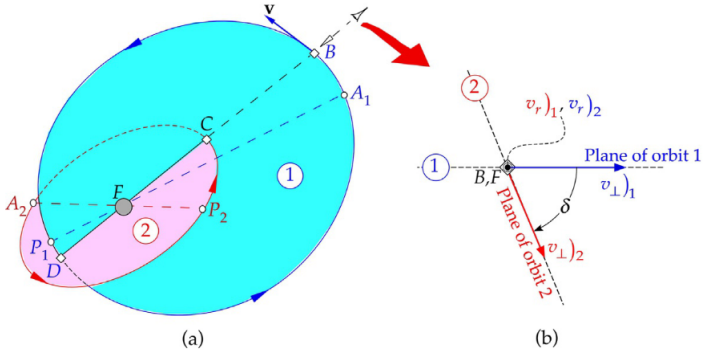

Figure 2.9: (a) Two noncoplanar orbits around F. (b) Line of intersection between the two orbital planes [4]

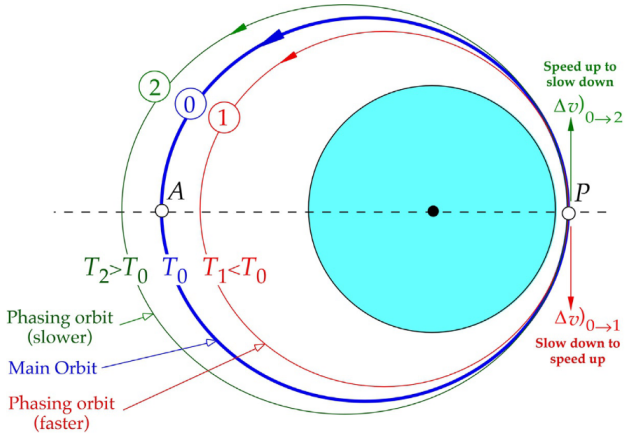

Figure 2.10: Example of phasing manoeuvre [4]

and manoeuvre time. In particular, it can be written that $\Delta T = n\Delta T_p$, with $T_p = 2\pi\sqrt{\frac{a^3}{\mu}}$, whereby ΔT is uniquely tied to Δa.
Note that if the required phasing is more than 180°, then it is better to phase in the opposite direction. In this case, the orbit is called a *catching orbit* and has a semi-major axis smaller than the starting orbit. The required impulses are performed at the same point at different times, they have the same modulus, same direction but opposite verse, as shown in fig. 2.10.

Transfer between coplanar circular orbits

In low-thrust missions, it is very often possible to approximate the orbit at any given time to a near-circular orbit, which is why this section will analyse transfers between near-circular orbits, both in the impulsive case and in the case of continuous thrust.

Wanting to move from an orbit with radius r_1 to an orbit with a greater (or smaller) radius r_2 in the same orbital plane, the transfer orbit must intersect both orbits: the periapsis shall be less than or equal to the radius of the departure orbit and the apoapsis shall be greater than or equal to the final radius. These relationships can be expressed through the following equations:

$$r_{pt} = \frac{p_t}{1+e_t} \leqslant r_1 \quad r_{at} = \frac{p_t}{1-e_t} \geqslant r_{r_2} \tag{2.48}$$

The combinations of semilatus rectum and eccentricity are infinite and can lead to elliptical, parabolic and hyperbolic transfers. It can be shown that the ellipse bitangent to the two orbits is the one with the lowest energy. The ΔV for this type of two impulses transfer is the lowest possible. If three impulses transfers are considered the argument does not apply, a biparabolic or bielliptical transfer may be more convenient, as reported in [3].
The bitangent elliptical transfer is called the *Hohmann transfer* and has the following characteristics:

$$r_{pt} = r_1 \quad r_{at} = r_2$$

$$a_t = \frac{r_1 + r_2}{2} \quad E_t = \frac{-\mu}{r_1 + r_2}$$

$$\Delta V_1 = V_{c1}\left(\sqrt{\frac{2r_2}{r_1 + r_2}} - 1\right) \quad \Delta V_2 = V_{c2}\left(1 - \sqrt{\frac{2r_1}{r_1 + r_2}}\right)$$

$$\Delta T_t = \frac{T_{pt}}{2} = \pi\sqrt{\frac{a_t^3}{\mu}}$$

A graphic representation is shown in figure 2.11. For transfers to smaller radii, the impulses have the same magnitude but the opposite direction.

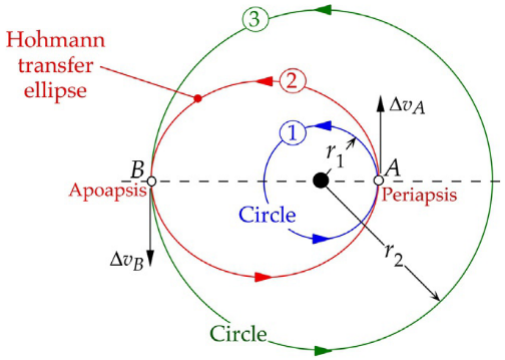

Figure 2.11: Hohmann Transfer [4]

2.5.3 Continuous thrust manoeuvres

This section covers the analysis of a continuous manoeuvre, using the Edelbaum's approximation. The assumptions introduced in the approximation are:

- Near-circular orbits ($a \approx p \approx r$; $e \approx 0$; $E \approx M \approx \nu$).
- Low inclination orbits ($i \approx 0$).
- Small accelerations compared to circular speed $V_c^2 = \frac{\mu}{r^2}$

These three assumptions make it possible to simplify the Gauss's equations for variations in the classical orbital parameters, obtaining:

$$\begin{aligned} \frac{V\dot{a}}{a} &= 2\frac{T_t}{m} \\ V\dot{e} &= 2\cos\nu\frac{T_t}{m} + \sin\nu\frac{T_r}{m} \\ V\dot{i} &= \cos(\omega+\nu)\frac{T_w}{m} \end{aligned}$$

Thrust, in a generic direction, can be broken down into tangential (T_t), radial (T_r) and normal (T_w).
By defining the α angle between the projection on the orbital plane of the thrust and the tangential direction and the β angle between the thrust and the orbital plane, it is possible to express these components as:

$$\begin{aligned} T_t &= T\cos\beta\cos\alpha \\ T_r &= T\cos\beta\sin\alpha \\ T_w &= T\sin\beta \end{aligned}$$

By integrating the simplified Gauss's equations on an orbit, we obtain:

$$\begin{aligned} \Delta a &= \frac{2aT}{nmV}\int_0^{2\pi}\cos\alpha\cos\beta\,d\nu \\ \Delta e &= \frac{T}{nmV}\int_0^{2\pi}(2\cos\nu\cos\alpha+\sin\nu\sin\alpha)\cos\beta\,d\nu \\ \Delta i &= \frac{T}{nmV}\int_0^{2\pi}\cos(\omega+\nu)\sin\beta\,d\nu \end{aligned}$$

In the case of eccentricity change, the reference of the true anomaly is chosen so that that the manoeuvre creates the major semi-axis in the direction of the chosen reference. Same for changes of inclination, the chosen reference will become the line of nodes of the final orbit.
In order to maximise the variation of semi-major axis a, it is trivial to have the thrust with $\alpha = \beta = 0$, so in the direction of the velocity, as in impulsive manoeuvres. To maximise

the variation of eccentricity e is more complicated, taking the equation inside the integral, deriving it and finding the optimum, one obtains an expression of the type:

$$\tan\alpha = \frac{\tan\nu}{2}; \quad \beta = 0 \tag{2.49}$$

This expression says that the direction of the thrust varies according to the true anomaly of the point at which it is located. It is possible to simplify the expression by imposing approximately $\nu = \alpha$ and thus have the thrust in the same direction in an inertial reference system.

Chapter 3

Mission definition

After providing a general introduction of the thesis, this chapter will aim to present the context in which the mission will take place in terms of the probe design, boundary conditions of the problem itself and the objectives to be achieved.

3.1 Near-Earth Objects

A *Near-Earth Object*, also known as NEO, is an object in the Solar system with an orbit intersecting that of the Earth. All the NEOs have a perihelion smaller than 1.3 AU and an aphelion bigger than 0.983 AU.
The Near-Earth objects can be divided in *Near-Earth Asteroids* (NEAs) and *Near-Earth Comets* (NECs). Comets fall into NECs group only if they have an orbital period of less than 200 years. Asteroids monitoring is important, as an impact of one of them with the Earth can cause catastrophic damage but also for possible scientific implications as they can be explored with low ΔV missions. NEAs are samples that make it possible to study the astronomical and geochemical aspects of the solar system, its history and evolution. With the New Space Economy NEAs are seen as a possible economic resource because of the material that can be extracted and brought to Earth at a reduced cost.
Among the NEAs there is a particular category of asteroids called *Potentially Hazardous Asteroids* (PHA). The asteroids in this category are constantly monitored for collision danger in certain time windows. The PHAs have a minimum *orbit intersection distance* (MOID) to the Earth's orbit less than or equal to 0.05 AU (less than 7.5 millions of kilometers) and a absolute magnitude smaller than 22, indicating a size bigger or equal to 150 meters. The magnitude is a measure of the brightness of an object, to calculate the size of the object the following formula should be used:

$$D = \frac{1329}{\sqrt{A}} \cdot 10^{-\frac{H}{5}}$$

With the above equation is possible to obtain the diameter D of an asteroid by knowing its albedo A, which is the percentage of reflected light compared to that received and the absolute magnitude H. The absolute magnitude can be easily measured but the albedo

depends on the chemical composition which can vary greatly. Albedo values are between 0.2 and 0.06. Taking into account a mean value of 0.15 for the albedo and a magnitude of 22, we obtain the diameter of a PHA. In the Solar system there are 1 million known asteroids and only 30000 of them can be classified as NEA. NEAs can be divided into the following groups:

- ***Amors***: Asteroids with an orbit outside the Earth's, therefore not intersecting.
- ***Apollos***: Asteroids with an orbit that intersects that of the Earth. Their semi-axis is greater than that of the Earth, but their perihelion is smaller than the Earth's aphelion.
- ***Atens***: Asteroids with an orbit that intersects that of the Earth. Their semi-major axis is smaller than that of the Earth, but their aphelion is bigger than the Earth's perihelion.
- ***Atiras***: Asteroids with an orbit inside the Earth's orbit, therefore not intersecting. They have a semi-major axis smaller than that of the Earth and an aphelion smaller than the Earth's perihelion.

NEAs are also divided into *numbered* and *unnumbered*: the former are object whose orbit is known more as results of repeated observations, while the accuracy of orbital parameters of the latter is less. When a new body is discovered, it is first added to the second category and then moved to the first category after a series of observations and studies.

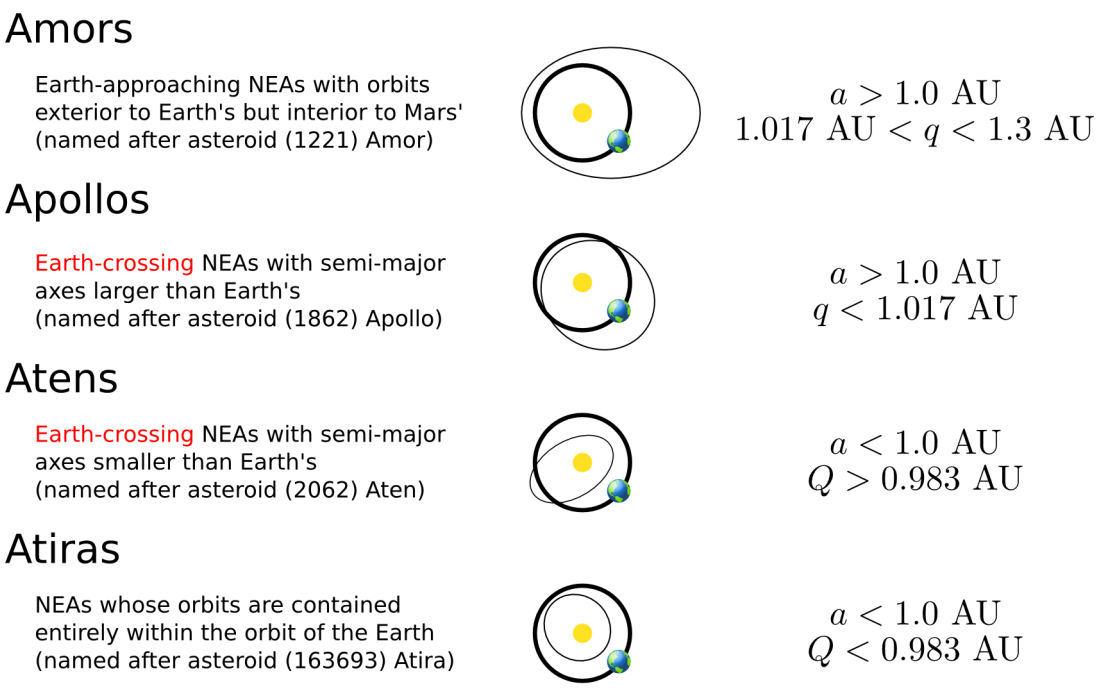

(q = perihelion distance, Q = aphelion distance, a = semi-major axis)

Figure 3.1: NEAs [5]

With reference to fig. 3.1, following the same nomenclature, are reported the parameters for Earth:

$$\text{Semi-major axis:} \quad a_\oplus = 1.0\text{AU}$$

$$\text{Aphelion:} \quad Q_\oplus = 1.017\text{AU}$$

$$\text{Perihelion:} \quad q_\oplus = 0.983\text{AU}$$

3.1.1 Astronomical and scientific aspects of NEAs

Spaceguard project started in 1998 with the aim of cataloguing NEAs and preventing their impacts with the Earth. At the beginning the monitoring was only for objects with a diameter bigger than 1 km. The research was then extended through NASA NEOWISE mission, with the aim of studying smaller bodies as well.
In fig. 3.2 is possible to observe all the NEOs discovered so far, divided by size. There are more than 30000 NEAs discovered, 800 of them have a diameter bigger than 1 km and 2400 NEAs are classified as PHAs, with 152 of them with a diameter bigger than 1 km. It is important to observe that the number of asteroids with a diameter bigger than 1 km is roughly constant: this is because they are easy to find, so it is estimated that almost all of them are now known.

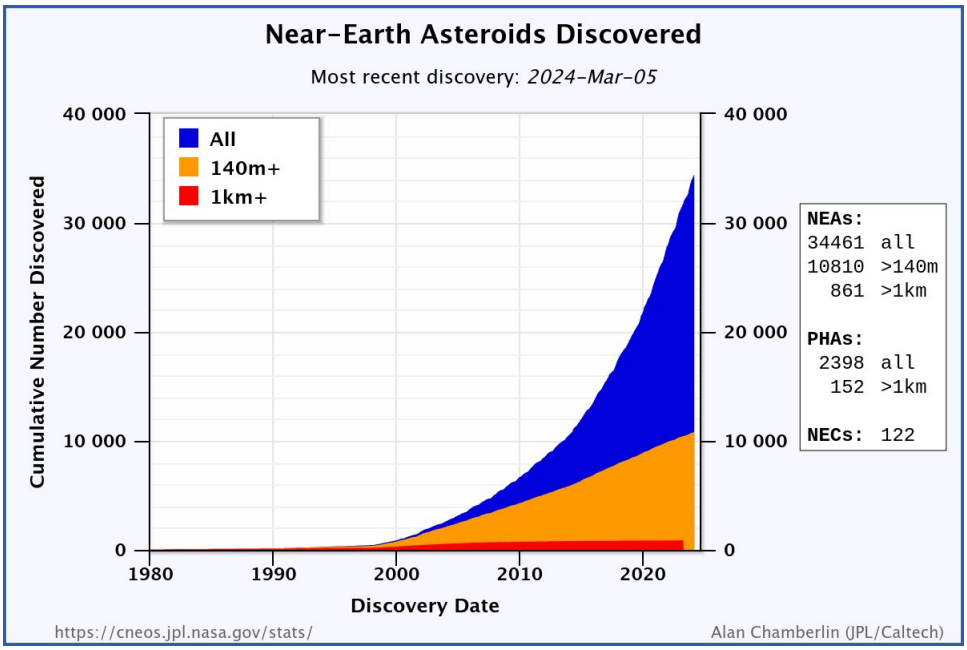

Figure 3.2: Discovered NEAs (Updated at 05 March 2024) [5]

The first objective of the *Spaceguard* project was surveillance and prevention of future impacts given the aforementioned energies involved, with consequent risks. Speaking of which, test missions have been studied and carried out with the goal of findings solutions to effectively deflect an asteroid from its collision course with Earth. Worth mentioning is the

DART mission that was the first-ever mission dedicated to investigating and demonstrating one method of asteroid deflection by changing an asteroid's motion in space through kinetic impact.
As mentioned before, NEAs are also important for the New Space Economy. In fact, they show a very diverse chemical and physical composition: silicates, basaltic compounds, carbonates and metals. This shows that their formation does not have a unique origin, making them an excellent source of information about the history of the solar system [6]. NEAs have various composition, rotational and aggregation properties: during the formation of the Solar system, micrometer-sized dust, called *chondrules*, aggregated to form centimeter-sized objects. They are subject to centrifugal accelerations that could be far stronger than gravitational or viscous forces, and the chondrules cluster as a result, is no longer able to grow. Once these aggregates have a size of a kilometer, the gravitational forces are strong enough to capture other dust or smaller bodies and create a proto-planet [7]. The transition from centimeter to kilometer has never been unambiguously clarified because of the *meter barrier*. When the object size is around one meter, the accretion becomes very difficult, because the energy holding the aggregate components together is not very strong, while their relative velocity, which generates a centrifugal force, goes up: neither gravity nor viscous forces can explain the change from centimeter to kilometer: some simulation shows that in presence of intense turbulent vortexes, it is possible to continue asteroid formation through the aggregation of dust [8].
The estimated lifetime of a NEA is only a few million years, they are usually eliminated through orbital decays towards the Sun, collisions with inner planets or by ejection from the solar system following a flyby with a large planet. This suggests that they did not originated in the present orbit, but actually come mainly from the main asteroid belt between Mars and Jupiter [9]. A proof has been provided by NASA OSIRIS-REx, the first U.S. mission to collect a sample from an asteroid. The collected sample from the NEA Bennu has the same composition of the asteroid Vesta from the main asteroid belt [10], which has suffered two strong impacts in the past, releasing many fragments [11]. There two main phenomena linked to the migration of asteroids towards more internal orbits: the *Kirkwood gaps* and the *Yarkovsky effect*.

Kirkwood Gaps

The main asteroid belt has some gaps in the density distribution of asteroids in the radial direction, this gaps are called *Kirkwood Gaps*. In fig. 3.3 is possible to see how for some semi-major axis values there are no asteroids. This happens because an asteroid in an orbit possessing a certain semi-major axis is in orbital resonance with Jupiter, that means that the orbital period of the planet and of the asteroid itself are in an integer ratio. This phenomenon is common with circular orbits, but it can happen also with eccentric or inclined orbits. For these NEAs, Jupiter's gravity generates considerable orbital disturbances, causing them to migrate to other regions of space, giving origin to these characteristic gaps named after the ratio of periods, for example 5:2 resonance. According to [13], about 61% of NEOs come from the inner asteroid belt, with a semimajor axis smaller than 2.5 AU, 24% of NEOs come from the central belt, with a semimajor axis between 2.5 and 2.8 AU, and 8% come from the outer asteroid belt, with a semimajor axis

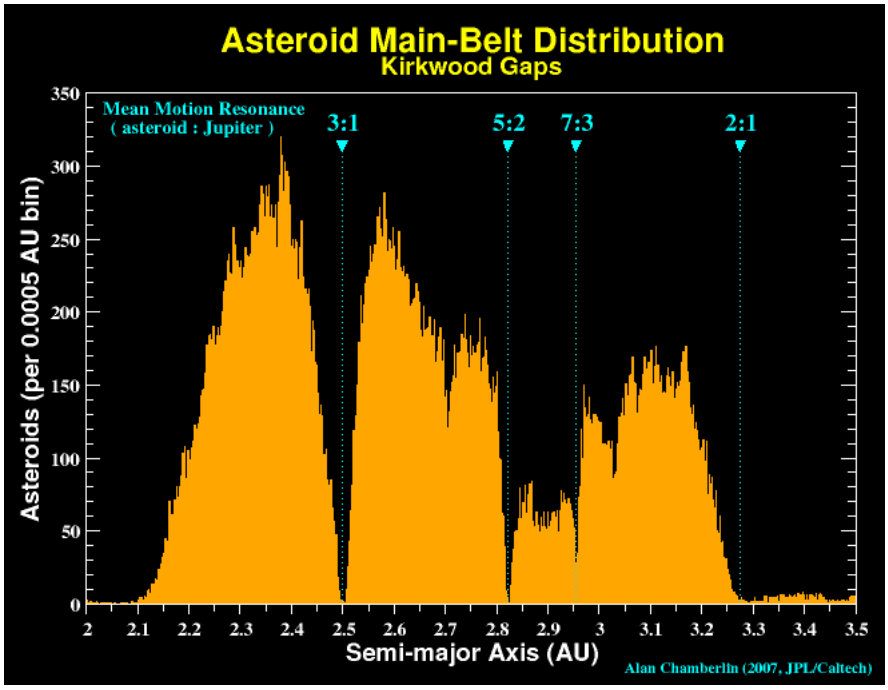

Figure 3.3: Kirkwood gaps in the asteroid main belt distribution [12]

bigger than 2.8 AU and 6% from Jupiter's comets.

Yarkovsky effect

Like any other object, an asteroid, when hit by solar radiation, will absorb energy and radiate it following the Stefan-Boltzmann law. Due to the thermal inertia, there is a time delay between the peak input and the peak output. If an asteroid possesses a rotation around its axis, the absorption peak would occur at "noon" while the emission peak in the afternoon, generating a non-zero and non-radial force. If, for example, the asteroid rotates in a prograde manner, the resulting force produces an increase in the semi-axis, in opposite if the spin is retrograde. If, on the other hand, the asteroid has no rotational motion, during its revolutionary motion half the satellite will be illuminated and the other half will not, following a 'seasonal' cycle. Referring to fig. 3.4, the absorption peak occurs at A and C, but the emission peak happens at B and D, generating a braking force that reduces the semi-major axis. According to [14], the forces generated by the Yarkovsky effect are very small, but they lead to significant variations over time, even to the extent of moving asteroids smaller than 20 km towards regions affected by gravitational resonance.

3.1.2 Planetary protection

As mentioned above, since the 1990s the observation of NEAs has been carried out for scientific reasons but above all for risk reasons. Indeed, the scientific community has

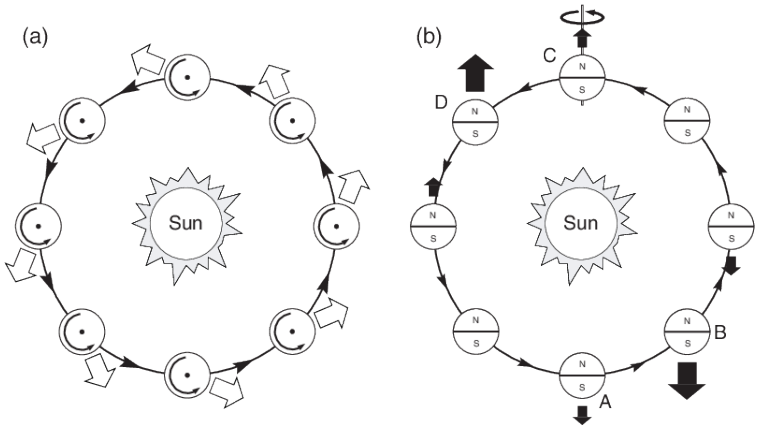

Figure 3.4: Yarkovsky effect [14]

always been aware that even small bodies can create large impact craters, and that the effect of such an impact can be recorded over even larger areas. With the ever-increasing awareness of the need to study these bodies in order to map them and possibly mitigate the risks of possible impacts, a number of organisations dealing with planetary protection have sprung up over the years. The most important is the *Planetary Defense Coordination Office* (PDCO), a planetary protection organisation founded by NASA in 2016. Its mission is to catalogue NEAs and PHAs whose orbits pass within 5 million km of Earth and which could strike it, and to help the US government coordinate efforts to mitigate or deflect potential threats once found. Observation is carried out through a variety of telescopes on the ground and in space. Nasa is currently developing *NEO Surveyor Space Telescope*, a satellite optimised for the search characterisation of near-Earth bodies, in order to accelerate the discovery of currently unknown asteroids [15].
There are other organisations involved in finding new NEOs, such as the *SpaceGuard Foundation* (SGF), a private non-profit organisation based in Frascati (Italy), whose aim is to protect the Earth from a possible impact threat.

Risks for the Earth

In recent years, episodes of small objects called *fireballs* have been documented: these are small asteroids burning in the atmosphere, so called because they are very bright. A famous example of *fireball* is the *Chelyabinsk meteor*, a NEO about 20 meters in diameter, which entered the Earth's atmosphere in the Ural region of Russia on 15 February 2013. The object exploded at an altitude of about 30 kilometers, creating a shock wave with an estimated kinetic energy equal to the energy of 30 atomic bombs dropped on Hiroshima (400-500 kilotons). Another episode occurred in February 2018, when the asteroid *2008 TC3*, 4 meters in diameter and 80 tonnes in weight, exploded about 37 km above the Sudan desert. Most of it disintegrated, but about 11 kg of debris that survived the explosion was collected on the ground. This was the first case of an asteroid impact that had been predicted prior to entry the atmosphere. In case of larger bodies, the impact with the

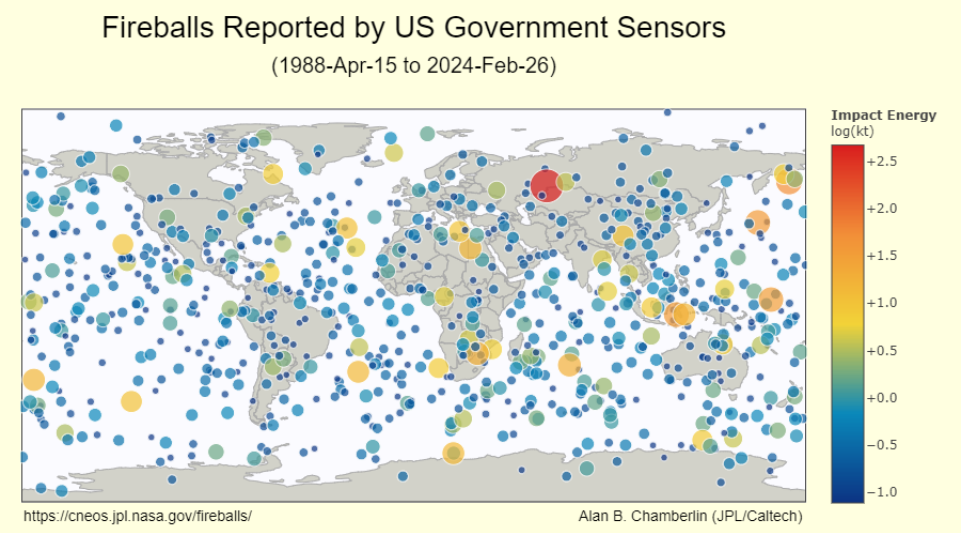

Figure 3.5: Fireballs entered the atmosphere between 1988 and 2024 [16]

Earth could have very serious consequences. In case of impact with a object with a size bigger than 1 km, the impact, already catastrophic itself, could trigger a series of chain effects such as tsunamis, earthquakes and, in the worst case scenario, climatic changes. There are two main scales used to assess the hazard of a possible collision: Torino scale and Palermo Scale.

Torino Scale

The Torino scale is a method for categorizing the impact hazard associated with near-Earth objects (NEOs) such as asteroids and comets.The scale has integer values from 0 to 10, where the individual risk value is a combination of the statistical probability of impact and its kinetic energy. The value 0 indicates a negligible impact, for example a very small asteroid that can't enter the Earth's atmosphere. The maximum value represents a definite threat, an asteroid large enough to cause a planetary catastrophe. The threat level is represented also by colours, as reported in fig 6.3:

- White: Asteroid too small to be a threat;
- Green: Current calculations show a collision is extremely unlikely. New telescopic observations very likely will lead to reassignment to Level 0;
- Yellow: meriting attention by astronomers. Current calculations give a 1% or greater chance of collision capable of localized destruction;
- Orange: Threatening. A close encounter by a large object posing a serious but still uncertain threat of a global catastrophe. Critical attention by astronomers is needed to determine conclusively whether a collision will occur;

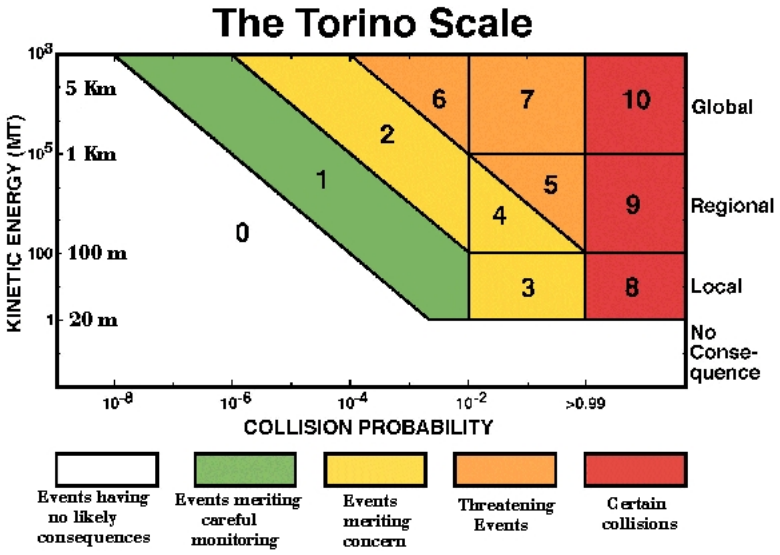

Figure 3.6: Torino Scale

- Red: Certain collision. The collision can cause localised destruction or a tsunami for small asteroids (1 event every 50-10000 years), while large asteroids can cause a global catastrophe (1 event every 100000 years). The asteroid that caused the Chicxulub impact, which caused the extinction of non-volatile dinosaurs, was estimated to be 10 on the Torino scale.

To far no observed asteroid has had a value other than zero. The asteroid with the highest value (4) is 2004 MN4 (Apophis), discovered on 24 December 2004, it has a size of 370 meters. The value 4 on the Torino scale translated into a probability of impact with the Earth of Friday 13 April 2029 of 2.7%. Further observations and calculations on the orbit led, on 28 December 2004, to the conclusion that the passage of 2029 would create no danger to the Earth, bringing the impact risk down to 0.

Palermo Scale

The Palermo Technical Impact Hazard Scale is a logarithmic scale used by astronomers to rate the potential hazard of impact of NEOs. The scale is used to assign a degree of priority to events that are ranked at the same level on the Torino scale. The scale can have both negative and positive values and compares the likelihood of the detected potential impact with the average risk posed by objects of the same size or larger over the years until the date of the potential impact. This average risk is known as *background risk*.
The values are defined using the following equation:

$$P = \log_{10}(\frac{p_i}{f_B \cdot T})$$

Where p_i is the impact probability, T the time interval and f_B is the background impact frequency.

Also for this scale the biggest value registered was for Apophis, with 1.10.

3.2 Multiple flyby missions

The use of spacecraft to study the physical properties of asteroids is very interesting from a scientific point of view, as discussed in the previous section. The simplest mission for this purpose is to send a probe into the asteroid belt and measure the effects of that environment in microgravity, gradually studying all the bodies it encounters. Such a mission has the advantage that it does not require a target object to arrive at, yet it would only obtain information on the most populous bodies in that particular celestial zone. Unfortunately, the largest asteroids are not so common in the belt, so they are not easily analysed. What instead can be realised is a mission with multiple flybys, as it would allow to test several NEAs with the same equipment, reducing costs.
For the target selection, different approaches may be used depending on the needs and preferences of the mission:

- Mission to asteroids selected on the basis of their orbital parameters so that they require low ΔV (subject of this thesis);
- missions that require the flyby of a particular asteroid for scientific purposes and can perform other subsequent or previous flybys without excessive additional costs;
- missions to the major planets of the solar system in which they pass in the vicinity of one or more asteroids (*New Horizons* mission [17])

This type of mission brings with it a non-negligible problem: it is necessary to know the orbital parameters of NEAs very accurately in order to intercept them. In fact, since they are small objects, even the smallest errors could jeopardise the success of the measurements. In order to collect more data and increase the scientific value of the mission, the inclusion of a final rendezvous may be considered: this manoeuvre adds greater complexity, but given the low gravity of the NEAs, no excessively complex approach manoeuvres are required and a slow close-in with the body under examination is sufficient.

3.3 Definition of Target Asteroids

The purpose of this thesis is to analyse the influence of asteroid orbital parameters and the phase angle between earth and asteroids on the mass of propellant consumed. To do this, fictitious asteroids are defined that require specific variations of certain orbital parameters (sometimes single, sometimes with simultaneous variations of some of them), choosing different phase angles with the earth, creating various possible combinations of orbital parameters.
Below are the values for the asteroids under consideration:

Designation	Epoch [MJD]	a [AU]	e	i [deg]	ω	Ω	M
REF	61771	1.1	0.1	2	0	0	-35.36529
AM	61771	1.05	0.1	2	0	0	116.36661
AP	61771	1.15	0.1	2	0	0	-8.301583
EM	61771	1.1	0.05	2	0	0	-35.36529
EP	61771	1.1	0.15	2	0	0	-35.36529
IM	61771	1.1	0.1	1	0	0	-35.36529
IP	61771	1.1	0.1	3	0	0	-35.36529

The mean anomaly values were set arbitrarily as the objective of optimisation. The epoch of each asteroid is expressed in Modified Julian Date and is equal to 01/01/2028.

3.4 Mission Features

The spacecraft used for this mission has an initial mass of 21 kg and is equipped with a thruster that has a nominal thrust (i.e. at 1 au) of 1 mN and an assumed constant specific impulse of 2100 s. This implies that the effective exhaust velocity c will also be constant and consequently the thrust will vary with the flow rate, which depends on the available electrical power, which in turn depends on the inverse of the square of the radius:

$$P_{elec} = \frac{P_{elec,1au}}{r^2}$$

$$P_T = \eta P_{elec} = \frac{1}{2}\dot{m}c^2 = \frac{Tc}{2} \rightarrow P_{elec} = \frac{Tc}{2}$$

where η is the propulsive efficiency assumed equal to 62.5% and r is measured in AU. With these values, the nominal electric power is 16.475 W. In reality, the propulsive efficiency is lower than assumed, so the nominal electrical power required will have to be higher.

3.5 Starting Assumptions

It is necessary to introduce some assumptions regarding the model used to study trajectories. These assumptions serve to simplify the analysis and can be considered acceptable since this is a preliminary feasibility study.

1. The first hypothesis, and perhaps the most unrealistic one, is to consider the orbital parameters of NEAs to be exact. In reality, these may be slightly different and may vary over time, depending on the number of observations made.

2. It is assumed that the satellite, upon departure, is already outside the Earth's gravitational sphere of influence and has zero velocity with respect to the Earth. This implies that the launch and escape phases from the sphere of influence are not taken into account in the analysis.

3. The earth's orbit was considered exactly circular, with a radius equal to one astronomical unit, zero eccentricity and zero inclination of the ecliptic.

Chapter 4

Mathematical Models

Before setting up the space trajectory optimisation problem, it is necessary to understand and choose models that represent the dynamics of a spacecraft in motion in space.
A *model* is defined as a set of ordinary differential equations representing the evolution, that is the time history, of the state of a system (Position and velocity). It can be written in the general form:

$$\dot{\mathbf{x}} = \mathbf{f}(\mathbf{x}(t), \mathbf{u}(t), t)$$

where t is the independent variable time, $\boldsymbol{x}$ is the state vector composed in general by n components capable of completely describe the current state of the system and $\boldsymbol{u}$ is the control vector, that is related to the input that can be implemented by the system to change its behaviour. It is important to notice that the dimension of the state vector is different from the dimension of the control vector because not all state variables can be controlled directly. The function $\boldsymbol{f}$ can be a linear matrix function or, in case of complex dynamics, a system of non-linear equations. In this thesis the state of the probe is well described by its position and velocity.
The mathematical model is not unambiguous: it is typically possible to create one that takes into account all the possible system-related phenomenologies, but is complex and difficult to apply. Depending of the study case, the mathematical model of the problem is usually derived by making specific simplifications from the general and complex model mentioned above, where certain phenomena are negligible on the overall motion of the spacecraft. For example, the action periods of the control vector can be orders of magnitude smaller than the manoeuvre times, so that an impulsive control model can be implemented without making major errors. As explained in Chapter 2, it is possible to move from the n-body problem to the two-body problem by ignoring the gravitational action of some bodies to that of other, closer or more massive bodies.
The mathematical model is therefore the first choice to make when defining an optimisation problem because it greatly influences the resolution of the problem and the accuracy of the results. Fig. 4.1 illustrates the various possibilities that can be encountered when defining the mathematical model for a spacecraft trajectory optimisation problem. It is necessary to select the type of transfer and the set of equation of motion involved, which respectively influence the form of vector $\vec{u}$ and the form of equations $f(\vec{x}(t), \vec{u}(t), t)$.

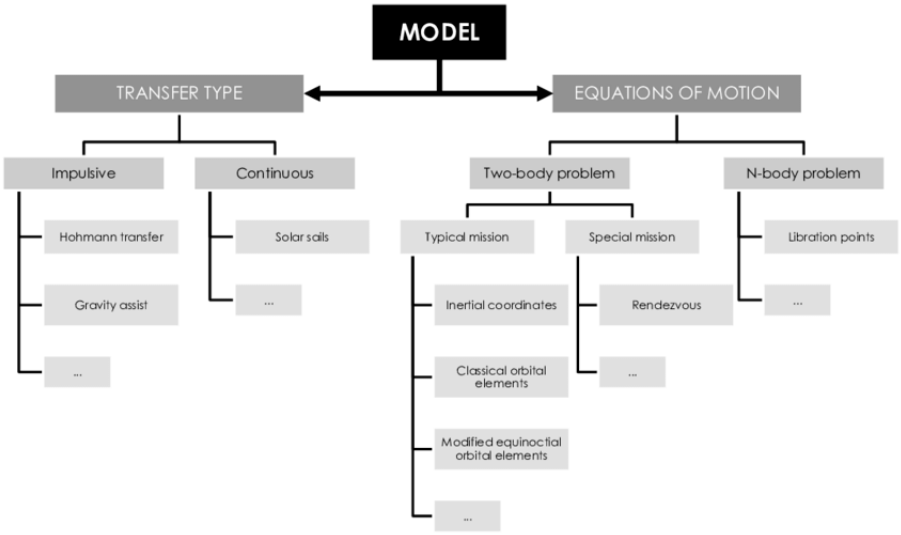

Figure 4.1: Mathematical model choice [18]

4.1 Transfer type

The type of travel largely influences the entire optimisation problem and especially its resolution. Depending on the type of mission, one may assume that the trips are impulsive if chemical propulsion is used, with the vector of the controls identically null throughout the trip but with possible discontinuities in speed, or continuous if electric propulsion is used, with a continuous trend of the $\vec{u}$ vector over time and no speed discontinuity, as the activation times of the control devices are very large and the accelerations are very small.

4.1.1 Impulsive model

As mentioned before, the impulsive model is applied when using chemical propulsion, characterised by a high level of thrust but low specific impulse which makes necessary only short ignitions to achieve the desired result. The model can also be used for low-thrust propulsion, as long as the ignition phases are short in relation to the overall mission duration and the final results contains non-negligible approximation errors.
For the impulsive model it is assumed that the system inputs are null, $\vec{u} = 0$, and that any action to vary the trajectory of the spacecraft can be regarded as an instantaneous change in velocity ΔV, that will bring to an energy change. This increase is physically created by actuating a propulsive force for a certain time, but if the force is very large, the action times are very small and can be considered as zero ($\Delta t = 0$). This last simplification leads to a further assumption: the satellite's position is constant during the ignition phase of the thruster. This type of model is very simple and relatively accurate for the simulation of trajectories characterised by large accelerations and very rapid responses of the propulsion system to commanded manoeuvres. In such situations, variations in orbital parameters are usually very large and occur in a very short time. An example of trajectory with impulsive

thrust is shown in fig. 4.2.

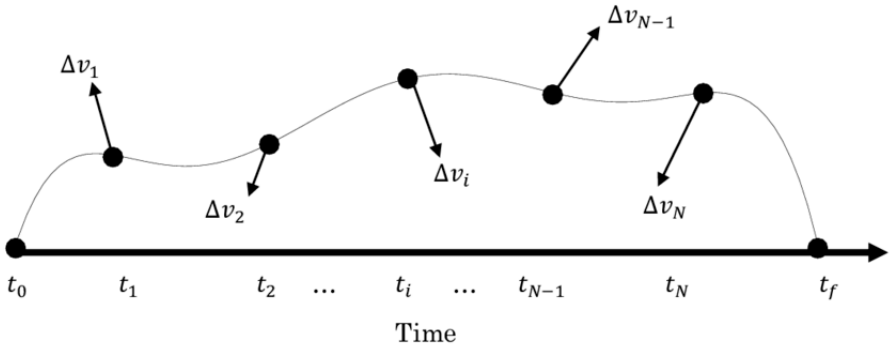

Figure 4.2: Impulsive transfer [18]

When an impulsive model is used, each time segment between one impulse and the next is simply calculated by propagating the Keplerian model, in which the body is subject to gravitational forces (and possible perturbations) and therefore follows very precise trajectories, which in the case of two body model, coincide with the family of conics. In the latter case, it is not necessary to integrate any equation of motion, because knowing the initial conditions of the segment it is possible to employ an analitycal solution in closed form.
The optimisation problem in this case is therefore to find the optimal time instant, modulus and direction of the different ΔV impulses to realise the mission by optimising the desired parameters, for example mission duration or final mass. This leads, among the advantages of the impulsive travel model, to a very low computational burden in the absence of perturbations.
A concept between impulsive and continuous transfer is the *impulsive thrusting*: in this model the trajectory is locally considered as continuous during the period in which the thruster is active, while overall is treated as impulsive. In this model, the thrust phases are usually very short compared to the mission times and are therefore modelled as isolated arcs, so that optimisation can only be performed on these specific, discrete arcs. If the required ΔV at the beginning of a segment is zero, the optimisation starts by keeping the impulse value at zero.

4.1.2 Continuous model

Continuous models are generally more accurate than impulsive models with velocity discontinuities, however they are very complex because in the differential equations system the input ($\vec{u}$(t)) (the known term of the equations) is non-zero. This type of model shall be used when thrust occurs over a time span that is not negligible compared to the mission duration and therefore the impulsive model is no longer able to produce reliable results. Thrust in a continuous model is extremely low, even lower than the gravitation force that keeps the spacecraft in orbit, the transfer times are orders of magnitude greater than those of high thrust propulsion. The combination of these two characteristics leads one to

think that for most of the trajectory the thrusters are fired at a certain level of thrust and variable direction, justifying the need for the continuous model.
The higher accuracy of continuous models is a characteristic that is always observed, however, when thrust is very large, the computational disadvantage of the continuous model can be very heavy to achieve a slightly better accuracy, so this model is not usually employed. This is why comparing an impulsive model to a continuous one is the equivalent to making a comparison between a high thrust mission and a low thrust mission. In the general case of applying the n-body model, the problem will become an extended version of the one presented in the previous chapter:

$$\ddot{\mathbf{r}} = -G \sum_{i=1}^{n} \frac{m_i}{r^3} \mathbf{r} + \Gamma \tag{4.1}$$

where Γ is a vector containing accelerations other than gravitational ones, including the thrust associated with the command vector $\mathbf{u}(\mathrm{t})$ or perturbations due to solar pressure or atmospheric resistance. The $\mathbf{r}$ vector contained in the equation can be expressed as $\mathbf{r} - \mathbf{r_i}$, with $\mathbf{r}$ position of the spacecraft, $\mathbf{r_i}$ is the position of the i-th body characterised by a certain mass m_i and G is the gravitational parameter. In this case the vector $[0, \Gamma]^T$ is analogous to the controls vector, while the vector $[\mathbf{r}, \dot{\mathbf{r}}]^T$ is the state vector. The equation becomes:

$$\frac{\partial}{\partial t} \begin{bmatrix} \mathbf{r} \\ \dot{\mathbf{r}} \end{bmatrix} = \begin{bmatrix} \dot{\mathbf{r}} \\ -G \sum_{i=1}^{n} \frac{m_i}{r^3} \mathbf{r} \end{bmatrix} + \begin{bmatrix} 0 \\ \mathbf{\Gamma} \end{bmatrix}$$

It is important to notice that by setting the controls vector to 0 and considering velocity discontinuities, the equation will be the one for the impulsive case, as the latter is a simplification of the continuous model.
The above equation for a two-body problem is the equation used to propagate an orbit in the heliocentric field. In the case where the orbit can be considered unperturbed and the controls vector is zero, propagation is not necessary because it is sufficient to denote the orbital parameters, which remain constant.

4.1.3 Choice of transfer type

Comparing the characteristics of the asteroids' orbits discussed in Chapter 2 with the characteristics of the transfer types reported here, the wisest choice is to employ a continuous transfer model: in fact, the asteroids under analysis have orbits that require significant variations in the satellite's trajectory in order for them to be reached and, making use of a low-thrust propulsion system, it is clear that long implementation times will be required. This choice will certainly complicate the problem, but will also lead to a better optimisation as one will have the possibility to act on the command vector by searching for an optimal form for the chosen trajectory and increasing the flexibility of the solution.

4.2 Equations of motion

It is necessary to choose the equations of motion according to the simplifications considered in the dynamics to which the spacecraft is subjected, in a mission, one can switch from one

equation model to another depending on the relative position of the vehicle with respect to other celestial bodies. There are many aspects that influence the choice and possible simplifying assumptions that can be implemented; the main one being the choice of how many bodies to consider for the realisation of the gravitational model, i.e. whether to opt for a 2, 3 or n-body problem. For example, in an interplanetary trip, a restricted two-body mathematical model is assumed for the planetocentric and heliocentric phases, but near the beginning of the spheres of influence of the two planets, the gravitational interactions of the latter are comparable with those due to the Sun, so a restricted three-body model or, in the case of the Earth-Moon-Sun system, a restricted N-body model should be employed. Another example concerns rendezvous, for which the equations of the restricted two-body problem are used until the chaser vehicle is in the vicinity of the target vehicle, at which point the Hill equations begin to be used.

4.2.1 Two body problem

The two-body problem describes the mutual gravitational interaction of two massive bodies considered as material points. In this model, the mass of one of the two bodies (the spacecraft) is much smaller than the mass of the other body, called the main body, around which the former orbits. Usually,with this additional assumption, the model is referred to as the restricted two-body problem. This is the case, for example, with a satellite orbiting the Earth, or in a heliocentric field and sufficiently distant from other bodies. If the mass of the vehicle is neglected, its force contribution on the larger body can also be seen as zero; moreover, a reference system solid to the larger, non-rotating body can be seen as inertial, which allows any quantity in this reference system to be derived without considering relative motion.
Another possible approach to the problem is the solution using the orbital parameters already presented in 2.4. This option is easy to understand physically and has the advantage of having a clear position of the body without going through a state vector, but it is complex to extend it to other shapes and reference systems.
In a two-body model, as in the N-body model, the most stringent assumption that leads to errors is that only gravitational forces are considered, neglecting all others, including thrust. Not omitting the other forces, which may be important (especially if derived from the propulsion system), the two-body model can be expressed with the non-Keplerian two-body equation:

$$\ddot{\mathbf{r}} = -\frac{\mu}{r^3}\mathbf{r} + \gamma$$

where $\mathbf{r}$ is the position of the secondary body with respect to a reference system fixed at the centre of mass of the primary body, $\mu = GM$ is the product of the universal gravitation constant and the mass of the largest body and γ is the acceleration generated by the thrusters plus disturbance accelerations. It is possible to write the above equation with the state vector:

$$\frac{\partial}{\partial t}\begin{bmatrix}\mathbf{r}\\ \dot{\mathbf{r}}\end{bmatrix} = \begin{bmatrix}\dot{\mathbf{r}}\\ -\frac{\mu}{r^3}\mathbf{r}\end{bmatrix} + \begin{bmatrix}0\\ \gamma\end{bmatrix}$$

These motion equations are used in trajectory optimisation problems, particurarly when orbits are perturbed and a low-thrust propulsion is used. Usually the motion equations

are written in Cartesian or cylindrical coordinates, or using classical or equinoctial orbital parameters. Neglecting perturbations (which, if there were any, would simply add to the propulsive forces), the equations of motion in terms of orbital parameters are the Gauss equations:

$$\begin{aligned}
\frac{\partial a}{\partial t} &= 2a^2 \sin\theta \frac{\gamma_r}{n\sqrt{p}} + 2a^2 \frac{p}{r} \frac{\gamma_t}{n\sqrt{p}} \\
\frac{\partial e}{\partial t} &= p \sin\theta \frac{\gamma_r}{n\sqrt{p}} + p(\cos\theta + \cos E) \frac{\gamma_t}{n\sqrt{p}} \\
\frac{\partial i}{\partial t} &= r \cos(\theta + \omega) \frac{\gamma_w}{n\sqrt{p}} \\
\frac{\partial \omega}{\partial t} &= -\frac{p \cos\theta}{e} \frac{\gamma_r}{n\sqrt{p}} + \frac{r+p}{e} \sin\theta \frac{\gamma_t}{n\sqrt{p}} - r \sin(\theta + \omega) \cot i \frac{\gamma_w}{n\sqrt{p}} \\
\frac{\partial \Omega}{\partial t} &= \frac{\gamma_w r \sin(\theta + \omega)}{n\sqrt{p} \sin i} \\
\frac{\partial M}{\partial t} &= \frac{\sqrt{1+e^2}}{e} ((p \cos\theta - 2er) \frac{\gamma_r}{n\sqrt{p}} - (r+p) \sin\theta \frac{\gamma_t}{n\sqrt{p}})
\end{aligned}$$

Where a, e, i, Ω, ω, M and p are respectively semi-major axis, eccentricity, inclination, longitude of the ascending node, argument of periapsis, mean anomaly and semilatus rectum of the osculating orbit of the trajectory at the considered point. n is the *mean motion*, which is the angular velocity around the main body and θ is the angular velocity (called ν in chapter 2). The γ_i parameters represent the radial, tangential and normal accelerations.
The advantage of using these equations is that they derive the variations in orbital parameters directly from the knowledge of accelerations, without needing the physical variables of position and velocity. As already stated in chapter 2, one or more of the six orbital parameters may not be defined and this leads to singularity in the Gauss equations. To avoid singularities it is possible to use different parameterisations, for example the modified equinoctial orbital parameters [19].
Although the classical orbital elements are often used for their intuitive physical meaning, the physical parameters of the vehicle, i.e. position and velocity, are almost always used in the trajectory optimisation problem. The physical parameters do not give immediate information about the orbit under consideration, unlike the classical orbital elements, but it is easy to extend them into other forms, they do not suffer from singularity and have much simpler equations. By way of comparison, the pros and cons of each proposed solution can be analysed in Table 4.1.

4.2.2 N-body problem

When the mission involves the probe's stay in space subject to different gravitational forces due to different masses, the most appropriate choice is the n-body model. This model can be useful for missions to the Moon, or to Saturn and Jupiter, characterised by large masses and many natural satellites.

	Inertial Coordinates	Classical Orbital Parameters	Modified Equinoctial Orbital parameters
Physical significance	Normal	High	Low
Coordinates transformation	Easy	Difficult	Difficult
Singularities	No	Yes	No
Equations complexity	Low	High	Medium

Table 4.1: Comparison of three possible approaches to the restricted two-body problem [18]

4.2.3 Choice of the equations set

The asteroids being considered are very small in size and their gravitational interaction with the vehicle is completely negligible compared to that of the Sun. Furthermore, interaction times between the bodies are negligible in the case of flybys (high relative velocities). The trajectory is completely in the heliocentric field and no other interaction is present, so it is possible to use the ordinary differential equations of the restricted two-body model, with the addition of the known term given by the propulsive system, which is non-zero only in the sections where the thrust is non-zero.
The general form of the problem is given for clarification:

$$\frac{\partial}{\partial t}\begin{bmatrix}\mathbf{r}\\ \dot{\mathbf{r}}\end{bmatrix} = \begin{bmatrix}\dot{\mathbf{r}}\\ -\frac{\mu}{r^3}\mathbf{r}\end{bmatrix} + \begin{bmatrix}0\\ \mathbf{\Gamma}\end{bmatrix}$$

where Γ is the controls vector. The following are then defined: radius r, latitude θ, longitude ϕ and the radial velocity $u = \dot{r}$, tangential velocity in East direction v and tangential velocity in North direction w, all in relation to local reference. The flow equation was then added, which is not specific to the model but is a characteristic of the propulsion system. The differential equations system is:

$$\frac{\partial}{\partial t}\begin{bmatrix}r\\ \theta\\ \phi\\ u\\ v\\ w\\ m\end{bmatrix} = \begin{bmatrix}u\\ \frac{v}{r\cos\phi}\\ \frac{w}{r}\\ -\frac{1}{r^2}+\frac{v^2}{r}+\frac{w^2}{r}\\ -\frac{uv}{r}+\frac{vw}{r}\tan\phi\\ -\frac{uw}{r}+\frac{v^2}{r}\tan\phi\\ 0\end{bmatrix} + \begin{bmatrix}0\\ 0\\ 0\\ \frac{T}{m}\sin\gamma_T\\ \frac{T}{m}\cos\gamma_T\cos\psi_T\\ \frac{T}{m}\cos\gamma_T\sin\psi_T\\ -\frac{T}{c}\end{bmatrix}$$

Where γ_T and ψ_T are the elevation angles (flight path angle) and heading angle (heading) of the thrust vector T and determine its direction.
However, the problem is not yet complete: although through this set of equations a solution can be found by imposing the appropriate boundary conditions, this will only be one of the possible trajectories that the probe can follow and there is no information on its quality in terms of consumption. It then becomes necessary to introduce mathematical elements that allow us to understand whether the result found is optimal or not. The next step is to define the appropriate mathematical optimisation tool and the choice of a procedure for finding a solution, aspects that will be dealt with in the next two chapters.

Chapter 5

Mission goals

After outlining the problem by defining a set of differential equations, its boundary conditions must be defined in order to find a solution. This chapter will therefore deal with the second macro-step that needs to be followed in order to optimise a space trajectory: the choice of objective to be achieved. It is based on the requirements of the mission: whether it is necessary to carry a certain mass of payload as far as possible, at the lowest propulsive cost or in the shortest possible time, but also whether it is necessary that the load factor (inertial, thermal or radiative) on the vehicle is always reasonable (in order to avoid structural failure or malfunctioning) or that propulsion times do not exceed a certain threshold.
Objectives are mathematically translated into objective functions, which are functions (often scalar) with several variables that outline an important quantity of the mission. They are also called cost functions, not because they represent an economic cost, but because they represent something that is difficult to achieve and therefore one wants to minimise the quantity. Usually in optimal control terminology we refer to *cost functions*, while in computer language we speak of *objective functions*. In some cases, they are represented by physical, tangible quantities (such as a mass, a value of ΔV, transfer time or acceleration) and in order to achieve an optimum, they must be minimised or maximised. However, this is not always true, as it is very common to have to optimise several aspects, such as maximising the final mass while minimising the travel time or external loads. In this case, the optimum of one parameter does not coincide with the optimum of the others and it will be necessary to introduce an overall cost function to maximise/minimise that takes into account the different physical quantities appropriately weighted; adding together a term representing a time and one representing a mass yields absolutely nothing physical. It is therefore obvious that the objective is not unique but varies from mission to mission.

5.1 Types of objective functions

The most general form of an objective function is the Bolza cost function, defined as:

$$J(\mathbf{x}, \mathbf{u}, t) = h(\mathbf{x}(t_f), t_f) + \int_{t_0}^{t_f} g(\mathbf{x}(t), \mathbf{u}(t), t)$$

Where t_0 and t_f are the start time and stop time of the transfer, $\mathbf{x}$ is the state vector and $\mathbf{u}$ is the controls vector. It can be seen that in general a cost function can be composed of a part that depends only on the end conditions, also called the *Mayer term* and a piece that depends on the entire path taken, called the *Lagrange term*. Usually only the Mayer

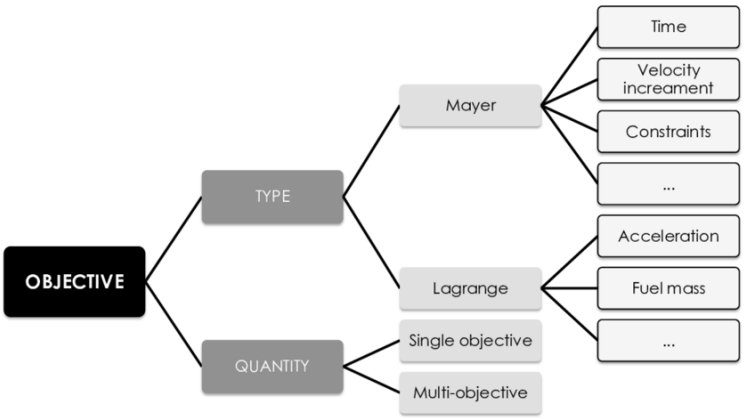

Figure 5.1: Taxonomy of objectives in trajectory optimisation [18]

term or the Lagrange term is present, depending on what is being optimised. It is not uncommon to encounter problems that possess cost functions with both terms, but it is much more common for only Mayer's term to appear as it is often the 'end result' that is most important. The subdivision according to the type of objective is widely used, but it is not the only one: it is also possible to categorise an objective function according to the number of objectives to be achieved and how they are integrated with each other. If there is only one objective, it is possible that the function is a physical parameter, if there are several, this is rarely the case.
Although the objective functions can be very numerous, the space trajectory optimisation problem can be basically reduced to two macro-cases: minimising mission time (expressed in Mayer form), and minimising vehicle control (expressed in Lagrange form).

5.1.1 Mayer objective functions

This category includes all the objective functions connected to a characteristic variable (typically state) related to the final instant of the trajectory.

Time

The simplest objective function is the transfer time. It can be written in a very general way that if one wants to minimise time, the cost function takes the form:

$$J = t_f$$

Velocity increase

The goal can also be to minimise the *propulsive distance*, which is the propulsive effort to reach a given goal. In this case, it is common to express the cost function in terms of ΔV. In fact, this objective can be seen as the sum of the speed increments ΔV given by the single pulses (for the impulsive case), while in the case of a continuous model the form is slightly different.

$$J = \sum_{i=0}^{N} |\Delta V_i|$$

Note that such an objective function is closely linked to propellant consumption, since obtaining a ΔV is the cause of the difference between final and initial mass. It is therefore an excellent objective function when one wants to save propellant.

Start and End conditions

Typically, the initial and final conditions represent constraints on the boundary of the problem, for example representing the starting point and destination of the trajectory. However, in some cases it is possible to treat them as goals, for example if one wants to cover the greatest distance with a certain amount of propellant. The cost function will have the following form:

$$J = \phi(\mathbf{x}(t_0), \mathbf{x}(t_f))$$

where ϕ is the *constraints function*.

5.1.2 Lagrange objective functions

These types of functions are used when the parameters to be optimised are a variable quantity during the mission and their evolution is the objective of the optimisation itself. The cost here is expressed with an integral function over time, whose integrand function is an appropriate combination of state variables and controls.

Acceleration

A function often used in space travel is the integral of the square modulus of acceleration over the entire trajectory:

$$J = \frac{1}{2} \int_{t_0}^{t_f} \gamma^2 \, dt$$

Acceleration is to be interpreted as that provided by the propulsion system, excluding perturbative contributions. Minimising this integral corresponds to minimising the use of thrust in the transfer.
Another very common formulation especially for low-thrust missions and continuous model is the following:

$$J = \Delta V = \int_{t_0}^{t_f} \sqrt{\gamma_x^2 + \gamma_y^2 + \gamma_z^2} \, dt$$

Where γ_i is the acceleration along the i-axis. With this formulation, the modulus of acceleration is integrated over time, thus obtaining an increase in velocity. It is therefore an extension of the objective function for ΔV previously expressed with Mayer's formulation to the case with a continuous thrust model.
In some optimisation studies, this function has been equivalently written as:

$$J = \int_{t_0}^{t_f} \frac{T}{m}\, dt$$

Where T and m are the modulus of thrust and the mass of the spacecraft, respectively.
If the effective exhaust velocity is constant (c = cost), As already mentioned in Chapter 2, the thrust is proportional to the mass flow rate:

$$T = m\dot{c} \quad \Rightarrow \quad T \quad \propto \quad \dot{m}$$

And considering an average mass m_{avg} over the transfer, the objective function, being an integral over the total duration, is proportional to:

$$J \quad \propto \quad \frac{m_f - m_o}{m_{avg}}$$

Assuming the initial mass fixed, the objective function becomes dependent only on the final mass, leading to a form similar to the Mayer function seen above.

Propellant mass

The mass of propellant is a function of the energy required for the transfer. There are several objective functions concerning the propellant mass, both in Mayer's form and in Lagrange's form, for the last case an example is:

$$J = \int_{t_0}^{t_f} m_p\, dt$$

where m_p is the propellant mass. In such a function, there is a dependency with the type of path and the time taken to travel it. If one were to use Mayer's form (e.g. $J = m_f$) this dependency would be lost, every optimal trajectory would have the same value as a cost function, regardless of the time taken or the route taken.

5.1.3 Other objective functions

The above cost functions are the most commonly used in space trajectory optimisation, but they are not the only ones. For example, more complex functions are used to obtain more regular trajectories, to manage constellations of satellites (where it is necessary to include collisions, path length, travel time and consumed propellant in the objective function).

5.2 Scalarisation of the objective function

As mentioned earlier, it is possible that there are multiple objectives and it is necessary to introduce multiple terms within the cost function. A trade-off therefore occurs, as the optimum of one aspect is generally not coincident with the optimum of another and, indeed, very often they are conflicting, for example if one wanted to minimise both consumption and mission duration.
Objective functions are therefore also categorised according to the number of objectives. The concept behind these trade-offs is similar to the increase in the cost function that is made in the case of constrained optimisation (A): constraints are added to the objective function and multiplied by a weighting coefficient, resulting in an *augmented function*. Also in this case, the various objective functions are scaled into a single objective function by summing them with certain weights.
Scaling of the objective functions is the most difficult process in creating an appropriate total objective function, as there are infinite combinations of the weights of the individual functions. A general objective function that has both a Mayer term and a Lagrange term is the following:

$$J(\mathbf{x}, \mathbf{u}, t) = h(\mathbf{x}(t_f), t_f) + \alpha \int_{t_0}^{t_f} g(\mathbf{x}(t), \mathbf{u}(t), t)$$

Where α is the weight determining the relative importance between the two terms. Usually α is chosen in order to bring the two terms on the same order of magnitude (they often differ, and by a lot) and also to choose which one should be more important than the other. In the case of having several objective functions in the Mayer form and in the Lagrange form, the process of scalarisation becomes more labour-intensive. In the event that functions are not weighted:

$$J = \sum_{i=1}^{n} J_i$$

It is possible to sum them with weights:

$$J = \sum_{i=1}^{n} \alpha_i J_i$$

Or using the weights to normalize the functions:

$$J = \sum_{i=1}^{n} \frac{J_i}{\alpha_i}$$

There is no single deterministic method for choosing the weights of individual functions. A lot of research has been done to obtain some specific criteria, such as that for choosing the maximum possible time step and so on.

5.3 Choice of the objective function

For the problem under study, it was decided to choose a simple Mayer formulation of the objective function:

$$J = m_f$$

The aim of the thesis is to find the optimal phase angle between earth and asteroid that maximises the objective function, which is the final mass. To do this, we started from a list of asteroids defined in 3.3, which have an arbitrary phasing value. After determining the final mass values for the asteroids, the next step is to optimise the mission by focusing on the phase angle. Optimisation will be carried out using the fortran code esatstar.for, which requires an input attempt solution and parameters passed via the command line, including the iteration number, the integration step, the starting asteroid (in this case the Earth), the arrival asteroid, the duration of the transfer, the initial mass (as a percentage of the reference mass of 21 kg) and the start time.
The main feature of this script is the *tstar* value that can be set in the attempt solution. There are two possibilities:

- If *tstar* is equal to zero, the script optimises the trajectory considering the orbital input parameters;
- Setting a non-zero value of *tstar* in the attempt solution, the code goes for a solution that can be defined as 'time free', moving the asteroid to the most favourable position, that means, to the most favourable phase angle.

The *tstar* value obtained at the end of the convergence, can be used to calculate the ΔM that must be applied to the current mean anomaly to move the asteroid to the optimum position. In fact, the value of ΔM in radians can be expressed as:

$$\Delta M = \sqrt{a^3} \cdot t_{star}$$

As final analysis, the relationship between variations in mean anomaly and propellant consumption will be explored. This analysis is carried out by locking the *tstar* value to the optimal value and applying the desired variations to the mean anomaly value chosen arbitrarily in the definition of asteroids.
Referring to the final mass equation derived from the Tsiolkovsky equation, the final mass is a function of c, m_0 and ΔV. In this case, the effective exhaust velocity and initial mass are fixed, so the final mass is uniquely related to the propulsive effort of the trajectory. By maximising the final mass, we are therefore minimising ΔV.

Chapter 6

Solving methods and theory of optimal control

In this chapter, the solution aspects of the trajectory optimisation process will be analysed, so how to find the optimal control that minimises the objective function while respecting the objectives and equations of motion.
Before delving into resolution approaches, it is convenient to distinguish two terms that are usually used synonymously: *trajectory optimisation* and *optimal control*. Trajectories optimisation occurs when the system's inputs are static parameters and it is necessary to find those that optimise the objective function, while optimal control occurs when these inputs are functions and it is necessary to find those that optimise the objective function.
In the previous chapters, the mathematical tools necessary for the solution of the problem were introduced, in particular in Chap. 4, the set of equations describing the satellite's dynamics in its trajectory was defined, while in Chap. 5, the cost function used to define the optimisation parameters and boundary conditions was introduced, even though expressed in a qualitative rather than quantitative manner. In particular, boundary conditions can be derived from the start and end points, while constraints can be written from physical, path or time limits (e.g. thrust between a minimum and a maximum value, there is no point in looking for solutions that require higher levels of thrust than can be achieved).
Schematically, the problem can be represented as in figure 6.1: the aim is to find the control evolution that minimises a certain cost function along a trajectory that follows laws of dynamics, with certain initial and final conditions and respecting a set of path constraints.
In general, there are two types of approaches to solving optimisation problems: the analytical approach and the numerical approach. Numerical approaches are divided into direct and indirect methods, in which various techniques can be used.

6.1 Optimal Control Theory

Optimal control theory is based on the writing of auxiliary equations, called Lagrange multipliers, related to both the physical variables of the problem and the optimal condition.

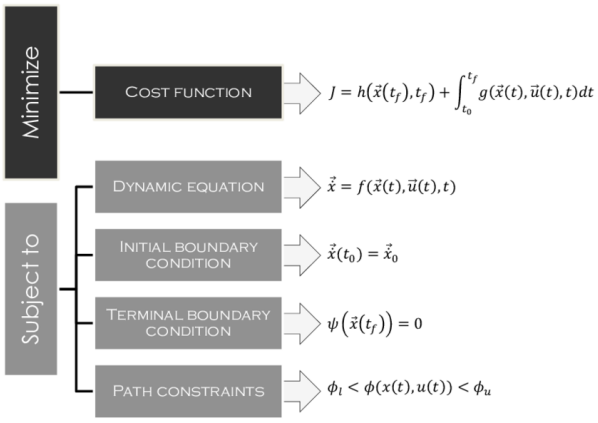

Figure 6.1: Mathematical representation of a spacecraft trajectory optimisation problem [18]

The generic system to which optimal control theory applies is described by a vector of state variables **x**. The differential equations describing the evolution between the initial and final instants (boundary conditions) are functions of **x**, the controls vector u and the independent time variable t, and have this form:

$$\frac{d\mathbf{x}}{dt} = f(\mathbf{x}, \mathbf{u}, t)$$

It is convenient to divide the trajectory into a number n of sub-intervals, called arcs, within which the variables are continuous. The j-th interval begins at $t_{(j-1)_+}$ and ends at time $t_{(j)_-}$, and the values that the variables assume at its extremes are $x_{(j-1)_+}$ and $x_{(j)_-}$, where the signs - and + indicate the values assumed immediately before and immediately after the point considered. The system is also subject to mixed boundary conditions, meaning that it involves the values of the state variables and the independent variable at both external and internal boundaries.

$$\mathbf{x} = (\mathbf{x}_{(j-1)_+}, \mathbf{x}_{(j)_-}, t_{(j-1)_+}, t_{(j)_-}) = 0$$

It is useful to rewrite the functional by introducing Lagrange multipliers, constants μ related to boundary conditions and variables λ, associated to state equation:

$$J^* = \phi + \mu^{\mathbf{T}}\mathbf{x} + \sum_j \int_{t_{(j-1)_+}}^{t_{(j)_-}} (\mathbf{\Phi} + \lambda^T(\mathbf{f} - \dot{x}))\, dt \quad j = 1, ..., n$$

The two functionals J and J^* depend on time, state variables **x** and their derivative $\dot{x}$ and from controls vector **u**. Lagrange multipliers for discrete constraints (boundary conditions), are not functions of time, whereas those within the integral have a time dependency and are true additional variables. If the boundary conditions and equations of state are met, it holds that $J = J^*$. Integrating by parts to eliminate the dependence on $\dot{x}$ and

differentiating is possible to obtain the variation of the functional δJ^*.

$$\begin{aligned}\delta J^* = &(-H_{(j-1)_+} + \frac{\partial \phi}{\partial t_{(j-1)_+}} + \mu^T \frac{\partial \mathbf{x}}{\partial t_{(j-1)_+}})\delta t_{(j-1)_+} \\ &+ (H_{(j)_-} + \frac{\partial \phi}{\partial t_{(j)_-}} + \mu^T \frac{\partial \mathbf{x}}{\partial t_{(j)_-}})\delta t_{(j)_-} \\ &+ (-\boldsymbol{\lambda}^{\mathbf{T}}{}_{(j-1)_+} + \frac{\partial \phi}{\partial \mathbf{x}_{(j-1)_+}} + \mu^T \frac{\partial \mathbf{x}}{\partial t_{(j-1)_+}})\delta x_{(j-1)_+} \\ &+ (-\boldsymbol{\lambda}^{\mathbf{T}}{}_{(j)_-} + \frac{\partial \phi}{\partial \mathbf{x}_{(j)_-}} + \mu^T \frac{\partial \mathbf{x}}{\partial t_{(j)_-}})\delta x_{(j)_-} \\ &+ \sum_j \int_{t_{(j-1)_+}}^{t_{(j)_-}} ((\frac{\partial H}{\partial \mathbf{x}} + \dot{\lambda}^T) + \frac{\partial H}{\partial \mathbf{u}}\delta \mathbf{u})\, dt \quad j = 1, ..., n\end{aligned}$$

Where H is the Hamiltonian.

$$H = \Phi + \lambda^T \mathbf{f}$$

The necessary condition of optimum requires the stationarity of the potential, and thus the cancellation of its derivative for any choice of variations $\delta\mathbf{x}$, $\delta\mathbf{u}$, $\delta x_{(j-1)_+}$, $\delta x_{(j)_-}$, $\delta t_{(j-1)_+}$, $\delta t_{(j)_-}$ compatible with the differential equations and boundary conditions. By setting the variation of the functional equal to 0, the relations known as the *Euler-Lagrange* equations for the added variables are derived:

$$\dot{\lambda} = -\frac{\partial H}{\partial \mathbf{x}}$$

and those for the controls:

$$0 = -\frac{\partial H}{\partial \mathbf{u}}$$

With this last equation, it is possible to determine the optimal value of control γ_T and ψ_T, it is sufficient to derive the Hamiltonian with respect to γ_T and ψ_T and set them equal to zero.

$$\frac{\partial H}{\partial \gamma_T} = 0$$

$$\frac{\partial H}{\partial \psi_T} = 0$$

Optimum values for thrust angles can be obtained from these:

$$\sin \gamma_T = \frac{\lambda_u}{\lambda_V}$$

$$\cos \gamma_T \cos \psi_T = \frac{\lambda_v}{\lambda_V}$$

$$\cos \gamma_T \sin \psi_T = \frac{\lambda_w}{\lambda_V}$$

Where $\lambda_V = \sqrt{\lambda_u^2 + \lambda_v^2 + \lambda_w^2}$.
The first set of equations is called the set of added equations because they concern co-state variables. The second set is called the set of control equations. Then there are other time-independent parameters for which additional sets of equations must be written, including transversality conditions. These conditions concern the time window that is considered, if parameters such as time or initial and final position are taken into account in the optimisation.
It is important to note that the control laws are independent of the search for the optimum of the functional J*. If one of the controls is subject to a constraint, it must belong to a given domain of allowability. In the presence of such a constraint, the optimal value of the control at each point of the trajectory is the one that, belonging to the admissibility domain, makes the Hamiltonian maximal, if maxima of J are sought, and vice versa. This principle is called *Pontryagin's Maximum Principle*. There are two possibilities:

- The optimum control value is given by the Euler-Lagrange equations for the controls if it falls within the domain of eligibility and therefore the constraint does not intervene there;
- The optimal value is at the extremes of the domain, meaning that the control assumes the maximum or minimum value if the value provided by the previous equation is outside the domain of admissibility.

There is a special case if the Hamiltonian is linear with respect to one of the controls subject to constraints, since in the Euler Lagrange equation for the controls, the control does not appear explicitly and therefore cannot be determined. If J is to be maximised, there are two possibilities:

- If in the Hamiltonian equation the coefficient of the control in question is non-zero, H is maximised by the maximum value of the control if the coefficient is positive and minimum if negative (*bang-bang* control), in accordance with Pontryagin's principle;
- If in the same equation the coefficient of the control in question is identically zero during a finite interval of time (singular arc), then it is necessary to impose the cancellation of all successive derivatives of the coefficient with respect to time, until the control appears explicitly in one of them. The optimal control is then determined by setting this last derivative equal to zero.

6.2 Solving approaches

6.2.1 Analytical approach

The analytical approach consists of finding an analytical solution for the optimal trajectory. Obviously, an analytical solution is always desirable, because it does not inconvenience computational power to solve the problem and because they are exact, error-free solutions. Such solutions are only obtainable in very special and simple cases (e.g. in the case of increasing the semi-axis major with low thrust) and very often without considering the

perturbative effects. The complexities that the analytical solution cannot overcome are mathematical (of the dynamics model) or concern the complexity of the objective functions. An example of an analytical solution concerns the impulsive Hohmann manoeuvre, the result is exact but for an extremely simple problem. An example on the continuum concerns the Edelbaum manoeuvre, which requires many very particular and heavy assumptions to be maintained in a slightly more general case. In the case of the continuous domain, the optimisation process generally consists of the application of optimal control theory and Pontryagin's principle, as with indirect numerical methods. In the process, the presence of the additional variables further complicates the problem, which becomes difficult to solve analytically.

6.2.2 Numerical approach

Numerical approaches have now become widely used in the field of optimisation, as the computational power installed in the latest ordinary computers is now sufficient to solve even rather complex cases. Two major categories of methods can be distinguished: direct methods and indirect methods. Fig. 6.2 shows the division.

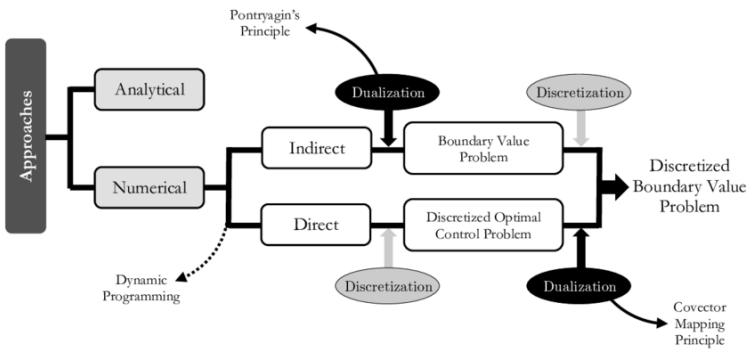

Figure 6.2: Solving approaches [18]

6.3 Solving algorithms

Solving algorithms consist of programming that allows to obtain numerically what one wants to obtain. Apart from analytical approaches, for which no iteration is required to obtain the solution, which is derived directly from the problem and is exact, numerical approaches require thousands of iterations following certain algorithms. A solving method for optimal control problems, whether indirect or direct, must consist of three basic elements:

1. An algorithm for solving differential equations and integrating functions;
2. An algorithm for solving non-linear systems of algebraic equations;
3. A solving algorithm for non-linear optimisation problems.

In an indirect method, the numerical solution of differential equations is combined with the solution of non-linear systems of algebraic equations derived from an boundary condition problem, whereas in a direct method, the solution of the problem is combined with programming and non-linear optimisation.
In this section the three basic elements of a solving method will be analysed.

6.3.1 Solving differential equations

Consider a problem like:

$$\dot{x} = f(x(t), t)$$

with $x(t_i) = x_i$. Consider a time span $[t_i, t_{i+1}]$ over which the solution is to be found. By integrating, it is possible to obtain:

$$x_{i+1} = x_i + \int_{t_i}^{t_{i+1}} f(x(t'), t')\, dt'$$

Numerically, this expression can be solved in several ways. The solution of the differential equation at each step t_k is obtained sequentially from the solution information at the previous and current steps. This family of methods is called *time marching*. Depending on the number and type of previous steps required to determine the value of the next step, these methods are divided into *multiple-step* and *multiple-stage*.
In the first category, the solution is obtained from a predefined number of previous steps. The simplest multi-step method is *Euler's method*, with the explicit form:

$$x_{k+1} = x_k + h_k[f_k]$$

or implicit:

$$x_{k+1} = x_k + h_k[f_{k+1}]$$

Other more complex and accurate methods use more than one time step in the calculation, for example the *Adams-Moulton* method, an implicit method, which was chosen for the realisation of the algorithm in this thesis in a variable step and order form. Expressions up to fourth order are given:

$$\begin{aligned}
j = -1: &\quad \mathbf{x}_{k+1} = \mathbf{x}_k + h \cdot \mathbf{f}_{k+1} \\
j = 0: &\quad \mathbf{x}_{k+1} = \mathbf{x}_k + \frac{h}{2} \cdot (\mathbf{f}_{k+1} + \mathbf{f}_k) \\
j = 1: &\quad \mathbf{x}_{k+1} = \mathbf{x}_k + h \cdot (\frac{5}{12}\mathbf{f}_{k+1} + \frac{2}{3}\mathbf{f}_k - \frac{1}{12}\mathbf{f}_{k-1}) \\
j = 2: &\quad \mathbf{x}_{k+1} = \mathbf{x}_k + h \cdot (\frac{3}{8}\mathbf{f}_{k+1} + \frac{19}{24}\mathbf{f}_k - \frac{5}{24}\mathbf{f}_{k-1} + \frac{1}{24}\mathbf{f}_{k-2})
\end{aligned}$$

In the second category, sub-intervals $[\tau_j, \tau_{j+1}]$ are considered, the overall integral can then be approximated in quadrature on the sub-intervals using the most appropriate quadrature method, from a simple trapezium method to the Cavalieri-Simpson method.

$$\int_{t_i}^{t_{i+1}} f(x(s), s)\, ds \simeq h_i \sum_{j=1}^{K} \beta_j f(x_j, \tau_j)$$

In this method, however, it is necessary to know the intermediate values of the function at each interval; these values can be obtained as:

$$x(\tau_j) = x(t_i) + h_i \sum_{l=1}^{K} \gamma_l f(x_l, \tau_l)$$

where γ is a coefficient determined by the method.
In the generic case where the objective function is a Bolza function, the integral term will also have to be discretized. The objective function, in particular, will have to be discretized using the same method that was used for the equations of motion for reasons of consistency. Each Bolza function can thus be converted into a Mayer function by adding the state x_{n+1} and the respective differential equation:

$$\dot{x}_{n+1} = L(\mathbf{x}(t), \mathbf{u}(t), t, \mathbf{p})$$

with the initial condition $x_{n+1}(t_0) = -$. The Mayer's function will be of the type:

$$J = \Phi(\mathbf{x}(t_0), t_0, \mathbf{x}(t_f), t_f, \mathbf{p}) + x_{n+1}(t_f)$$

Translating the optimal control problem into algorithms (Indirect Methods)

Optimum control theory can be transformed into a programming problem, in particular the trajectory is not discretised, but the point solution is the result of numerical integration of the necessary conditions of the optimum.
First of all, an overall variable is denoted:

$$\mathbf{y} = [u_0, x_1, u_1, x_2, ..., ..., x_M, u_M]$$

The time step, generally variable, is in this case considered constant and equal to $h = \frac{t_f}{M}$.
The generic derivative at the k-th point can be discretely evaluated as:

$$\dot{\mathbf{x}} = \frac{\mathbf{x}_k - \mathbf{x}_{k-1}}{h}$$

Substituting this approximation into the equations of dynamics, a non-linear discrete system of the type is found:

$$c_k(\mathbf{y}) = \mathbf{x}_k - \mathbf{x}_{k-1} - h\mathbf{f}(\mathbf{x}_{k-1}, \mathbf{u}_{k-1}) = 0$$

for each k from 1 to M.
The augmented Lagrangian function is writable as:

$$L(\mathbf{y}, \lambda) = \phi(\mathbf{x_M}) - \sum_{k=1}^{M} \lambda_{\mathbf{k}}{}^T [\mathbf{x}_k - \mathbf{x}_{k-1} - h\mathbf{f}(\mathbf{x}_{k-1}, \mathbf{u}_{k-1})]$$

So the necessary conditions (control equations and added equations), the equations of motion and transversality in the discrete case can be derived:

$$\begin{aligned}
\lambda_{k+1} - \lambda + h\lambda_{k+1}^T \frac{\partial \mathbf{f}}{\partial \mathbf{x}_k} &= 0 \\
h\lambda_{k+1}^T \frac{\partial \mathbf{f}}{\partial \mathbf{u}_k} &= 0 \\
\mathbf{x}_{k+1} - \mathbf{x} - h\lambda_{k+1}^T \frac{\partial \mathbf{f}}{\partial \lambda_k} &= 0 \\
-\lambda_M + \frac{\partial \phi}{\partial \mathbf{x}_M} &= 0
\end{aligned}$$

6.3.2 Solving non-linear algebraic systems

Non-linear programming algorithms are based on gradient methods, and use *line search* strategies to increase the global convergence domain.
The most widely used and intuitive non-linear programming algorithms are based on Newton's method or its derivatives. Although at first sight it appears that such algorithms are very convenient, several problems arise: an initial estimate of all the parameters of the problem is required. In direct methods, the state vector and the vector of controls at each node are parameters and it is necessary to guess them all. An initial estimate that is far from the optimal solution may lead to non-convergence of the trajectory or convergence to a solution that is not globally optimal.
The basic algorithm for solving a non-linear programming problem is the one proposed by Newton centuries ago. There is a non-linear algebraic equation of the type:

$$\mathbf{a}(\mathbf{x}) = 0$$

And a root is to be found $\mathbf{x}^*$. The first step is to give an initial estimate of the root, x. It is possible to find a better estimate of the root via an expression of the type:

$$\tilde{\mathbf{x}} = \mathbf{x} + \alpha \mathbf{p}$$

Where $\mathbf{p}$ is a *pointing vector*, calculated by solving the linear equation:

$$[A](\mathbf{x})\mathbf{p} = -\mathbf{a}(\mathbf{x})$$

Where A is the derivative matrix of the non-linear equations, that is $\nabla \mathbf{a}$.
In Newton's original method $\alpha = 1$, as $\mathbf{a}$ is replaced by its Taylor series expansion stopped at first order (a linear term is obtained), however, it is possible to vary this value to stabilise iterations and avoid divergence for values of $\mathbf{x}$ too far from the root. In practice, it varies to reduce the length of the step that is taken, a procedure known as line search, which in the thesis work is taken to $\alpha = 0.01$.
Of course, this is only valid if the matrix A is non-singular and thus if it is possible to invert it and if the initial estimate of the solution is close enough to the true root. If these two assumptions are correct and the method works, it can be shown to have quadratic convergence.

6.3.3 Solving non-linear optimisation problems

The last fundamental element consists of algorithms for solving non-linear optimisation problems. They consist in determining the vector $\mathbf{x}$ that can minimise a function $f(\mathbf{x})$ subject to equality or inequality constraints. The algorithms fall into two macro-categories: those based on gradient methods and heuristic algorithms.
In a gradient method, an initial estimate of the vector $\mathbf{x}$ is made, from which, for each iteration, a search direction is defined in the space of dimension n and a step length to find the next iteration. Basically, α_k and $\mathbf{p}_k$ are searched for such that:

$$f(\mathbf{x}_{k+1}) \leqslant f(\mathbf{x}_k) + K\alpha_k \nabla f^T(\mathbf{x}_k)\mathbf{p}_k$$

The search direction is calculated by solving the quadratic programming problem of type:

$$\min_p \frac{1}{e}\mathbf{p}^T[W]\mathbf{p} + \nabla f^T(\mathbf{x}_k)\mathbf{p}$$

Such that the constraints c_i:

$$\nabla c_i^T(\mathbf{x}_k)\mathbf{p} - c_i(\mathbf{x}_k) = 0$$

Where i is the generic active or inactive constraint. $[W]$ is the semi-definite positive matrix representing the Hessian matrix approximation of the Lagrangian function $L = f(\mathbf{x}) - \lambda^T\mathbf{c}$. The best known algorithm for solving such a problem is the *Broyden-Fletcher-Goldfarb-Shanno* algorithm.
A gradient-based optimisation method is a local method that finds optimal solutions that tend to be local. A heuristic method, on the other hand, is a global method: the search for trajectories is done stochastically and not deterministically. In the class of heuristic algorithms are all genetic algorithms, that is, those that have an evolutionary approach: an initial population of possible solutions is drawn up, each solution in the group having a particular *fitness*, reflecting the quality of a certain gene. Genes are recombined and mutated (as genes are recombined in successive generations of the population), until only the genes with the best fitnesses survive, finding the best solution to the optimisation problem.

6.4 Resolution methods

This section will describe the direct and indirect methods in more detail, outlining their advantages and disadvantages.
Indirect methods are based on variational calculus, which allows first-order optimal conditions to be found. They lead to an boundary condition problem that has optimal trajectories as its solution, each of which is then analysed to see whether it respects the constraints and boundary conditions and whether there is a maximum, minimum or saddle, after which the one with the lowest cost is selected.
Direct methods discretise the state vector and the control vector to obtain a non-linear optimisation problem.
The reason for the choice of names can be seen from this definition: indirect optimisation

solves the optimal problem by transforming it into a problem with equivalent boundary conditions, the solution of which is obtained by integration, whereas direct optimisation simply discretises the infinite-dimensional problem into a finite-dimensional one in which the unknowns involved are the discretisations of the trajectory and the vector of controls, and derives the optimal control directly by non-linear programming.

6.4.1 Direct methods

In direct methods, the solution is found in an approximate manner by parameterisation of state and control variables. If only the control vector is approximated, this is referred to as the parameterised control method, whereas if both the control vector and the state vector are approximated, this is referred to as the parameterised state and control method. In either case, the problem is solved as a non-linear optimisation. The parameterisation is carried out by means of a time discretization, which means that the trajectory is divided into a finite number of points, each of which is an optimisation parameter. Between the points into which the trajectory is divided, consistency with the equations of motion is ensured by numerically integrating them from one point to the next. This leads to the generation of constraint expressions (the end point of one integration must coincide with the start point of the next) of a non-linear type. This category of methods has its advantages: they are very easy to implement and have a very large convergence domain. Compared to indirect methods, Lagrange multipliers are not involved, so the size of the problem is reduced.

6.4.2 Indirect methods

For indirect methods, essentially the same techniques are used as for direct methods, but the resolution philosophy is fundamentally different. The problem is solved by writing and solving in time the first-order mathematical conditions required for the optimum. Such conditions make it possible to derive equations in which state variables and added variables (called co-state variables) appear with apparently no physical meaning. The necessary conditions are based on Pontryagin's principle, explained above. The problem with indirect methods is that it is very often difficult to find an initial estimate of the solution (required for the calculation), especially since it is not possible to work out the values (or at least the orders of magnitude) of the Lagrange multipliers to be used.

6.5 Numerical solving techniques

Numerical techniques consist of the numerical procedures that can be used to solve the optimum problem. They can be used indiscriminately for direct methods and indirect methods, although some techniques are peculiar to one of the two methods.

6.5.1 Shooting Technique

Shooting techniques are used to calculate the time history of state variables once the time history of the control vector is known. The advantage of using these techniques is to use

a very small number of optimisation variables. Shooting techniques can be divided into *single-shooting* and *multi-shooting* techniques.
In direct shooting techniques, the vector of controls is temporally parameterised using specific functions:

$$\mathbf{u}(t) \simeq \sum_{i=1}^{m} a_i \psi_i(t)$$

Where $\psi_i(t)$ are known functions, whereas the parameters a are the one to be determined in the optimisation process. Once these parameters have been found, the equations of dynamics are verified by direct integration with *time-marching* algorithms. In the previous writing, the single-shooting technique was used, where the controls were interpolated throughout the domain. This technique can be extended to *multi-shooting*: the problem is subdivided into $M + 1$ subintervals where controls are approximated with the same formulation as above. However, continuity conditions must be introduced at the various interfaces:

$$\mathbf{x}(t_{j_-}) - \mathbf{x}(t_{j_+}) = 0$$

This extension increases the size of the problem, as the states at the beginning of each interval are variables in the problem.
For a direct *single-shooting* method, the resolution procedure is rather simple to apply:

1. **Input**: initial estimation of the parameters of the vector of controls
2. **While** the objective function is not minimal and the constraints are not satisfied:
   (a) Integration of the trajectory from t_0 to t_f
   (b) Calculation of error on target conditions
   (c) Recalculation of initial conditions by shifting the objective function to a lower value;
3. **End While**
4. **Output**: Optimum parameter values and optimal trajectory

The technique can also be implemented for indirect methods, just introduce the added variables. First, an initial estimate of the variables is made at one end of the time interval, often the initial one, after which the system of equations of optimal control theory is integrated to the other end. Upon arrival, the conditions at the other extreme are compared with the conditions at that edge, if they differ by an amount greater than the imposed limit, the calculation is repeated by changing the conditions at the other extreme until convergence.
A key advantage of shooting techniques is that the equations of motion are imposed automatically by numerical integration and do not appear as constraints. This effectively reduces the calculation time due to the reduction in the number of constraints applied. An indirect method with simple shooting techniques is very easy to implement, however it presents some major numerical difficulties due to the malconditioning of Hamiltonian dynamics. This leads to an easy amplification of the errors made on the initial estimation

of the variables at the starting boundary, making the convergence domain very small and thus leading to serious difficulties in convergence to the optimal solution. The problem of malconditioning is particularly acute when the optimal control problem is hyper-sensitive, i.e. when the integration interval is very long compared to the time scale of the Hamiltonian system in the vicinity of the optimal solution.
To overcome these computational problems and make convergence less sensitive, a multi-shooting indirect method can be implemented: the integration time interval is divided into sub-intervals and the indirect method is applied to each of them using simple shooting techniques. In this case, it is necessary to satisfy continuity by imposing the following conditions:

$$\mathbf{y}(t_{j_-}) = \mathbf{y}(t_{j_+})$$

Where $\mathbf{y}$ is:

$$\mathbf{y}(t) = \begin{bmatrix} \mathbf{x}(t) \\ \lambda(t) \end{bmatrix}$$

where $\lambda(t)$ are the Lagrange multipliers associated with the state variables, also known as co-state variables. The problem with indirect multi-shooting methods is the increase in problem size and the increase in variables for which an initial estimate must be found.
A simple shooting algorithm for indirect methods is the following:

1. **Input** Initial estimation of unknown initial conditions
2. **While** Error at end conditions is larger than a certain tolerance:
   (a) Integration of the trajectory from t_0 to t_f
   (b) Calculation of error on target conditions
   (c) Modification of unknown initial conditions;
3. **End While**
4. **Output**: Optimal trajectory

For indirect methods with shooting techniques, it is useful to note that:

- When a variable is assigned to an extreme, the corresponding added variable is unbound;
- When an extreme variable does not appear in the boundary conditions, the corresponding co-state is null;
- When a variable is continuous and unconstrained at any point, the corresponding co-state variable is also continuous and unconstrained at that point;
- When a variable is continuous and assigned at any point, the corresponding added variable has a discontinuity and is unbound at that point;
- If the time at one end is free, the Hamiltonian is zero at that point;
- If the time at one end is assigned, the Hamiltonian is unbound at that point;

- If time at an intermediate point is assigned, the Hamiltonian has a discontinuity and is unbound at that point.

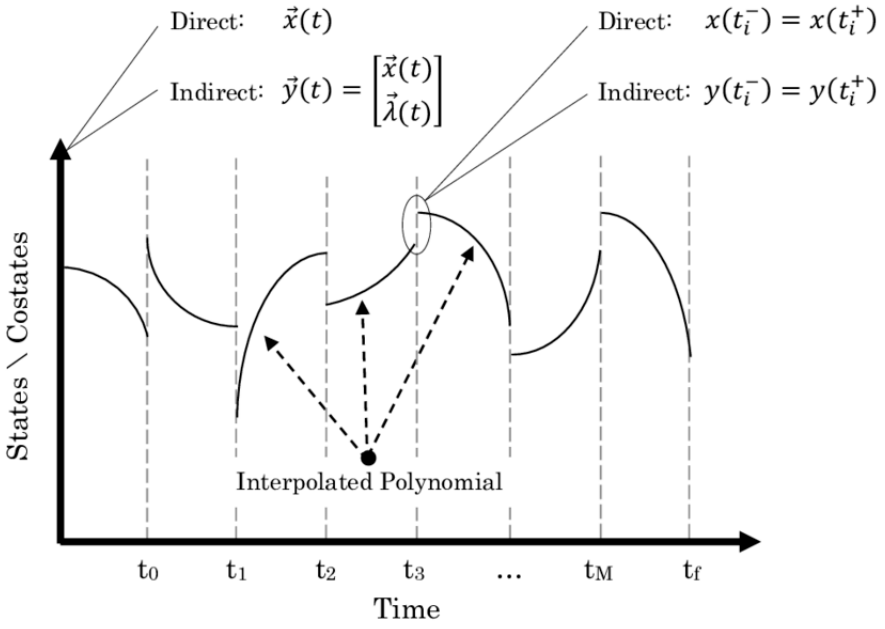

Figure 6.3: Shooting technique for a direct and indirect case[18]

6.6 Choice of solving method

In the light of what has been presented so far, the use of an analytical approach for finding the solution can be ruled out with certainty as it does not exist, given that for the trajectories considered, it is impossible to trace back to simple cases. Comparing the merits and demerits of direct and indirect methods, the question arises as to whether a less precise (and potentially sub-optimal) solution typical of direct methods is preferable to a solution with high precision but difficult to achieve due to the small convergence domain, i.e. an indirect method. Given the limited amount of fuel and the low thrust of the propulsion system, the aim is to obtain as correct a trajectory as possible in order to minimise subsequent corrections and minimise propellant usage, so it is clear that the indirect method is preferable. The techniques used are shooting techniques because of the simplicity of application to the case under consideration. In the present case, a simple shooting technique is used for trajectories, in which only the variables at the beginning of the arc need to be estimated. A code with an Adams-Moulton step and variable order integrator for solving ordinary differential equations and Newton's method for solving systems of non-linear equations was used for the calculation. The Hamiltonian has the following form:

$$H = \lambda^T \mathbf{f} + \mu^T \mathbf{g} + TS_F$$

Where SF is the switching function and is equal to:

$$SF = \frac{\lambda_v^T \mathbf{T}}{mT} - \frac{\lambda_m}{c}$$

With λ_m being the Lagrange coefficient of mass, λ_v being the added variables that compete with the last three equations of dynamics, those of velocities *(u, v, w)*, $\mathbf{g}$ is the vector of boundary conditions to which are associated Lagrange multipliers (constant over time) μ. Considering the equation defined in chapter 4, it is possible to write the Hamiltonian as:

$$\begin{aligned} H = {} & \lambda_r u + \lambda_\theta \frac{v}{r\cos\phi} + \lambda_\phi \frac{w}{r} \\ & + \lambda_u(-\frac{\mu}{r^2} + \frac{v^2}{2} + \frac{w^2}{2} + \frac{T}{m}\sin\gamma_T) \\ & + \lambda_v(-\frac{uv}{r} + \frac{vw}{r}\tan\phi + \frac{T}{m}\cos\gamma_T\cos\psi_T) \\ & + \lambda_w(-\frac{uw}{r} + \frac{v^2}{r}\tan\phi + \frac{T}{m}\cos\gamma_T\sin\psi_T) - \lambda_m\frac{T}{c} \end{aligned}$$

The direction of the thrust and its modulus are typically the control variables, which must maximise H in accordance with Pontryagin's Maximum Principle. The optimal direction of the thrust is obviously parallel to the added velocity vector λ_V. The thrust module, on the other hand, is derived from a *bang-bang* control mode:

- maximum if SF > 0;
- minimum(null) if SF < 0;
- Singular arch is SF $= 0$.

Since a constant effective exhaust velocity has been implemented, the modulus of the thrust is directly proportional to the flow rate and thus to the thrust power.

6.7 Boundary conditions

After obtaining the differential equations, it is necessary to impose the boundary conditions. In the case of rendezvous-only missions such as the one dealt with in this thesis, the spacecraft (S/C) at time t0 will have the same position and speed as the Earth and a certain initial mass:

$$\begin{aligned} \mathbf{r}_{S/C}(t_0) &= \mathbf{r}_{Earth}(t_0) \\ \mathbf{V}_{S/C}(t_0) &= \mathbf{V}_{Earth}(t_0) \\ m_0(t_0) &= 21\text{kg} \end{aligned}$$

When the asteroid is reached at time t_f, the position and speed of the aircraft must be equal to that of the object just reached:

$$\begin{aligned} \mathbf{r}_{S/C}(t_f) &= \mathbf{r}_{Asteroid}(t_f) \\ \mathbf{V}_{S/C}(t_f) &= \mathbf{V}_{Asteroid}(t_f) \end{aligned}$$

6.8 Initial Conditions

Initial conditions are required to carry out the integration of the differential equations. These values are contained inside the vector **p**:

$$\mathbf{p} = \begin{bmatrix} t_0 \\ t_f \\ r_0 \\ \theta_0 \\ \phi_0 \\ u_0 \\ v_0 \\ w_0 \\ \lambda_{r_0} \\ \lambda_{\theta_0} \\ \lambda_{\phi_0} \\ \lambda_{u_0} \\ \lambda_{v_0} \\ \lambda_{w_0} \end{bmatrix}$$

In the vector **p**:

- t_0 and t_f are the departure time from Earth and the arrival time at the asteroid;
- r_0, θ_0 and ϕ_0 represent the initial position of the spacecraft;
- u_0, v_0 and w_0 represent the initial velocity of the spacecraft;
- λ_{r_0}, λ_{θ_0}, λ_{ϕ_0}, λ_{u_0}, λ_{v_0} and λ_{w_0} represent the initial added variables.

As mentioned above, the added variables are indispensable for obtaining the optimal thrust direction:

$$T \sin \gamma_T = T \frac{\lambda_u}{\lambda_V}$$

$$T \cos \gamma_T \cos \phi_T = T \frac{\lambda_v}{\lambda_V}$$

$$T \cos \gamma_T \sin \phi_T = T \frac{\lambda_w}{\lambda_V}$$

The thrust obtained is parallel to the primer vector λ_V.
The quantities contained in the vector **p** are not all known a priori, so the problem goes from being a *boundary condition problem* (BVP) to an *initial condition problem* (IVP). The problem is solved with a shooting method, i.e. an initial solution of attempt **p** is assumed and the system of differential equations is integrated. The results are then compared with the boundary conditions: if the error is less than a certain tolerance, the initial values chosen are correct, otherwise a new set of initial parameters must be chosen. When the initial values are found, the optimal solution of the trajectory is also found, and

consequently also all information on how the quantities vary over time.
Before delving into the results, it's important to highlight that the script works with dimensionless parameters, in particular:

- The distances become dimensionless using the Sun-Earth mean distance:

$$r_{conv} = 1.4959 * 10^8 \text{km}$$

- The velocities become dimensionless using the Earth circular velocity:

$$V_conv = \sqrt{\frac{\mu_\odot}{r_{conv}}} = 29.784 \text{km/s}$$

- The accelerations become dimensionless using the Earth acceleration around the sun:

$$a_{conv} = \frac{\mu_\odot}{r_{conv}}^2 = 5.93 \cdot 10^{-6} \text{km}/s^2$$

- The time become dimensionless using the relation:

$$t_{conv} = \frac{V_{conv}}{a_{conv} * 86400} = 58.1324 \text{days}$$

- The dates are dimensionless and start from 1/1/2000 with a value of 0, to continue with the time t_{conv}.

Chapter 7

Results

After defining the mission, its purposes and characteristics, and after delving into the physical and mathematical models and strategies applied to optimise the trajectory, it is now possible to present and analyse the results obtained.
For ease of reading, the orbital parameters of the asteroids under consideration are given below, the choice of which was discussed in Chapter 3.3.

Designation	Epoch [MJD]	a [AU]	e [AU]	i [deg]	ω	Ω	M [deg]
REF	61771	1.1	0.1	2	0	0	-35.36529
AM	61771	1.05	0.1	2	0	0	116.36661
AP	61771	1.15	0.1	2	0	0	-8.301583
EM	61771	1.1	0.05	2	0	0	-35.36529
EP	61771	1.1	0.15	2	0	0	-35.36529
IM	61771	1.1	0.1	1	0	0	-35.36529
IP	61771	1.1	0.1	3	0	0	-35.36529

Table 7.1: Main asteroids in analysis

Designation	Epoch [MJD]	a [AU]	e [AU]	i [deg]	ω	Ω	M [deg]
REF	61771	1.1	0.1	2	0	0	-35.36529
AM1	61771	1.075	0.1	2	0	0	124.81543
AP1	61771	1.125	0.1	2	0	0	-12.49047
EM1	61771	1.1	0.075	2	0	0	-35.36529
EP1	61771	1.1	0.125	2	0	0	-35.36529
IM1	61771	1.1	0.1	1.5	0	0	-35.36529
IP1	61771	1.1	0.1	2.5	0	0	-35.36529

Table 7.2: Intermediate Asteroids

Intermediate asteroids will only be used to verify that the code is working correctly and that the chosen initial conditions do not cause the problem to converge to incorrect values.

Three Fortran codes were used to carry out the trajectory analyses, which were developed to solve the optimal problem through an iterative procedure, the aim of which is to find a thrust strategy that allows the mission to be completed with the highest possible final mass.

7.1 Initial case

The first analysis was carried out by studying the trajectories to the various asteroids, using the orbital parameters defined during the asteroid selection phase, and looking for the minimum mission duration for each asteroid.
The minimum duration for each trajectory to converge is 988.25 days, which corresponds to approximately 2.7 years. This duration will be used in every discussion from now on.
The attempt solution required for the code to run was completed by using as the arrival time the time returned by the *scanesa.for* script with which the asteroids were classified and as the departure time, the arrival time from which the desired mission duration was subtracted. The objective of this initial analysis phase was to obtain the departure and arrival dates of the trips and the final optimised mass values, the value of which was obtained by passing the script a value of t_0 equal to zero,which triggers the search for the optimal departure date.
At the end of this analysis, the optimal final mass and consumed propellant values were collected and are reported below. From the values of consumed propellant mass, it can

DES	DEPARTURE	ARRIVAL	**FINAL MASS (kg)**	**FUEL MASS (kg)**
REF	8/ 5/2031	21/ 1/2034	18.7536	2.2464
AM	13/ 3/2026	25/11/2028	18.9454	2.0546
AM1	14/ 4/2027	27/12/2029	18.8716	2.1284
AP1	8/ 5/2030	21/ 1/2033	18.3887	2.6113
AP	20/ 6/2030	4/ 3/2033	18.3387	2.6613
EM	30/ 4/2031	13/ 1/2034	19.1905	1.8095
EM1	6/ 5/2031	18/ 1/2034	19.0386	1.9614
EP1	12/ 5/2031	24/ 1/2034	18.3679	2.6321
EP	29/ 3/2030	11/12/2032	17.2994	3.7006
IM	4/ 5/2031	17/ 1/2034	19.1226	1.8774
IM1	6/ 5/2031	19/ 1/2034	18.9597	2.0403
IP1	12/ 5/2031	24/ 1/2034	18.5067	2.4933
IP	16/ 5/2031	28/ 1/2034	18.2031	2.7969

be deduced that the most difficult asteroids to reach, in other words those requiring greater propulsive effort and fuel consumption, are those with increased orbital parameters compared to the reference case, while the easiest asteroids to reach are those with smaller orbital parameters compared to the reference case. It should be noted that the easiest asteroid and the hardest to reach asteroid both fall into the group of asteroids with a varied eccentricity. The graphs containing the final mass and the propellant mass trends for the various asteroids under consideration are shown below.

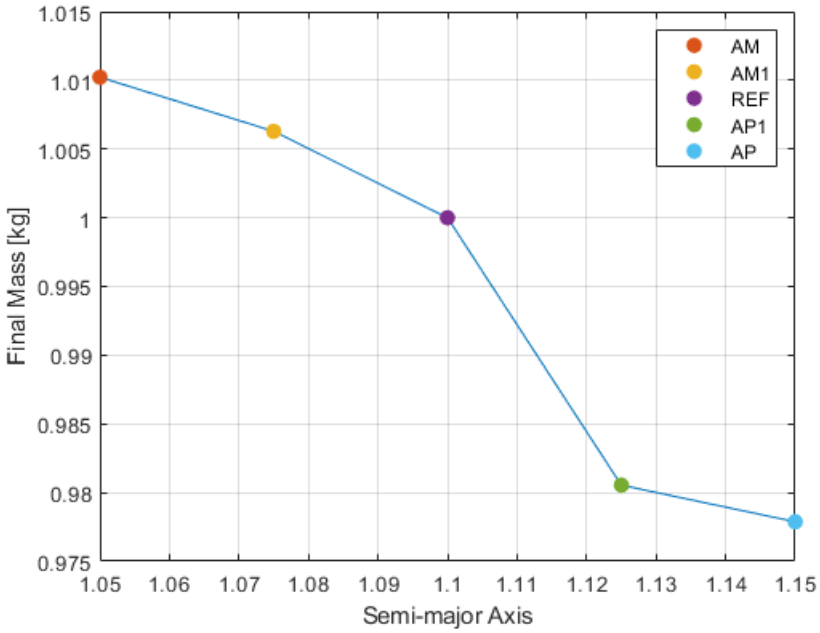

Figure 7.1: Relationship between semimajor-axis and final mass

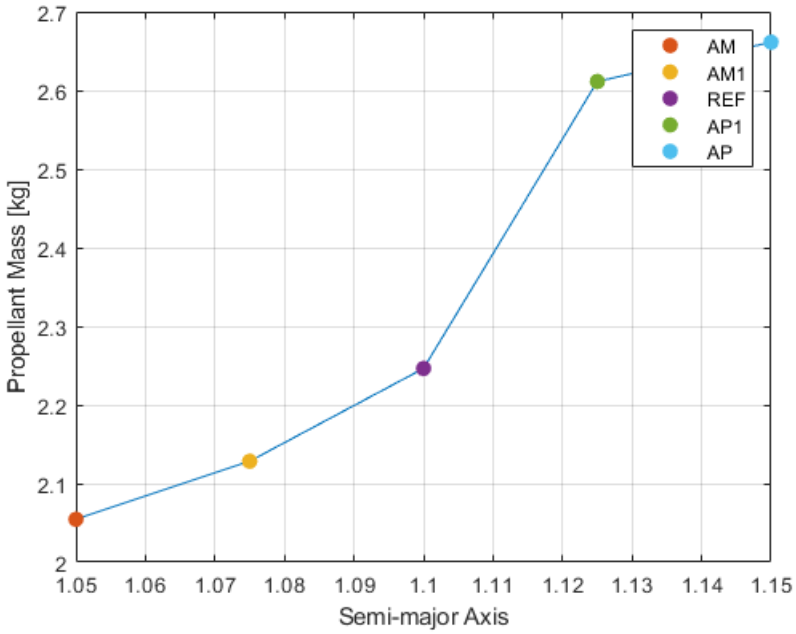

Figure 7.2: Relationship between semimajor-axis and propellant mass

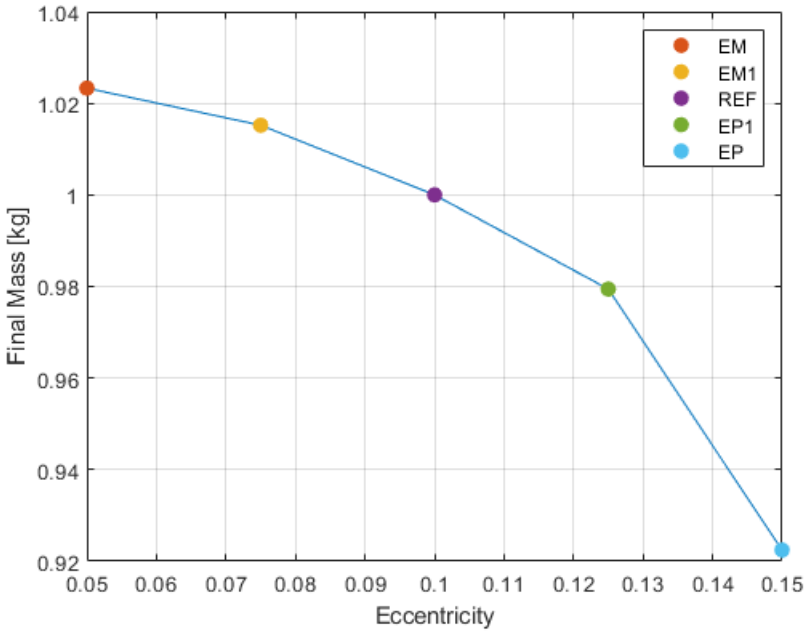

Figure 7.3: Relationship between eccentricity and final mass

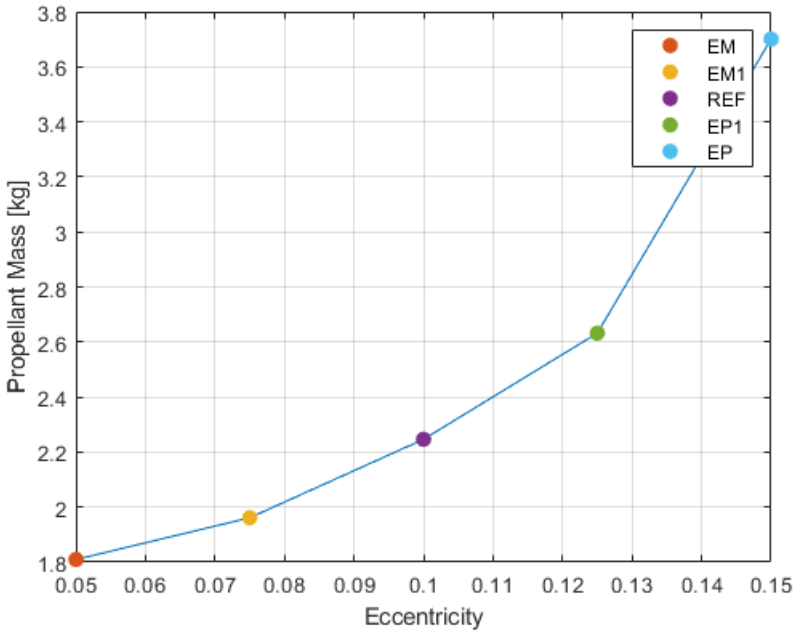

Figure 7.4: Relationship between eccentricity and propellant mass

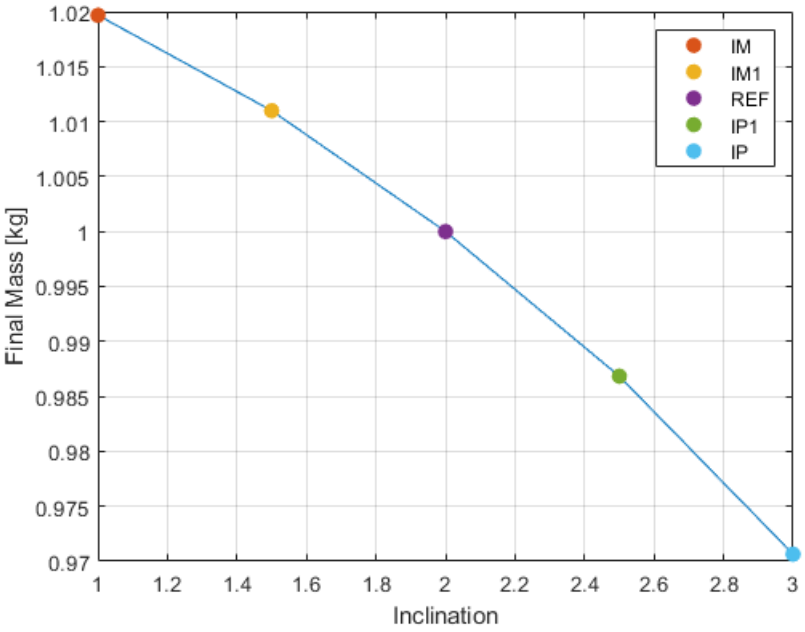

Figure 7.5: Relationship between inclination and final mass

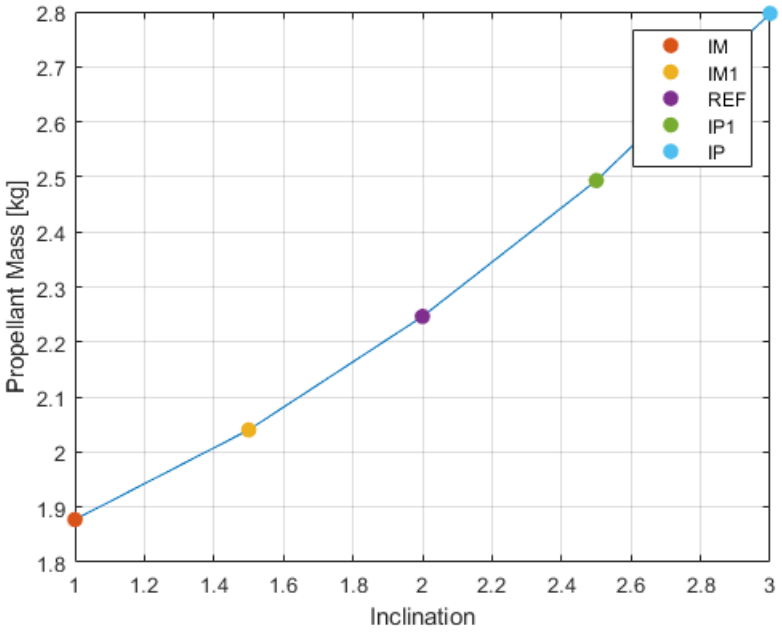

Figure 7.6: Relationship between inclination and propellant mass

7.2 Finding the optimal mean anomaly

After determining the final mass values for the asteroids under examination, the next step is to optimise the mission by focusing on another crucial aspect: the mean anomaly. The objective of this section is to identify the optimal mean anomaly value for the asteroids that, while keeping the mission duration constant and equal to 988.25 days, maximizes the final mass of the spacecraft. This optimisation is essential because an increase in the final mass corresponds to a reduction in the amount of propellant required to reach the target asteroid. Changing the mean anomaly of asteroids obviously also changes the phase angle between asteroid and earth, so optimising the mean anomaly results in optimising the phase angle between earth and asteroid at t_0. The new optimised final mass values are shown in the tables below:

DES	DEPARTURE	ARRIVAL	**FINAL MASS (kg)**	**FUEL MASS (kg)**
REF	15/ 5/2031	27/ 1/2034	18.8353	2.1647
AM	19/ 3/2030	1/12/2032	19.0411	1.9589
AM1	13/ 4/2027	26/12/2029	18.8781	2.1219
AP1	3/ 6/2030	15/ 2/2033	18.5941	2.4059
AP	3/ 7/2030	18/ 3/2033	18.4405	2.5595
EM	6/ 5/2031	19/ 1/2034	19.2187	1.7813
EM1	6/ 5/2031	18/ 1/2034	19.0422	1.9578
EP1	12/ 5/2031	25/ 1/2034	18.3840	2.6160
EP	20/ 5/2030	1/ 2/2033	18.0189	2.9810
IM	10/ 5/2031	23/ 1/2034	19.2124	1.7876
IM1	7/ 5/2031	19/ 1/2034	18.9662	2.0338
IP1	11/ 5/2031	24/ 1/2034	18.5147	2.4853
IP	20/ 5/2031	1/ 2/2034	18.2840	2.7160

Table 7.3: Final mass relative to optimum M

DES	**FUEL MASS (kg)** (M_{OPT})	**FUEL MASS (kg)**	**Δ Fuel Mass**
REF	2.1647	2.2464	-3.6369
AM	1.9589	2.0546	-4.6578
AM1	2.1219	2.1284	-0.3054
AP1	2.4059	2.6113	-7.8658
AP	2.5595	2.6613	-3.8252
EM	1.7813	1.8095	-1.5584
EM1	1.9578	1.9614	-0.1835
EP1	2.6160	2.6321	-0.6117
EP	2.9810	3.7006	-19.4455
IM	1.7876	1.8774	-4.7832
IM1	2.0338	2.0403	-0.3186
IP1	2.4853	2.4933	-0.3209
IP	2.7160	2.7969	-2.8925

Table 7.4: Final mass with optimum M VS Final mass

As can be seen from table 7.4, lower propellant consumption is achieved if the "time free" solution is used and the code calculates the optimal position of the asteroid at the time of departure.
Before delving into the trajectories to reach the various asteroids, please note that from this point on, only the main asteroids will be used for the analyses and how the mean anomalies of these have been changed by applying the ΔM calculated using the tstar value.

Designation	Epoch [MJD]	a [AU]	e [AU]	i [deg]	ω	Ω	M [deg]
REF	61771	1.1	0.1	2	0	0	-29.35517
AM	61771	1.05	0.1	2	0	0	125.42800
AP	61771	1.15	0.1	2	0	0	6.31658
EM	61771	1.1	0.05	2	0	0	-31.46614
EP	61771	1.1	0.15	2	0	0	-87.71435
IM	61771	1.1	0.1	1	0	0	-29.89938
IP	61771	1.1	0.1	3	0	0	-28.95264

Table 7.5: Main asteroids in analysis with the optimal mean anomaly

7.2.1 REF

The first trajectory analysed is that directed towards the reference asteroid REF, whose orbital parameters are given below:

a	e	i	Ω	ω	M
1.1 AU	0.1	2°	0	0	-29.355°

Table 7.6: Orbital parameters of REF at epoch 61771 MJD

As explained above, this is the optimal starting position for this asteroid while the optimal departure date is shown in the following table:

Asteroid	Departure Date	Arrival Date	ΔV
REF	15/05/2031	27/01/2034	2.240325 km/s

The duration of the mission is approximately 2 years and 8 months.

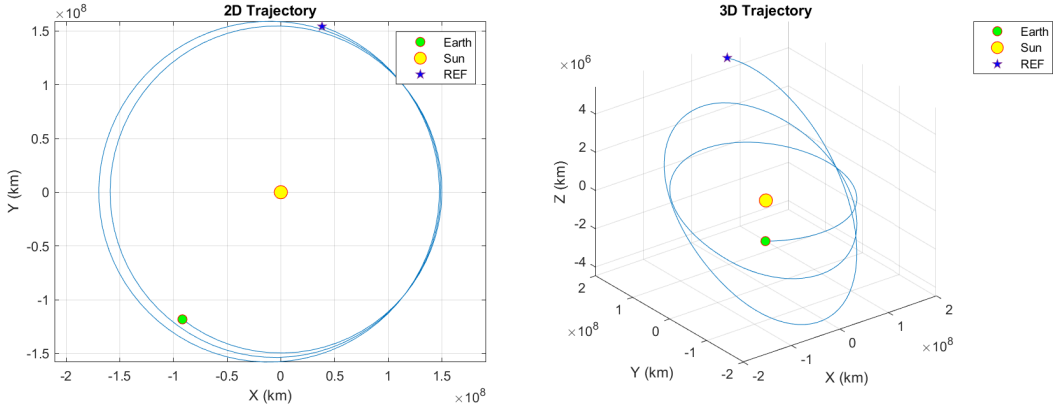

Figure 7.7: 2D and 3D Trajectories in a heliocentric reference frame

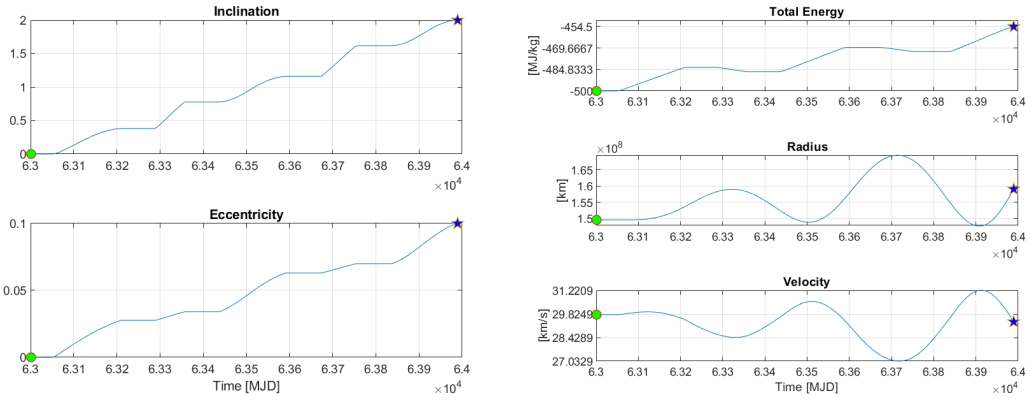

Figure 7.8: Trends of inclination, eccentricity, energy, velocity and radius

From the eccentricity and inclination graphs 7.8, it can be deduced that the engines are

on for most of the transfer, with short periods of non-propelled coasting. The semi-axis change is carried out mainly in the final part, in fact the graphs show how the speed decreases and the radius increases before reaching the asteroid under examination.
The final mass of the spacecraft is 18.83 kg, so the propellant consumption is about 2.1647 kg, with the trend reported in 7.9.

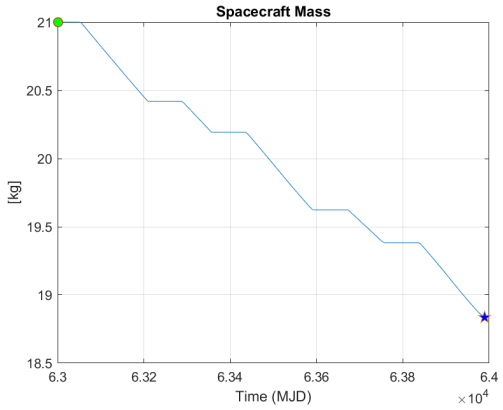

Figure 7.9: Total Mass versus Time

At the moment of departure the spacecraft has its engines switched off and the thrust strategy consists of five distinct moments of thrust. It can be seen that there are longer thrust moments interspersed with shorter ones and that thrust always occurs on all three axes.

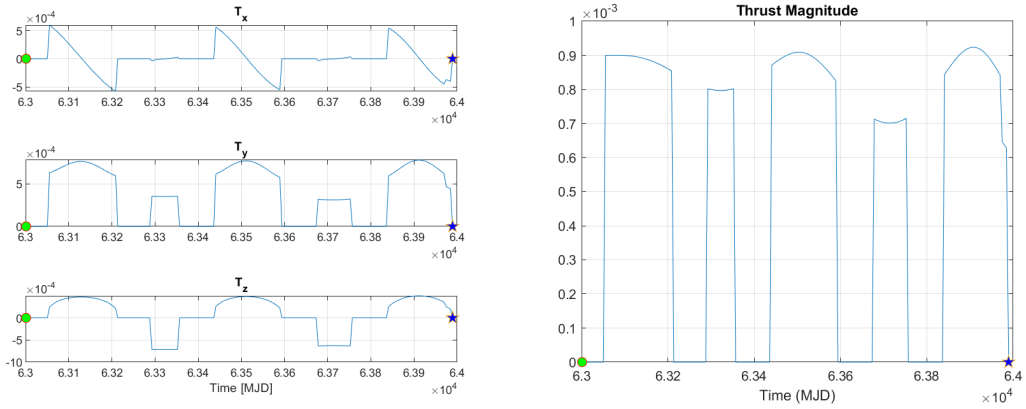

Figure 7.10: Components and magnitude of thrust T

7.2.2 AM

The second asteroid under analysis is AM, whose orbital parameters are given below:

a	**e**	**i**	Ω	ω	**M**
1.05 AU	0.1	2°	0	0	125.428°

Table 7.7: Orbital parameters of AM at epoch 61771 MJD

As explained above, this is the optimal starting position for this asteroid while the optimal departure date is shown in the following table:

Asteroid	**Departure Date**	**Arrival Date**	ΔV
AM	19/03/2030	1/12/2032	2.016587 km/s

The duration of the mission is approximately 2 years and 8 months.

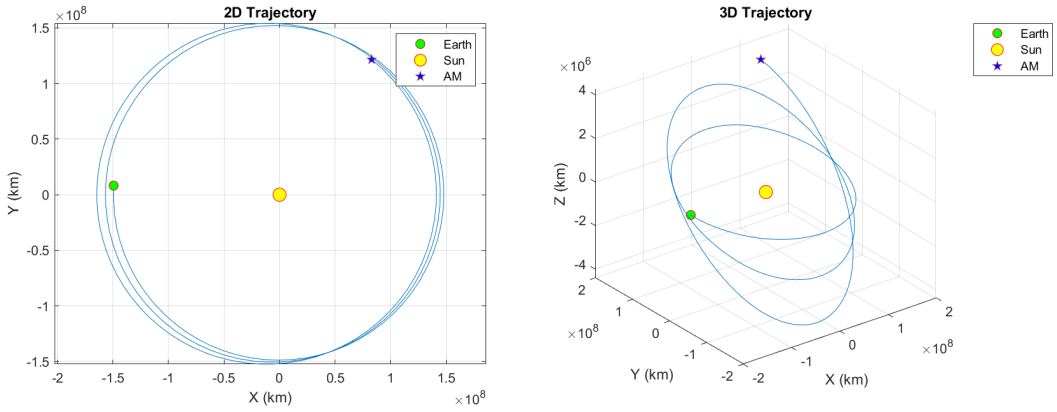

Figure 7.11: 2D and 3D Trajectories in a heliocentric reference frame

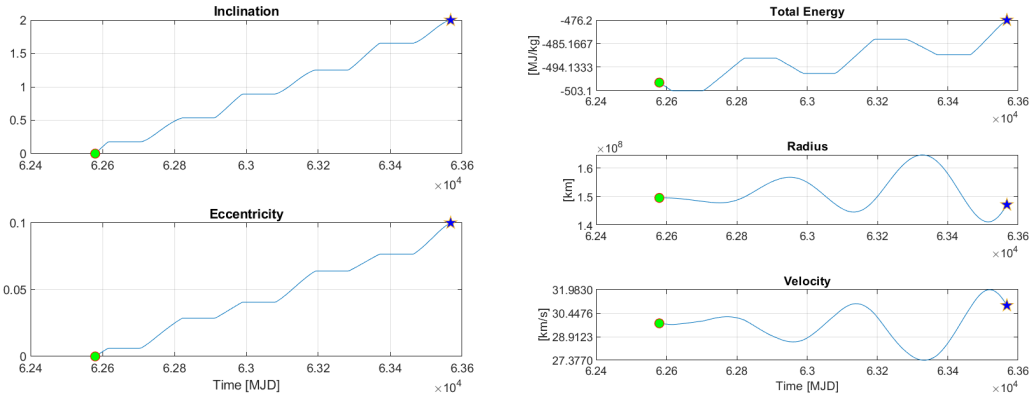

Figure 7.12: Trends of inclination, eccentricity, energy, velocity and radius

From the eccentricity and inclination graphs 7.12, it can be deduced that the engines are

on for most of the transfer, with short periods of non-propelled coasting. The semi-axis change is carried out mainly in the final part, in fact the graphs show how the speed increases and the radius decreases before reaching the asteroid under examination.
The final mass of the spacecraft is 19.04 kg, so the propellant consumption is about 1.9589 kg, with the trend reported in 7.13.

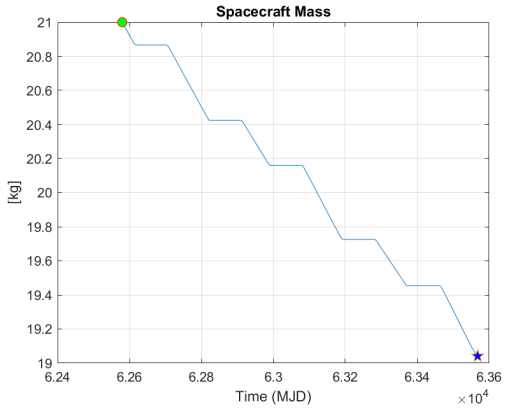

Figure 7.13: Total Mass versus Time

At the moment of departure the spacecraft has its engines switched on and the thrust strategy consists of six distinct moments of thrust. It can be seen that there are longer thrust moments interspersed with shorter ones. Note also how the spacecraft arrives at the rendezvous with the asteroid with the thrusters still on.

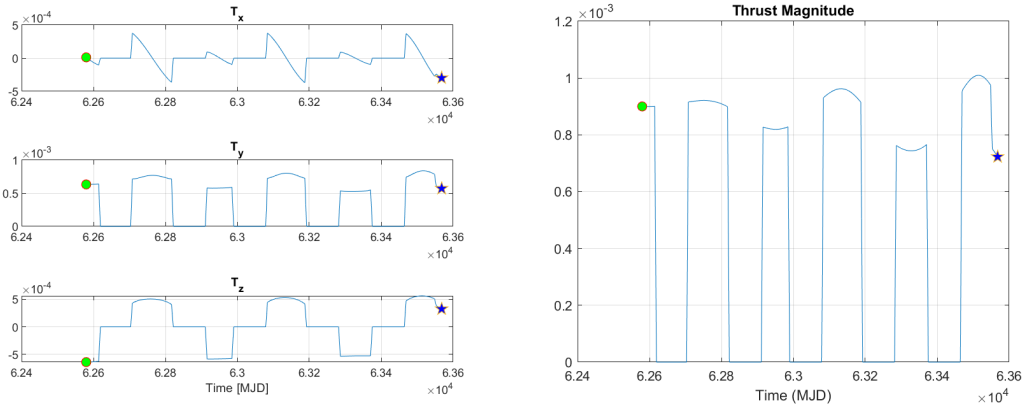

Figure 7.14: Components and magnitude of thrust T

7.2.3 AP

The next asteroid under analysis is AP, whose orbital parameters are given below:

a	e	i	Ω	ω	M
1.15 AU	0.1	2°	0	0	6.316°

Table 7.8: Orbital parameters of AP at epoch 61771 MJD

As explained above, this is the optimal starting position for this asteroid while the optimal departure date is shown in the following table:

Asteroid	Departure Date	Arrival Date	ΔV
AP	03/07/2030	18/03/2033	2.676608 km/s

The duration of the mission is approximately 2 years and 8 months.

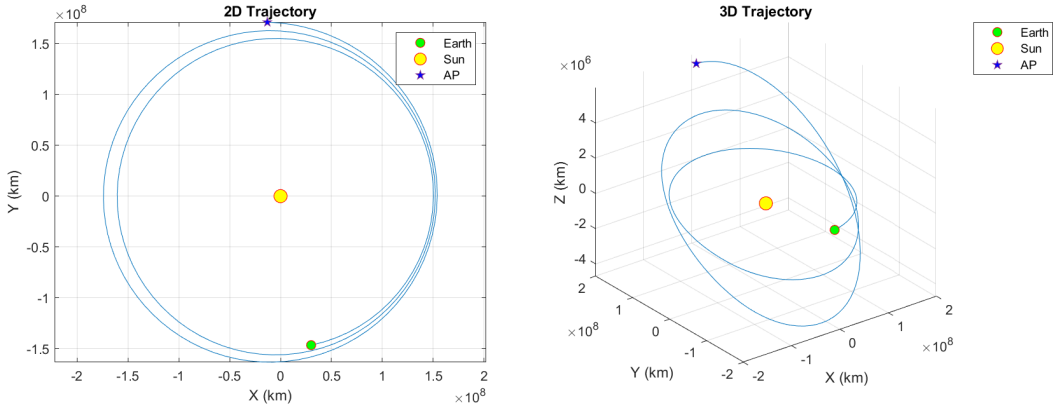

Figure 7.15: 2D and 3D Trajectories in a heliocentric reference frame

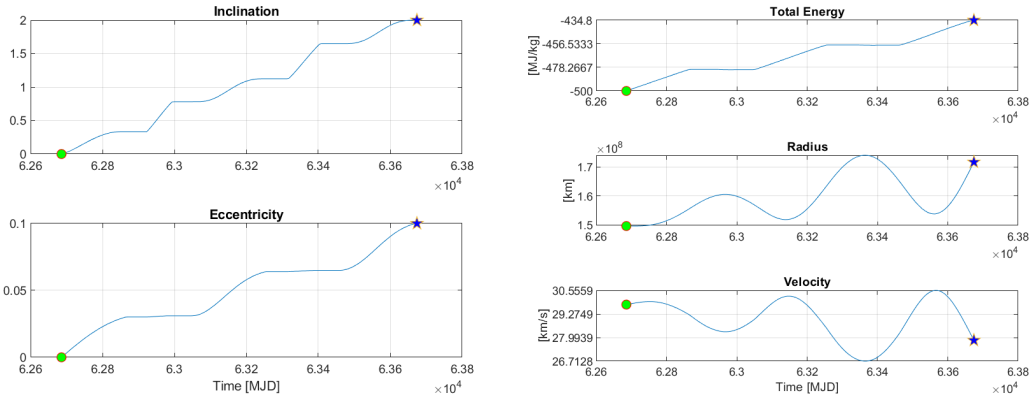

Figure 7.16: Trends of inclination, eccentricity, energy, velocity and radius

From the eccentricity and inclination graphs 7.16, it can be deduced that the engines are

on for most of the transfer, with short periods of non-propelled coasting. The semi-axis change is carried out mainly in the final part, in fact the graphs show how the speed decreases and the radius increases before reaching the asteroid under examination.
The final mass of the spacecraft is 18.44 kg, so the propellant consumption is about 2.5595 kg, with the trend reported in 7.17.

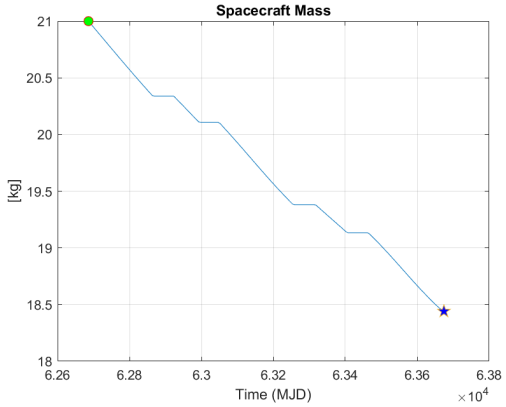

Figure 7.17: Total Mass versus Time

At the moment of departure the spacecraft has its engines switched on and the thrust strategy consists of 5 distinct moments of thrust. It can be seen that there are longer thrust moments interspersed with shorter ones. Note also how the spacecraft arrives at the rendezvous with the asteroid with the thrusters still on.

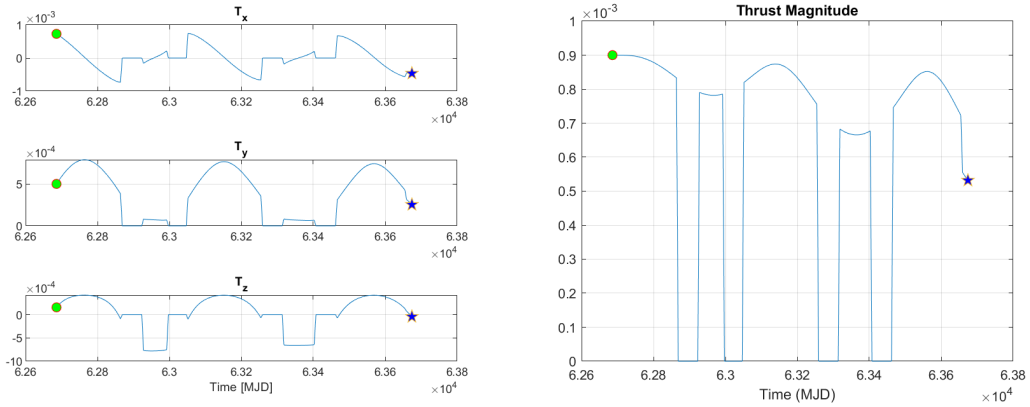

Figure 7.18: Components and magnitude of thrust T

7.2.4 EM

Now the family of asteroids with a variation in eccentricity value with respect to the reference asteroid is analysed. The first asteroid analysed is EM, whose orbital parameters

are given below:

a	**e**	**i**	Ω	ω	**M**
1.1 AU	0.05	2°	0	0	-31.466°

Table 7.9: Orbital parameters of EM at epoch 61771 MJD

As explained above, this is the optimal starting position for this asteroid while the optimal departure date is shown in the following table:

Asteroid	**Departure Date**	**Arrival Date**	ΔV
EM	06/05/2031	19/01/2034	1.825364 km/s

The duration of the mission is approximately 2 years and 8 months.

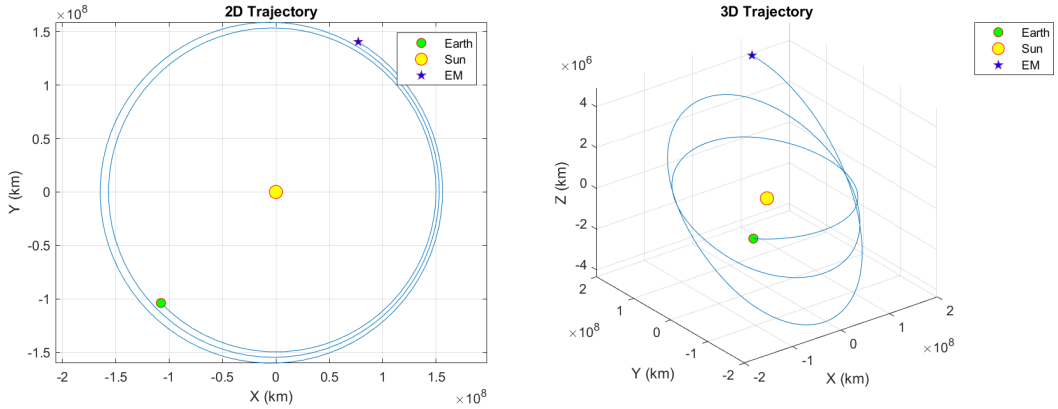

Figure 7.19: 2D and 3D Trajectories in a heliocentric reference frame

From the eccentricity and inclination graphs 7.20, it can be deduced that the engines are on for most of the transfer, with short periods of non-propelled coasting.
The final mass of the spacecraft is 19.22 kg, so the propellant consumption is about 1.7813 kg, with the trend reported in 7.21.

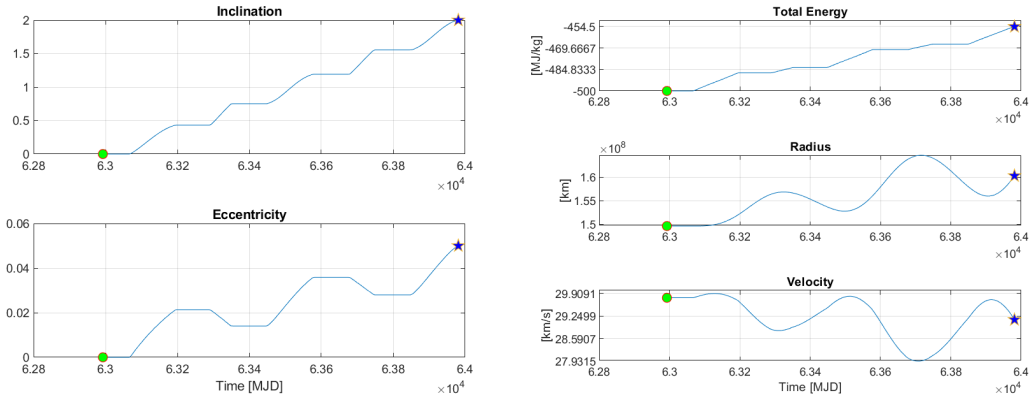

Figure 7.20: Trends of inclination, eccentricity, energy, velocity and radius

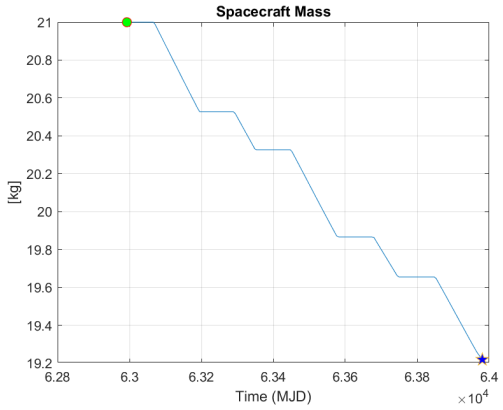

Figure 7.21: Total Mass versus Time

At the moment of departure the spacecraft has its engines switched off and it does a short period of coasting and the thrust strategy consists of 5 distinct moments of thrust. It can be seen that there are longer thrust moments interspersed with shorter ones. Note also how the spacecraft arrives at the rendezvous with the asteroid with the thrusters off and how the thruster when is on has always the three components different from zero.

7.2.5 EP

In the family of asteroids with a variation in eccentricity value with respect to the reference asteroid there is EP, whose orbital parameters are given below:

a	**e**	**i**	Ω	ω	**M**
1.1 AU	0.15	2°	0	0	-87.714°

Table 7.10: Orbital parameters of EP at epoch 61771 MJD

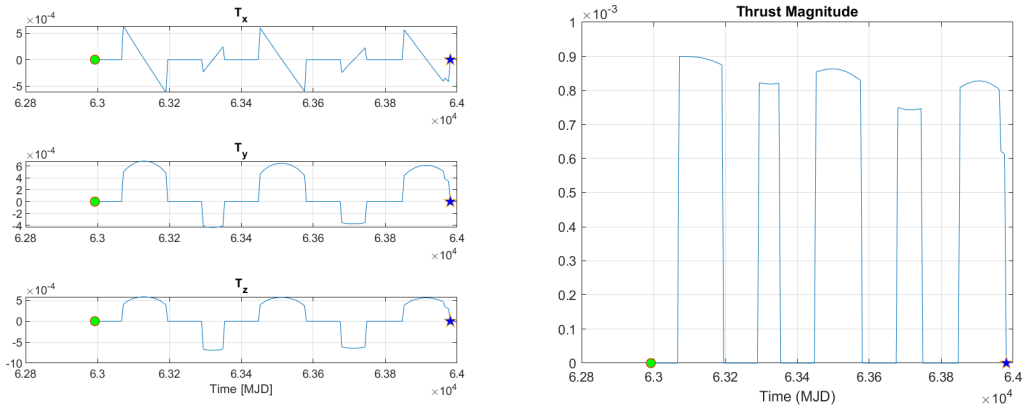

Figure 7.22: Components and magnitude of thrust T

This is the optimal starting position for this asteroid while the optimal departure date is shown in the following table:

Asteroid	**Departure Date**	**Arrival Date**	ΔV
EP	20/05/2030	01/02/2033	3.152850 km/s

The duration of the mission is approximately 2 years and 8 months.

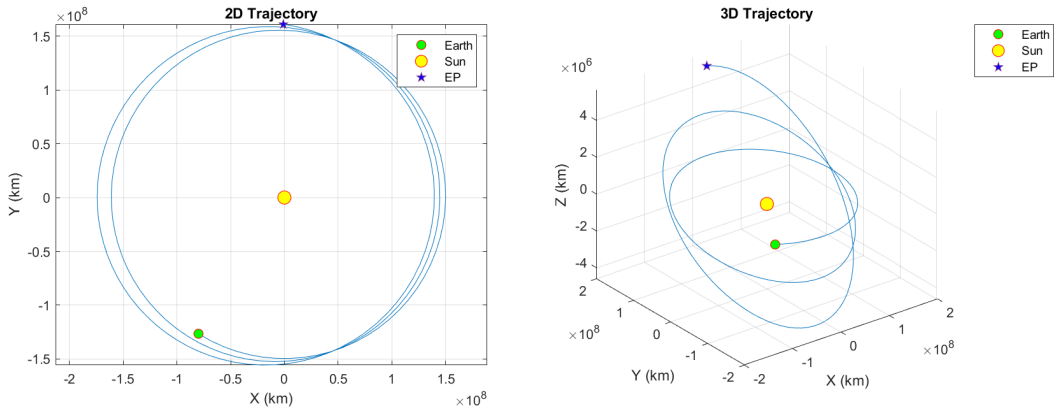

Figure 7.23: 2D and 3D Trajectories in a heliocentric reference frame

From the eccentricity and inclination graphs 7.24, it can be deduced that the engines are on for most of the transfer, with short periods of non-propelled coasting.
The final mass of the spacecraft is 18.01 kg, so the propellant consumption is about 2.9810 kg, with the trend reported in 7.25. Consequently, EP is the most onerous asteroid to reach in terms of consumption.

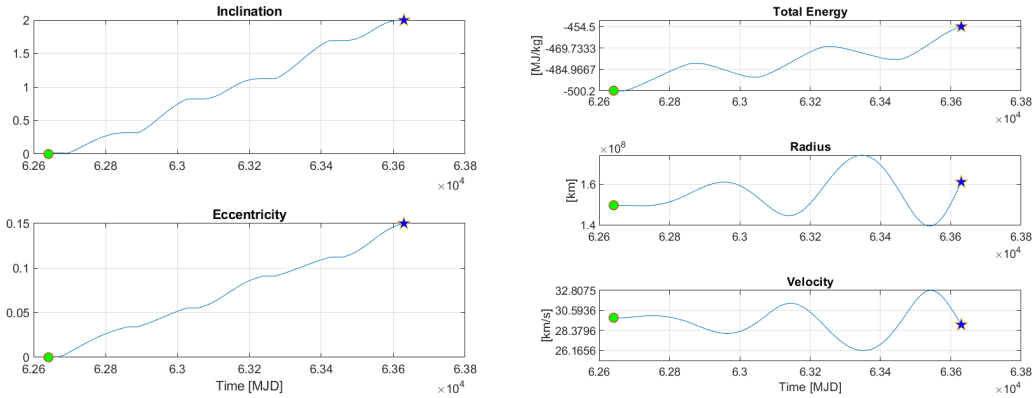

Figure 7.24: Trends of inclination, eccentricity, energy, velocity and radius

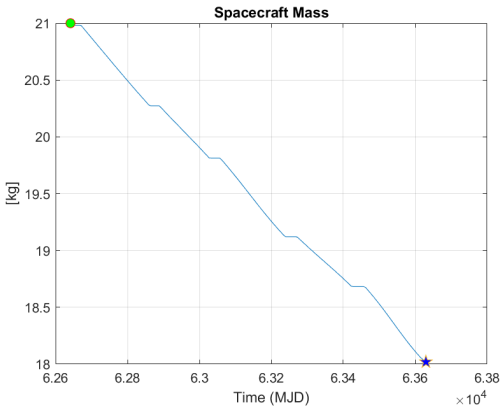

Figure 7.25: Total Mass versus Time

At the moment of departure the spacecraft has its engines switched on and the thrust strategy consists of 6 distinct moments of thrust. It can be seen that there are longer thrust moments interspersed with shorter ones. Note also how the spacecraft arrives at the rendezvous with the asteroid with the thrusters on and how the thruster when is on has always the three components different from zero.

7.2.6 IM

Now the family of asteroids with a variation in inclination value with respect to the reference asteroid is analysed. The first asteroid analysed is IM, whose orbital parameters are given below:

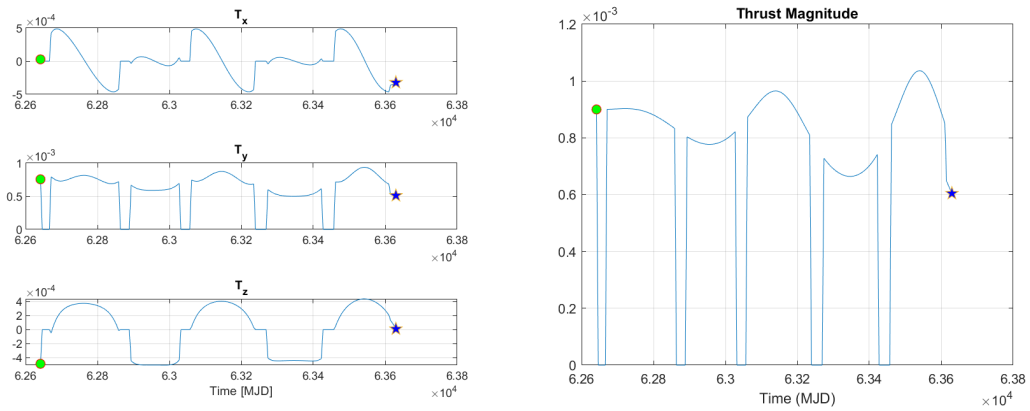

Figure 7.26: Components and magnitude of thrust T

a	e	i	Ω	ω	M
1.1 AU	0.1	1°	0	0	-29.890°

Table 7.11: Orbital parameters of IM at epoch 61771 MJD

This is the optimal starting position for this asteroid while the optimal departure date is shown in the following table:

Asteroid	Departure Date	Arrival Date	ΔV
IM	10/05/2031	23/01/2034	1.832147 km/s

The duration of the mission is approximately 2 years and 8 months.

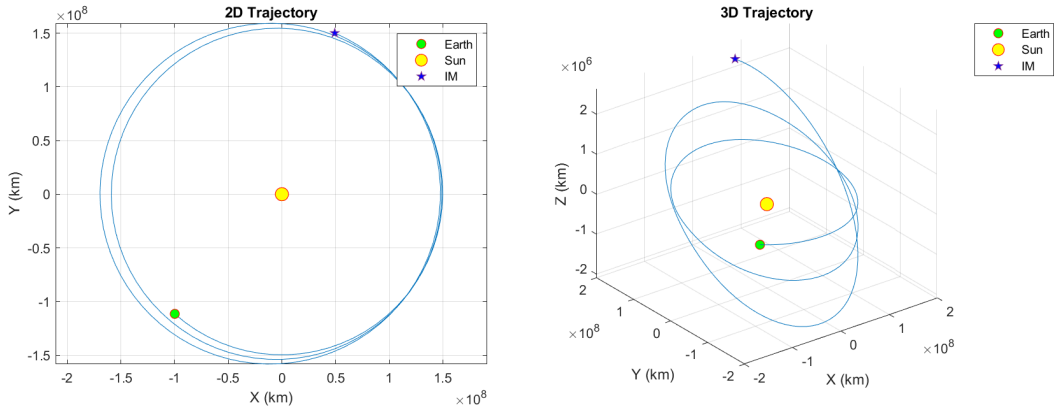

Figure 7.27: 2D and 3D Trajectories in a heliocentric reference frame

From the eccentricity and inclination graphs 7.28, it can be deduced that the engines are

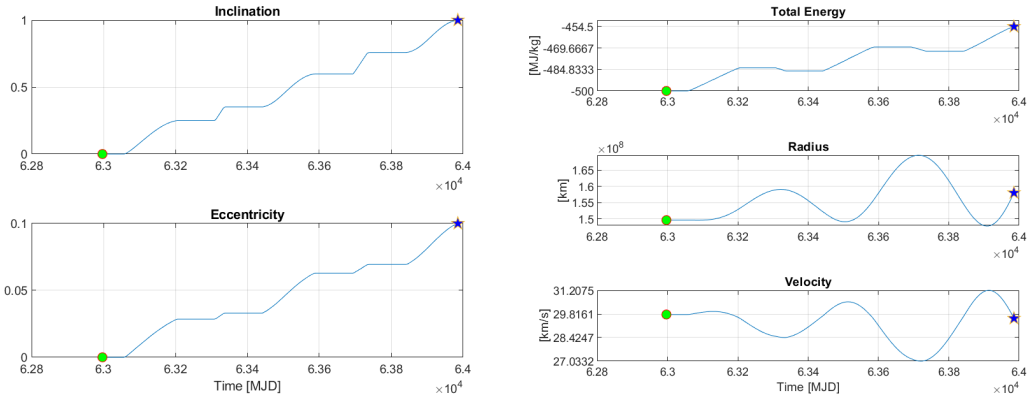

Figure 7.28: Trends of inclination, eccentricity, energy, velocity and radius

on for most of the transfer, with short periods of non-propelled coasting.
The final mass of the spacecraft is 19.21 kg, so the propellant consumption is about 1.7876 kg, with the trend reported in 7.29.

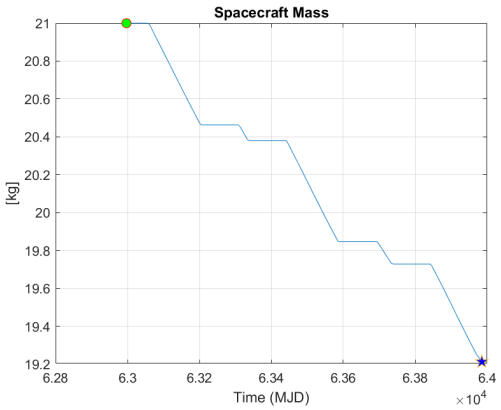

Figure 7.29: Total Mass versus Time

At the moment of departure the spacecraft has its engines switched off and the thrust strategy consists of 5 distinct moments of thrust. It can be seen that there are longer thrust moments interspersed with shorter ones. Note also how the spacecraft arrives at the rendezvous with the asteroid with the thrusters off and how, when the thruster is on, has always the three components different from zero.

7.2.7 IP

The last asteroid analysed is IP, whose orbital parameters are given below:

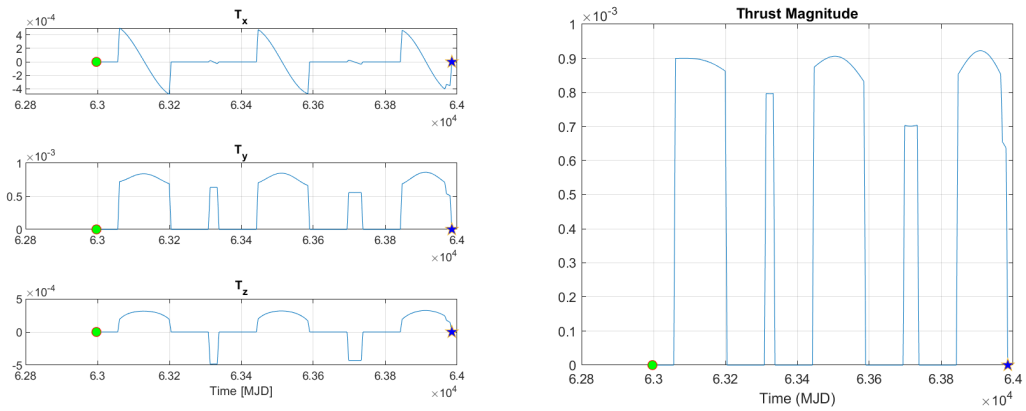

Figure 7.30: Components and magnitude of thrust T

a	e	i	Ω	ω	M
1.1 AU	0.1	3°	0	0	-28.952°

Table 7.12: Orbital parameters of IP at epoch 61771 MJD

This is the optimal starting position for this asteroid while the optimal departure date is shown in the following table:

Asteroid	Departure Date	Arrival Date	ΔV
IP	20/05/2031	01/02/2034	2.852169 km/s

The duration of the mission is approximately 2 years and 8 months.

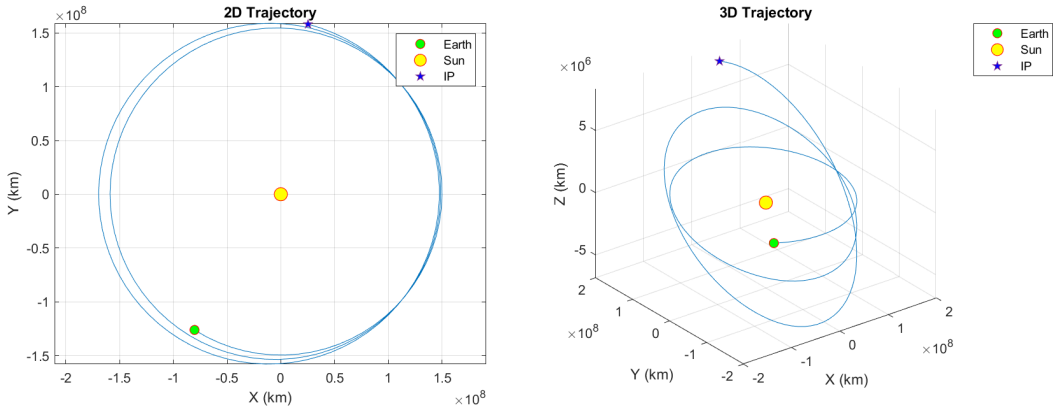

Figure 7.31: 2D and 3D Trajectories in a heliocentric reference frame

From the eccentricity and inclination graphs 7.32, it can be deduced that the engines are

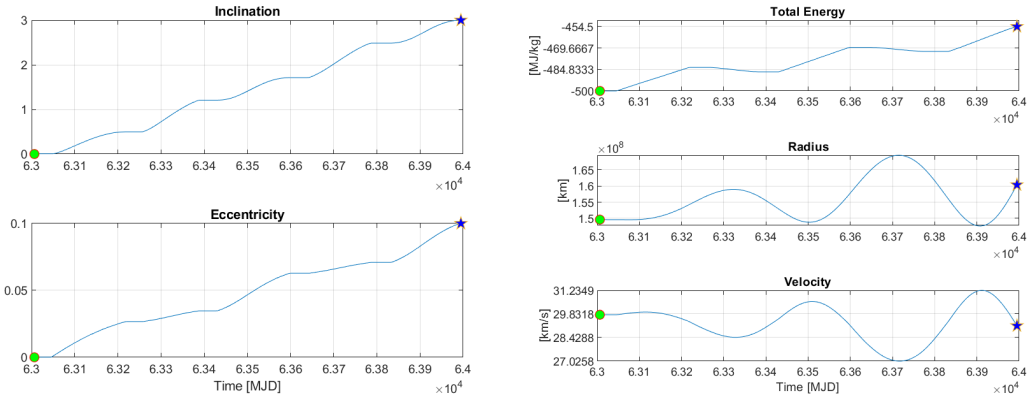

Figure 7.32: Trends of inclination, eccentricity, energy, velocity and radius

on for most of the transfer, with short periods of non-propelled coasting. The semi-axis change is carried out mainly in the final part, in fact the graphs show how the speed decreases and the radius increases before reaching the asteroid under examination.
The final mass of the spacecraft is 18.28 kg, so the propellant consumption is about 2.7160 kg, with the trend reported in 7.33.

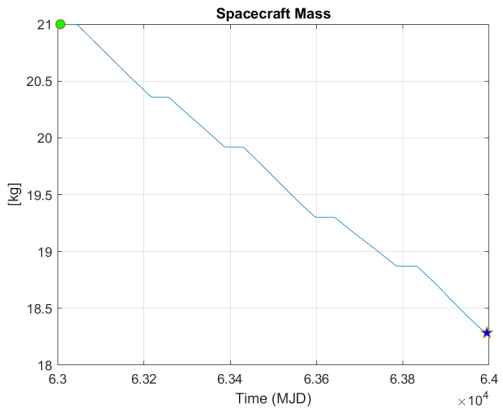

Figure 7.33: Total Mass versus Time

At the moment of departure the spacecraft has its engines switched on and the thrust strategy consists of 6 distinct moments of thrust. It can be seen that there are longer thrust moments interspersed with shorter ones. Note also how the spacecraft arrives at the rendezvous with the asteroid with the thrusters still on and how, when the thruster is on, has always the three components different from zero.

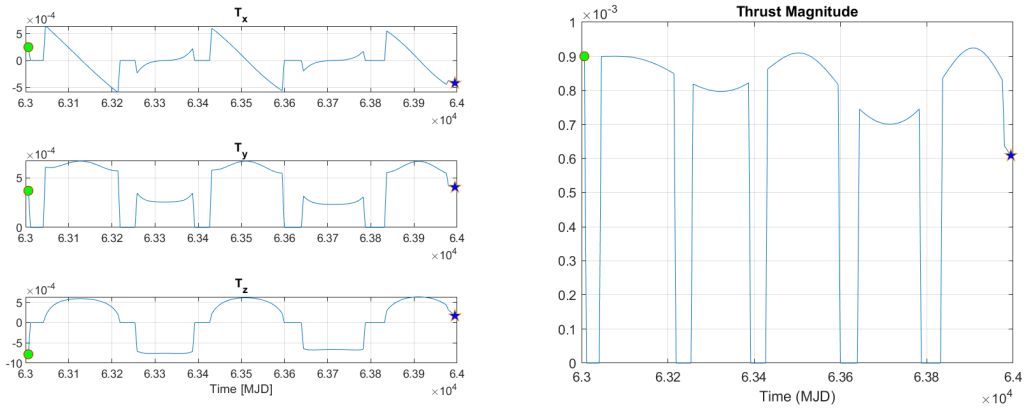

Figure 7.34: Components and magnitude of thrust T

7.3 Impact of Mean Anomaly Variations on Propellant Consumption

This section explores the relationship between variations in mean anomaly and propellant consumption. The subsequent analysis will explore several scenarios, each characterized by a different deviation from the mean anomaly optimum values found in the previous section. It will be evaluated the corresponding changes in propellant consumption, identifying patterns and quantifying the effects of these variations and understand whether the change in propellant mass is symmetrical, so if moving the asteroid forward by a ΔM or backward by the same amount generates the same effect.
This investigation aims to provide a comprehensive understanding of how maintaining or deviating from the optimum mean anomaly value affects propellant requirements, ultimately contributing to more efficient space missions and better propellant management, which allows the mass of transportable payload to be increased.
A total of six cases per asteroid will be analysed:

$$\Delta M = \left[-20°, \quad -10°, \quad -5°, \quad +5°, \quad +10°, \quad +20°\right]$$

After obtaining all the trajectories for each case under consideration, the results were analysed and plotted, which will be reported and discussed below.
The first thing analysed is the deviation of the final mass of the individual cases from the optimum case, the graph of which is shown in 7.35. It can be seen from the graph that the variations with respect to the reference case are not symmetrical, and in some cases they show a considerable difference, the causes of which will be investigated later. It should also be noted that the trajectories that are most affected by the shift from optimal M are those to reach the AP and EP asteroids, a phenomenon that is also confirmed by the graph 7.36, containing the trend in the mass of propellant consumed for various ΔM. The exact values of the final and consumed propellant masses are given in the appendix B.
The following table shows the percentage increase in propellant mass compared to the optimum case:

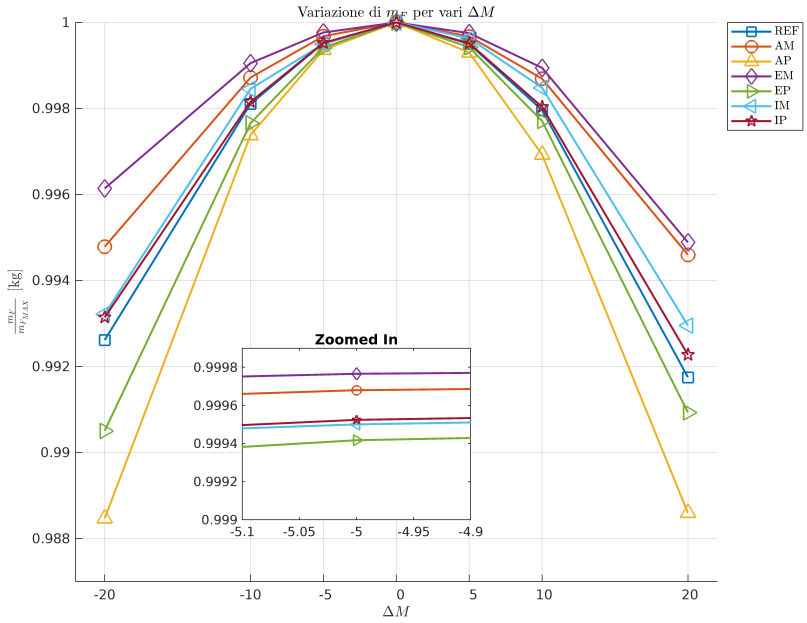

Figure 7.35: Final masses normalised to optimal case

DES	ΔM = -20	ΔM = -10	ΔM = -5	ΔM = 5	ΔM = 10	ΔM = 20
REF	6.4258	1.6492	0.4158	0.4342	1.7739	7.1788
AM	5.0682	1.2456	0.3114	0.3165	1.2711	5.2529
AP	8.3102	1.8871	0.4571	0.5040	2.2153	8.2164
EM	4.1655	1.0217	0.2526	0.2695	1.1396	5.5184
EP	5.7397	1.4156	0.3522	0.3489	1.3854	5.4814
IM	7.2891	1.6614	0.5370	0.3972	1.6335	7.5744
IP	4.6171	1.2445	0.3203	0.3277	1.3218	5.2025

Table 7.13: Percentage increase in consumed propellant mass

The data in the table confirm what was stated earlier, namely that the most critical cases are in the AP and EP trajectories and that the trends are not symmetrical.
Possible reasons for an asymmetrical mass trend and why for some asteroids the shift from the optimal M has a greater impact than for others will now be reported.

7.3.1 AM & AP

Analysing the graphs of the REF asteroid, it is possible to see the presence of 5 propelled arcs and in all 5 there is a change in inclination. During the first, third and fifth arcs, apoapsis variation occurs with almost constant periapsis, except for small variations due

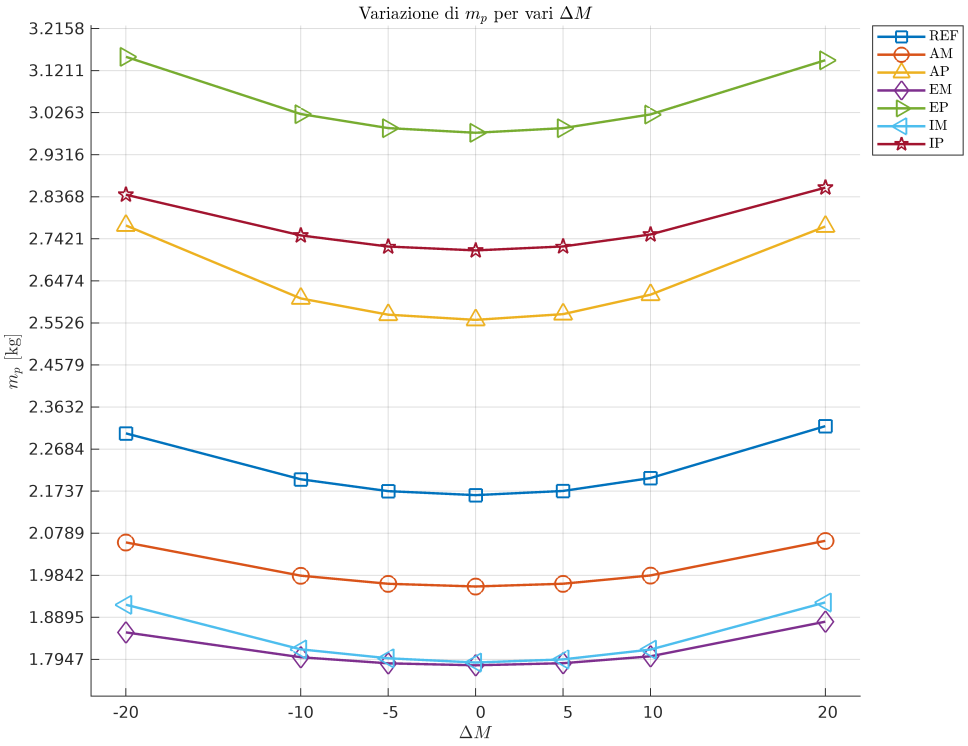

Figure 7.36: Propellant mass trend

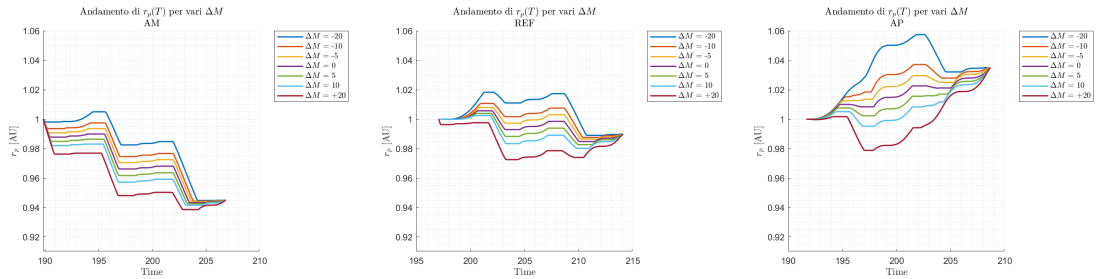

Figure 7.37: AM Periapsis **Figure 7.38:** REF Periapsis **Figure 7.39:** AP Periapsis

to the effect of applying a ΔV on an arc of finite length.In contrast, the periapsis is varied during the second and fourth arcs, phases in which the apoapsis is constant. Comparing the extreme cases $\Delta M = -20$ and $\Delta M = 20$, it can be seen that the latter is the more disadvantageous of the two, since it immediately goes to lower altitudes, in fact the periapsis decreases while the apoapsis remains constant and the spacecraft thus goes to orbits with an higher orbital velocity.
The case with $\Delta M = -20$ instead follows the optimal case $\Delta M = 0$ by initially increasing

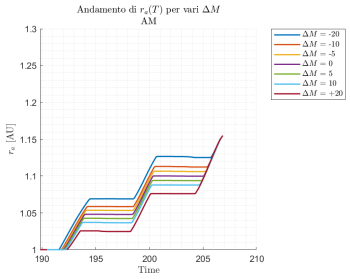

Figure 7.40: AM Apoapsis

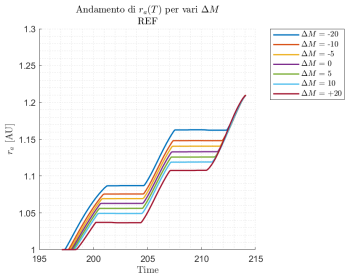

Figure 7.41: REF Apoapsis

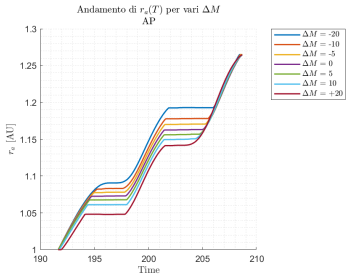

Figure 7.42: AP Apoapsis

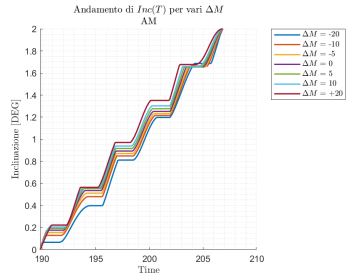

Figure 7.43: AM Inclination

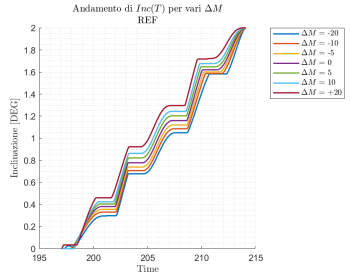

Figure 7.44: REF Inclination

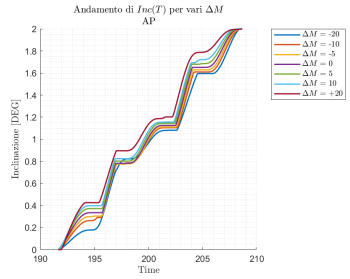

Figure 7.45: AP Inclination

the spacecraft's altitude. In fact, the apoapsis increases and the periapsis also has a slight increase. Determining factor for the higher cost of the case $\Delta M = +20$ is also the last propelled arc which has a very long duration compared to the previous ones.
The trajectory to reach asteroids AM and AP is different from that followed to reach asteroid REF and this is also reflected in the trends of apoapsis and periapsis. Regarding **AM**, it can be seen that it has 6 very short propulsive arcs, three (1, 3, 5) which modify the periapsis while keeping the apoapsis constant and three (2, 4, 6) which modify the apoapsis while maintaining the periapsis constant.
Comparing the $\Delta M = -20$ and $\Delta M = +20$ cases, it can be seen, as also in REF, that the $\Delta M = +20$ case presents an initial periapsis variation, with the spacecraft moving to orbits at lower altitudes, as the periapsis decreases and the apoapsis remains constant, and higher velocities, which penalises the mass of propellant consumed. The opposite case, on the other hand, decreases the periapsis slightly at first, resulting in a greater variation in the fifth propelled arc. With regard to the apoapsis variation, it can be seen that the case $\Delta M = +20$ has the last propelled arc very long compared to the others cases, a factor that increases the cost of the trajectory.
For **AP**, the trend of apoapsis and periapsis is different from the cases seen previously. The apoapsis has an increasing monotonic trend, while the periapsis shows different behaviour for the case $\Delta M = -20$ and $\Delta M = +20$. The second case is the most convenient for AP, with reduced propellant consumption. The case $\Delta M = -20$ is penalised by the fact that the spacecraft has to rise very high right from the start in order to decrease its angular velocity. It must therefore increase both periapsis and apoapsis and this leads

to an excessive increase in periapsis which must then be reduced in the final part of the trajectory. Concerning the case$\Delta M = +20$ where an increase in elevation is required, we see how the trends of periapsis and apoapsis are opposite. The apoapsis is increased at constant periapsis in the first arc in a way that is not as significant as in $\Delta M = -20$. Afterwards, the periapsis is raised to values slightly lower than the starting value. In fact, the periapsis lowering required to cope with the increase in apoapsis is less than that required in $\Delta M = -20$, which has a positive impact on fuel consumption. In general, it can be seen that for **REF** and **AP**, larger apoapsis variations and longer arcs are required and this is a disadvantage from a propulsive and propellant consumption point of view.

7.3.2 EM & EP

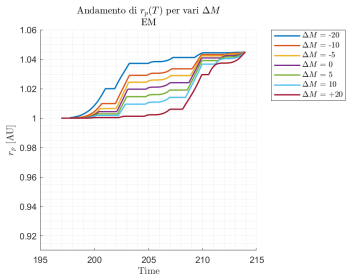

Figure 7.46: EM Periapsis

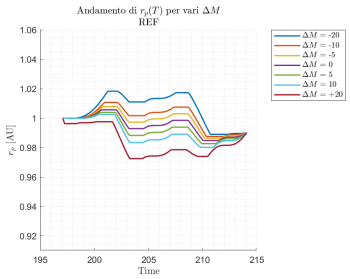

Figure 7.47: REF Periapsis

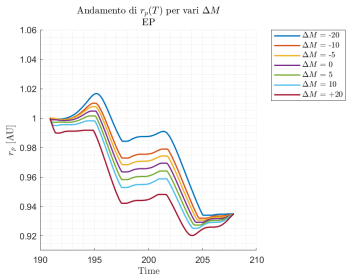

Figure 7.48: EP Periapsis

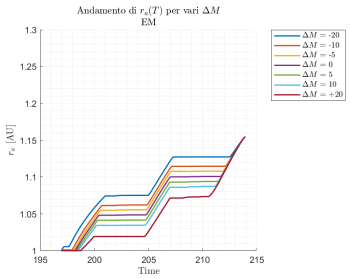

Figure 7.49: EM Apoapsis

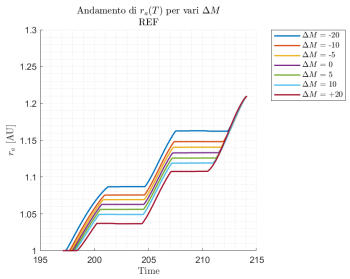

Figure 7.50: REF Apoapsis

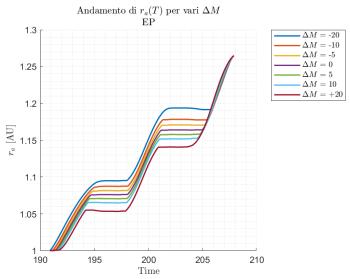

Figure 7.51: EP Apoapsis

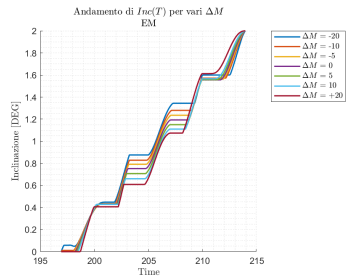

Figure 7.52: EM Inclination

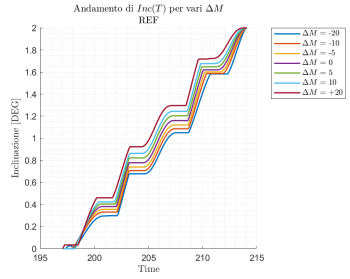

Figure 7.53: REF Inclination

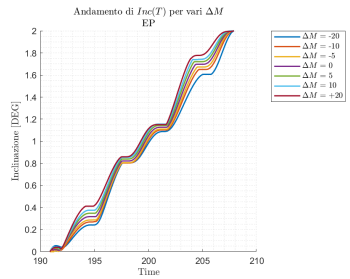

Figure 7.54: EP Inclination

The trajectory for **EM** shows an increasing monotonic pattern for both apoapsis and periapsis. The case $\Delta M = -20$ features an initial increase in apoapsis along with a slight increase in periapsis, rising in altitude at orbits with lower angular velocities. The difference between $\Delta M = -20$ and $\Delta M = +20$ lies in the slope of the propulsive arcs, in $\Delta M = -20$ there are shorter propulsive arcs, while in $\Delta M = +20$ there are longer propulsive arcs and, for the periapsis, concentrated in the final part of the trajectory. This is because $\Delta M = +20$ requires staying at low radii to increase angular velocity and inefficiently concentrate the increase in periapsis and apoapsis at the end. In fact, it has a

higher propellant consumption than the opposite case.
It should be noted that **EP** requires much greater apoapsis variations than in the other cases, which makes it necessary to decrease in periapsis.
EP has an increasing monotonic trend only for the apoapsis, while the periapsis has two different trends depending on the case. $\Delta M = -20$ follows the trend of the optimal case $\Delta M = 0$, increasing the altitude of the spacecraft, while the $\Delta M = +20$ case presents an initial decrease in periapsis, with the spacecraft going to lower altitudes and higher velocities.
Note the duration of the propulsive arcs, $\Delta M = -20$ has longer propulsive arcs than the opposite case, especially in the last arc due to the decrease in periapsis, caused by the excessive increase in apoapsis. In the case of $\Delta M = -20$, the periapsis is maintained at high values compared to the final value, while in the case of $\Delta M = +20$, it is reduced to values below the final value, so a shorter manoeuvre is required to reach the final value. This makes the case $\Delta M = -20$ more disadvantageous in terms of consumption. It should also be noted that the inclination varies in each propelled arc and the presence of small variations of periapsis together with apoapsis are due to the application of a ΔV on an arc of finite length.
In general, we can see that **EP** and **REF** have longer propelled arcs than **EM**, which makes the trajectory less effective and results in greater propellant consumption.

7.3.3 IM & IP

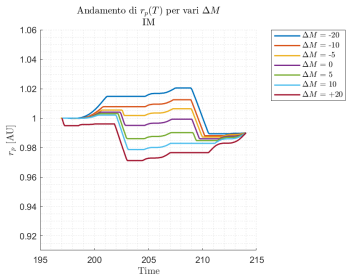

Figure 7.55: IM Periapsis

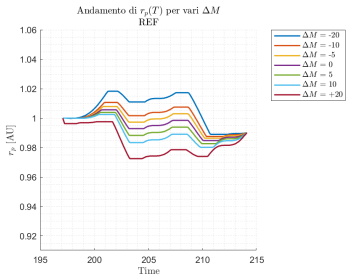

Figure 7.56: REF Periapsis

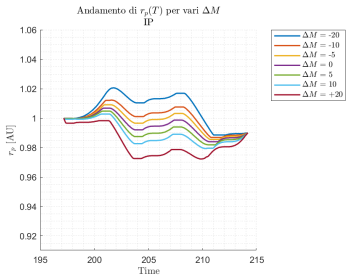

Figure 7.57: IP Periapsis

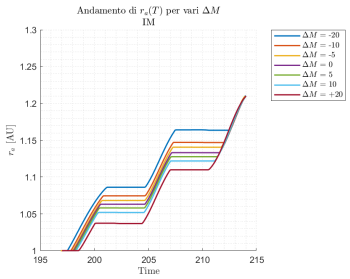

Figure 7.58: IM Apoapsis

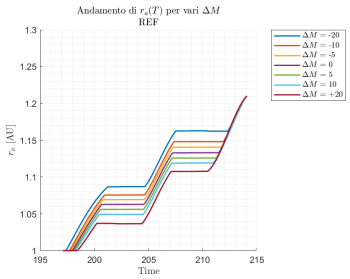

Figure 7.59: REF Apoapsis

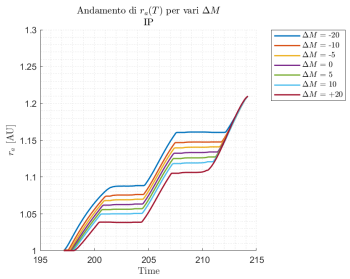

Figure 7.60: IP Apoapsis

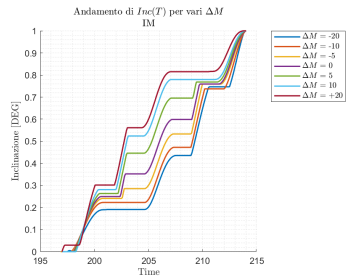

Figure 7.61: IM Inclination

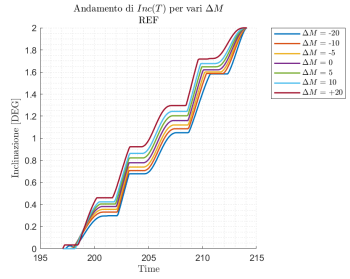

Figure 7.62: REF Inclination

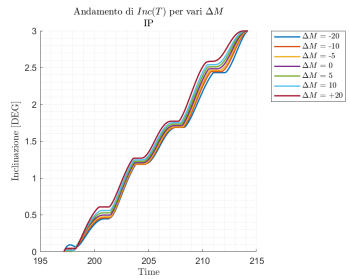

Figure 7.63: IP Inclination

The trajectory for **IM** has an increasing monotonous apoapsis pattern. With regard to periapsis, a distinction must be made between the cases $\Delta M = -20$ and $\Delta M = +20$. In fact, in the former case we see an initial increase in apoapsis at constant periapsis, a manoeuvre that causes the satellite to climb to altitude with lower speeds, while in the case of $\Delta M = +20$ we see an initial decrease in periapsis at constant apoapsis, a manoeuvre that causes the spacecraft to descend to altitude with higher speeds. This makes this case less convenient, as it has a higher propellant consumption than the case $\Delta M = -20$.
The trajectory for **IP** presents an increasing monotonic apoapsis pattern. The same

considerations made for **IM** apply to the periapsis, in fact also for IP the most convenient case is $\Delta M = -20$, which presents a lower propellant consumption than the case $\Delta M = +20$.
In general, we can see that for **IP** and **REF** we have propelled arcs for periapsis variation, of longer duration than for **IM**, which makes the trajectory less effective and leads to greater propellant consumption.

Chapter 8

Conclusions

In this thesis work, a set of fictitious asteroids, which fall into the category of near-earth objects, was created to study and analyse the influence of orbital parameters and phase angle on propellant consumption. The asteroids were chosen to ensure the feasibility of the mission with electric propulsion.
The optimal ΔV found and the mass of propellant consumed to reach each asteroid are now reported.

DES	**FUEL MASS (kg)** (M_{OPT})	ΔV **(km/s)** (M_{OPT})
REF	2.1647	2.2403
AM	1.9589	2.0165
AP	2.5595	2.6766
EM	1.7813	1.8253
EP	2.9810	3.1528
IM	1.7876	1.8321
IP	2.7160	2.8521

Table 8.1: Consumed propellant mass and ΔV generated

All trajectories have a ΔV of less than 3.5 km/s, which is a good result as these values are fully compatible with those achievable with electric propulsion. It is obvious that the more asteroids have orbital parameters different from those of the earth, the higher the ΔV. It should be noted that reaching asteroids that have orbits with greater eccentricity and inclination than those of the earth are the most onerous to reach in terms of consumption. Moreover, as ΔV increases, at fixed initial mass and specific impulse, more propellant will be required, which reduces the amount of payload the probe carries. A compromise or

trade-off is therefore required between the scientific return of the mission and the propulsive expenditure to carry it out. With regard to the optimal departure time, it should be noted that in order to reach the AP and EP asteroids, one must be very punctual, as a deviation from the optimal phase angle results in a sharp increase in the amount of propellant consumed. It should be noted that the indirect method has a limited convergence domain: it is possible that small variations in the tentative solution can determine a different final mass.
Furthermore, it must also be remembered that this is an initial feasibility study, so these trajectories represent preliminary mission solutions, which need to be studied in depth to validate them and make them achievable in all respects and that assumptions have been made as a starting point which should fall away when it is decided to delve into the study of these trajectories.

Appendix A

Optimisation problem

The optimum coincides, as required, with the minimum or maximum of a function with one or more variables, representing the cost or performance of a given phenomenon. Free optimisation will be discussed first, followed by the introduction of constraints, then moving on to constrained optimisation. Constraints can be either equality or inequality. The optimum is always sought (indistinctly maximum and minimum) with the exception of the problem with inequality constraints where the optimality conditions are not the same between minimum and maximum problems. One deals with the maximisation problem and then leads back to the minimum problem through simple considerations.

A.1 Maxima and minima of a scalar function

Theorem 1 *Let $f : D \subseteq \mathbb{R}^2 \to \mathbb{R}$ be a scalar function dependent on n real variables and x_0 a point inside the domain. Then:*

- *x_0 is a point of global maximum (or global minimum) for f if:*

$$f(x_0) \geqslant f(x) \quad (f(x_0) \leqslant f(x)) \quad \forall_x \in D$$

- *x_0 is a local maximum point (local minimum point) if:*

$$\exists_\delta \geqslant 0 : \forall_x \in I_\delta(x_0) \cap D \Rightarrow f(x_0) \geqslant f(x) \quad (f(x_0) \leqslant f(x))$$

The difference between a global optimum point and a local optimum point is that the latter is exclusively so in its vicinity I_δ whereas the former is so over the entire domain D.

Theorem 2 *If x_0 is a local maximum (or minimum) for the function f, then:*

- *if f is convex (concave), x_0 is a global maximum (minimum) for f;*
- *if f is strictly convex (strictly concave), x_0 is the only point of global maximum (minimum) for f.*

Theorem 3 *Weierstrass: Let $f : D \subseteq \mathbb{R}^n \to \mathbb{R}$ be a function of class C^1 and D a compact space of $\mathbb{R}^n$. Then, f admists at least one point of global maximum and one point of global minimum.*

A.2 Optimisation problem

Let $f : D \subseteq \mathbb{R}^n \to \mathbb{R}$ be a class C^2 function and β a property (constraining relationship) verified in the points $x \in K$ with $K = \{x \in \mathbb{R}^n : \beta(x)\}$. The function f is called objective function and β in the constraint condition. The set K is called binding set because it constrains the solution to be in the set $V = D \cap K$.

A.2.1 Maximisation problem

Let $f : D \subseteq \mathbb{R}^n \to \mathbb{R}$ be a class C^2 function submitted to the β constraint. A search is made for a point x_0 of global maximum for the function f in the admissible region.

$$x_0 \in D \cap K : f(x_0) \geqslant f(x) \forall_x \in D \cap K$$

Or:

$$x_0 = \max_{x \in V}[f(x)]$$

A.2.2 Minimisation problem

Let $f : D \subseteq \mathbb{R}^n \to \mathbb{R}$ be a class C^2 function submitted to the β constraint. A search is made for a point x_0 of global minimum for the function f in the admissible region.

$$x_0 \in D \cap K : f(x_0) \leqslant f(x) \forall_x \in D \cap K$$

Or:

$$x_0 = \min_{x \in V}[f(x)]$$

It is useful to note that finding the maximum of a function f is equivalent to finding the minimum of the function -f.
If $x_0 \in V$ is optimum for f in V, the $f(x_0)$ is optimum valore of f. x_0 is then a local (global) optimum if it meets the local (global) optimum condition of the problem. If the global (local) optimum in unique, then $x \in V$ is a point of strong optimum (or weak optimum).

A.3 Free optimisation

Free optimisation exists when no constraint is present, or more generally when:

$$K = D = V$$

The admissible set coincides with the domain of the function f, so the problem of maximisation or minimisation becomes the search for the point of maximum or minimum of the function f on its domain. To solve such a problem, differential calculus will be used, assuming that the function $f : D \subseteq \mathbb{R}^n \to \mathbb{R}$ and of C^2 class in $\mathbb{R}^n$.

Theorem 4 *The point $x_0 \in D$ is called stationary point for f if its gradient evaluated in x_0 is the null vector. Otherwise x_0 is said to be a regular point. In equations:*

$$\nabla f(x_0) = 0$$

Theorem 5 *Every local maximum or minimum point is a stationary point*

Note that the last theorem is not invertible, it is a necessary condition for the existence of maximum or minimum points, but it is not a sufficient condition.

Theorem 6 *Let $f : D \subseteq \mathbb{R}^n \to \mathbb{R}$ of class C^2 in $\mathbb{R}^n$ and $x_0 \in D$ a stationary point. Then the following propositions apply:*

- *If x_0 is a weak local minimum (or maximum) for f then the quadratic form associated to $H_f(x_0)$ is semidefinite positive (or negative);*
- *If the quadratic form associated to $H_f(x_0)$ is defined positive (or negative) then x_0 is a strong minimum (or maximum) point to f.*

A.4 Constrained optimisation

A.4.1 Optimisation with equality constraints

Let $V = K \cap D \subset D$ and β an equality vector relation that serves as a constraint. The latter can also be written in the form:

$$g(x) = 0$$

then the eligible region can be defined as:

$$V = \{x \in D \cap K : g(x) = 0\}$$

This optimization problem can be solved using two types of methods (under specific conditions): the *substitution method* and the *method of Lagrange multipliers*.

Substitution method

The constraint relations are h and can be specified as:

$$g(x) = 0 \quad \Leftrightarrow \quad \begin{cases} g_1(x_1, x_2, ..., x_n) = 0 \\ g_2(x_1, x_2, ..., x_n) = 0 \\ \dots \\ g_h(x_1, x_2, ..., x_n) = 0 \end{cases}$$

If each equation in the n variables x is explicable according to only one variable, they can be rewritten as:

$$\begin{cases} x_1 = \phi_1(x2, ..., x_n) \\ x_2 = \phi_2(x_1, ..., x_n) \\ \dots \\ x_h = \phi_h(x_1, x_2, ..., x_{h-1}, x_{h+1}, x_n) \end{cases}$$

And solving the system by substitution, it can be written:

$$\begin{cases} x_1 = \Phi_1(x_{h+1}, ..., x_n) \\ x_2 = \Phi_2(x_{h+1}, ..., x_n) \\ \dots \\ x_h = \Phi_h(h+1, ..., x_{h-1}, x_{h+1}, x_n) \end{cases}$$

The function to be optimised will be:

$$f(x) = f(x_1, x_2, ..., x_n) = f(\Phi_1, \Phi_2, ..., \Phi_h, x_{h+1}, x_{h+2}, ..., x_n)$$

That is:

$$f(x) = \Phi(x_{h+1}, x_{h+2}, ..., x_n)$$

a function with $n - h$ variables. The optimisation from this point is a free optimisation with $x_{h+1}, x_{h+2}, ..., x_n$ variables.
It can be seen that this resolution procedure involves direct explication of some variables as a function of others, which turns out to be analytically possible only if the expression of the constraint relation is known and if it is solvable in the variable of interest. In most cases this is not possible, so the method of Lagrange multipliers is used.

Method of Lagrange multipliers

Let $f : D \subseteq \mathbb{R}^n \to \mathbb{R}$ of class C^2 be an objective function and $g : D \subseteq \mathbb{R}^n \to \mathbb{R}^h$ of class C^1 a constraint function. The admissible region defined as $V = \{x \in \mathbb{R} : g(x) = 0\}$. The Lagrangian of f is defined as the scalar function $L : D \times \mathbb{R}^h \to \mathbb{R}$ written in the form:

$$L(x, \lambda) = f(x) + \lambda \cdot g(x)$$

with $\lambda = (\lambda_1, \lambda_2, ..., \lambda_h)$ the vector of size h of Lagrange multipliers.

$$\begin{aligned} \frac{\partial L}{\partial \lambda_i} &= g_i(x) \\ \frac{\partial L}{\partial x_i} &= \frac{\partial f}{\partial x_i} + \lambda \cdot \frac{\partial g}{\partial x_i} \\ \frac{\partial^2 L}{\partial x_i \partial \lambda_j} &= \frac{\partial g_j}{\partial x_i} \\ \frac{\partial L}{\partial \lambda_i \lambda_j} &= 0 \\ \frac{\partial^2 L}{\partial x_i \partial x_j} &= \frac{\partial^2 f}{\partial x_i \partial x_j} + \lambda \cdot \frac{\partial^2 g}{\partial x_i \partial x_j} \end{aligned}$$

H_f is defined as the matrix of the second derivatives of L with respect to the variables x_i, and G is defined as the matrix of mixed second derivatives with respect to the variables x_i and λ_j, it is possible to write:

$$G = \nabla g$$

and the Hessian matrix of L is composed of the following blocks:

$$\begin{bmatrix} H_f & G^T \\ G & 0 \end{bmatrix}$$

Definition 1 *The constraint is said to be qualified if the function g is regular throughout the admissible region, that is:*

$$\nabla g(x) \neq 0 \forall_x \in V$$

Theorem 7 *If g is regular at every point in the admissible region and the vector* $(\mathbf{x}, \lambda)$ *is a local solution to the problem:*

$$\max_{x,\lambda} L(x, \lambda)$$

Then $\boldsymbol{x}$ *is a local solution to constrained maximum problem for the function* f*.*

Theorem 8 *Let* $\boldsymbol{x}$ *be the local solution to the constrained maximum problem and* $G(\boldsymbol{x})$ *the matrix* $\nabla g_i(\boldsymbol{x})$,$i = 1,2,...,h$*. If* $G(\boldsymbol{x})$ *is of maximum rank, then exists a unique vector* λ *such that the vector* $(\mathbf{x}, \lambda)$ *is local solution of the problem:*

$$\max_{x,\lambda} L(x, \lambda)$$

The theorem just expressed is a necessary but not sufficient condition for determining the point of maximum (or minimum) bound of the function f. A second-order condition must be written:

Theorem 9 *Let the vector* $(\mathbf{x}, \lambda)$ *such that* $L(\mathbf{x}, \lambda) = 0$*, then:*

- *If* $\boldsymbol{x}$ *is a point of local maximum (or minimum) for the function f in the admissible region and* λ *its Lagrange multiplier, then the Hessian of L is semidefinite negative (or positive);*
- *If the Hessian of L is defined as negative (or positive) on the core of* $G(\mathbf{x})$*, then* $\mathbf{x}$ *is a point of local maximum (or minimum) of the function f in the admissible region V.*

A.4.2 Optimisation with inequality constraints

The optimisation problem does not always have constraint relations expressed through equations, but sometimes they can be unequalities. In this case it is not possible to find a general formulation of the problem and its resolution, since the optimum conditions are not the same in the case of the maximisation and minimisation problem.

Maximum problem with non-positive constraints

Let $f : D \subseteq \mathbb{R}^n \to \mathbb{R}$ the objective function of class C^2 and $g : K \subseteq \mathbb{R}^n \to \mathbb{R}^h$ a set of constraint functions of class C^1. Let $b \in \mathbb{R}$ a vector with h real components, the constraints are written in the following form:

$$g_i(x) \leqslant b_i$$

The admissible region can be defined as $V = \{x \in D \cap K : g(x) \leqslant b\}$. Inequalities for which equality holds are called active (saturated, stringent) constraints, while those for which inequality holds are called non-active constraints.
The problem of maximisation of the function f with h non-positivity constraints is formulated as:

$$\max_f f(x) : g(x) - b \leqslant 0$$

Note that if the constraint is of non-negativity, simply multiply both members to the left by -1.
At this point h Lagrange multipliers can be defined for each inequality contraint, writing a Lagrangian function $L : D \times \mathbb{R}^n \to \mathbb{R}^h$, defined as:

$$L(x, \lambda) = f(x) - \lambda \cdot (g(x) - b)$$

Theorem 10 *Let* $\mathbf{x}$ *be the local solution of the maximum problem and* g *such for which the gradients of the active constraints in* $\mathbf{x}$ *are linearly independent. Then there exists a* λ *such that the following properties are satisfied:*

$$\begin{aligned}
&\nabla_x L(\mathbf{x}, \lambda) = 0 \\
&\nabla_\lambda L(\mathbf{x}, \lambda) \wedge \lambda \cdot \nabla_\lambda L(\mathbf{x}, \lambda) = 0 \\
&\lambda \geqslant 0
\end{aligned}$$

Theorem 11 *Let* f *be a function of class* C^2 *weakly concave and* g *a function of class* C^1 *weakly convex for each* $i = 1, ...h$*. If* λ *and* $\mathbf{x}$ *exist such that the three previous relations are satisfied, if* $\nabla f(\mathbf{x}) \neq 0$*, then* $\mathbf{x}$ *is solution of the maximum problem.*

If the constraints are non-negativity for some variables, for example , expression such as $x > 0$ are added to the constraints. In this case the Lagrangian function does not change, but the condition becomes:

$$\begin{aligned}
&\nabla_x L(\mathbf{x}, \lambda) \leqslant 0 \wedge \mathbf{x}\nabla_x L(\mathbf{x}, \lambda) = 0 \\
&\nabla_\lambda L(\mathbf{x}, \lambda) \geqslant 0 \wedge \lambda\nabla_\lambda L(\mathbf{x}, \lambda) = 0 \\
&\mathbf{x}, \lambda \geqslant 0
\end{aligned}$$

For minimum problems, it is still necessary to solve a maximum problem, but where the objective function is denoted as $h(x) = -f(x)$.

Appendix B

Numerical Results

DES	ΔM = -20	ΔM = -10	ΔM = -5	ΔM = 0	ΔM = 5	ΔM = 10	ΔM = 20
REF	18.6962	18.7996	18.8263	18.8353	18.8259	18.7969	18.6799
AM	18.9418	19.0167	19.0350	19.0411	19.0349	19.0162	18.9382
AP	18.2278	18.3922	18.4288	18.4405	18.4276	18.3838	18.2302
EM	19.1445	19.2005	19.2142	19.2187	19.2139	19.1984	19.1204
EP	17.8479	17.9768	18.0085	18.0190	18.0086	17.9777	17.8556
IM	19.0821	19.1827	19.2028	19.2124	19.2053	19.1832	19.0770
IP	18.1586	18.2502	18.2753	18.2840	18.2751	18.2481	18.1427

Table B.1: Values of final mass in kg

DES	ΔM = -20	ΔM = -10	ΔM = -5	ΔM = 0	ΔM = 5	ΔM = 10	ΔM = 20
REF	2.3038	2.2004	2.1737	2.1647	2.1741	2.2031	2.3201
AM	2.0582	1.9833	1.9650	1.9589	1.9651	1.9838	2.0618
AP	2.7722	2.6078	2.5712	2.5595	2.5724	2.6162	2.7698
EM	1.8555	1.7995	1.7858	1.7813	1.7861	1.8016	1.8796
EP	3.1521	3.0232	2.9915	2.9810	2.9914	3.0223	3.1444
IM	1.9179	1.8173	1.7972	1.7876	1.7947	1.8168	1.9230
IP	2.8414	2.7498	2.7247	2.7160	2.7249	2.7519	2.8573

Table B.2: Values of propellant mass in kg

Bibliography

[1] Ulrich Walter. «Rocket Fundamentals». In: *Astronautics: The Physics of Space Flight*. Cham: Springer International Publishing, 2018, pp. 1–35. ISBN: 978-3-319-74373-8. DOI: 10.1007/978-3-319-74373-8_1. URL: https://doi.org/10.1007/978-3-319-74373-8_1 (cit. on p. 3).

[2] Benjamin Stahl and Robert Braun. «Low-Thrust Trajectory Optimization Tool to Assess Options for Near-Earth Asteroid Deflection». In: *AIAA/AAS Astrodynamics Specialist Conference and Exhibit* (Aug. 2008). DOI: 10.2514/6.2008-6255 (cit. on pp. 5, 8).

[3] Roger R. Bate, Donald D. Mueller, and Jerry E. White. *Fundamentals of Astrodynamics*. New York: Dover Publications, 1971 (cit. on pp. 7, 14, 26).

[4] Howard D Curtis. *Orbital mechanics for engineering students / Howard D. Curtis*. eng. 2nd ed. Elsevier aerospace engineering series. Kidlington, Oxford, UK ; Burlington, MA: Butterworth-Heinemann, 2010. ISBN: 9780123747785 (cit. on pp. 7, 16, 17, 24–26).

[5] URL: https://cneos.jpl.nasa.gov/about/neo_groups.html (cit. on pp. 30, 31).

[6] Shane D. Ross. «Near-Earth Asteroid Mining». In: 2002. URL: https://api.semanticscholar.org/CorpusID:52220910 (cit. on p. 32).

[7] Jürgen Blum and Gerhard Wurm. «The Growth Mechanisms of Macroscopic Bodies in Protoplanetary Disks». In: *Annual Review of Astronomy and Astrophysics* 46.1 (2008), pp. 21–56. DOI: 10.1146/annurev.astro.46.060407.145152. eprint: https://doi.org/10.1146/annurev.astro.46.060407.145152. URL: https://doi.org/10.1146/annurev.astro.46.060407.145152 (cit. on p. 32).

[8] Anders Johansen, Emmanuel Jacquet, Jeffrey N. Cuzzi, Alessandro Morbidelli, and Matthieu Gounelle. «New Paradigms for Asteroid Formation». In: *Asteroids IV*. University of Arizona Press, 2015, pp. 471–492. ISBN: 9780816532131. URL: http://www.jstor.org/stable/j.ctt18gzdvc.31 (visited on 03/08/2024) (cit. on p. 32).

[9] Tom Gehrels. *Asteroids III*. University of Arizona Press, 2002. ISBN: 9780816522811. URL: http://www.jstor.org/stable/j.ctv1v7zdn4 (visited on 03/08/2024) (cit. on p. 32).

[10] D. Dellagiustina et al. «Exogenic basalt on asteroid (101955) Bennu». In: *Nature Astronomy* (Sept. 2020). DOI: 10.1038/s41550-020-1195-z. URL: https://hal.science/hal-03038593 (cit. on p. 32).

[11] Paul Schenk et al. «The Geologically Recent Giant Impact Basins at Vesta's South Pole». In: *Science* 336.6082 (2012), pp. 694–697. DOI: 10.1126/science.1223272. eprint: https://www.science.org/doi/pdf/10.1126/science.1223272. URL: https://www.science.org/doi/abs/10.1126/science.1223272 (cit. on p. 32).

[12] URL: https://ssd.jpl.nasa.gov/diagrams/mb_hist.html (cit. on p. 33).

[13] William F. Bottke, Alessandro Morbidelli, Robert Jedicke, Jean-Marc Petit, Harold F. Levison, Patrick Michel, and Travis S. Metcalfe. «Debiased Orbital and Absolute Magnitude Distribution of the Near-Earth Objects». In: *Icarus* 156.2 (2002), pp. 399–433. ISSN: 0019-1035. DOI: https://doi.org/10.1006/icar.2001.6788. URL: https://www.sciencedirect.com/science/article/pii/S0019103501967880 (cit. on p. 32).

[14] William Jr, David Rubincam, and Miroslav Brož. «The Effect of Yarkovsky Thermal Forces on the Dynamical Evolution of Asteroids and Meteoroids». In: () (cit. on pp. 33, 34).

[15] URL: https://www.jpl.nasa.gov/missions/near-earth-object-surveyor (cit. on p. 34).

[16] URL: https://cneos.jpl.nasa.gov/fireballs/ (cit. on p. 35).

[17] URL: https://science.nasa.gov/mission/new-horizons (cit. on p. 37).

[18] Abolfazl Shirazi, Josu Ceberio, and Jose Lozano. «Spacecraft trajectory optimization: A review of models, objectives, approaches and solutions». In: *Progress in Aerospace Sciences* 102 (Aug. 2018). DOI: 10.1016/j.paerosci.2018.07.007 (cit. on pp. 40, 41, 45, 48, 54, 57, 65).

[19] John T. Betts. *Practical Methods for Optimal Control and Estimation Using Nonlinear Programming, Second Edition*. Second. Society for Industrial and Applied Mathematics, 2010. DOI: 10.1137/1.9780898718577. eprint: https://epubs.siam.org/doi/pdf/10.1137/1.9780898718577. URL: https://epubs.siam.org/doi/abs/10.1137/1.9780898718577 (cit. on p. 44).